VAPOR CHAMBER EMBEDDED WITH HOLLOW CONDENSER TUBES HEAT SINK

GOH WEN QIAN

A project report submitted in partial fulfillment of the

Requirements for the award of the degree of

Bachelor of Engineering (Hons) Industrial Engineering

Faculty of Engineering and Green Technology

Universiti Tunku Abdul Rahman

January 2017

DECLARATION

I hereby declare that this project report is based on my original work except for citations and quotations which have been duly acknowledged. I also declare that it has not been previously and concurrently submitted for any other degree or award at UTAR or other institutions.

Signature : _____

Name : _____Goh Wen Qian_____

ID No. : _____12AGB04025_____

Date : _____

APPROVAL FOR SUBMISSION

I certify that this project report entitled **"VAPOR CHAMBER EMBEDDED WITH HOLLOW CONDENSER TUBES HEAT SINK"** was prepared by **GOH WEN QIAN** has met the required standard for submission in partial fulfillment of the requirements for the award of Bachelor of Engineering (Hons) Industrial Engineering at Universiti Tunku Abdul Rahman.

Approved by,

Signature : _____

Supervisor : Prof. Ir. Dr. Ong Kok Seng

Date : _____

The copyright of this report belongs to the author under the terms of the copyright Act 1987 as qualified by Intellectual Property Policy of Universiti Tunku Abdul Rahman. Due acknowledgement shall always be made of the use of any material contained in, or derived from, this report.

© 2017, Goh Wen Qian. All right reserved.

Specially dedicated to

My beloved family

ACKNOWLEDGEMENT

Firstly, I would like to express my deepest gratitude and special thanks to my supervisor, Prof. Ir. Dr. Ong Kok Seng for his guidance, advices and supervision throughout the progress of the whole Final Year Project. I am grateful for his prompt replies to my questions. His suggestions and guidance throughout the Final Year Project contributed to the success of my project。

Besides that, I would like to thank Mr. Tan Choon Foong and Mr. Gabriel Goh for their precious guidance throughout the process of experimental set up. I truly appreciate the knowledge shared by them that helped me to get closer to my project.

Besides, I would also give my gratitude to Yat Ngai Solar Engineering Works (YN Solar) for the fabrication of the experimental apparatus that allowed me to complete the experimental investigation. Apart from that, I would like to thank the lab officers, Mr. Khairul and Mr. Syahrul for their help while working on my project.

Lastly, I would like to thank my parents and course mates who have offered me a great support, both mentally and physically, to complete this project.

VAPOR CHAMBER EMBEDDED WITH HOLLOW CONDENSER TUBES HEAT SINK

ABSTRACT

A novel vapor chamber with embedded hollow condenser tubes heat sink was designed and fabricated. Experiments were carried out to determine its thermal performance. The device was used to improve the thermal management of electronic packages. In this study, two vapor chambers heat sinks were tested using different fill ratios. Natural and forced convection as cooling model were employed and subjected to two different power inputs of 10W and 20W.

The results of this investigation showed that:

- ✓ Force Convection performs better with lower thermal resistance compared to Natural Convection.
- ✓ Under Natural Convection, lower Fill Ratio (FR=0.5) performs better.
- ✓ Under Forced Convection, higher Fill Ratio (FR=1.0) performs better.
- ✓ Under Natural Convection, lower Fill Ratio does not affect the performance of Vapor Chamber #1 & Vapor Chamber #2.
- ✓ Under Forced Convection and at low Fill Ratio, Vapor Chamber #2 performs better than Vapor Chamber #1.

TABLE OF CONTENTS

LIST OF FIGURES

LIST OF TABLES

LIST OF SYMBOLS/ABBREVIATIONS

V	Voltage input, V
I	Current input, A
P_{EH}	Power input to electric heater, W
P_{sat}	Saturation pressure, MPa
T_{sat}	Saturation temperature, ℃
T_{amb}	Ambient temperature, ℃
T_{ins}	Insulation temperature, ℃
T_{evap}	Temperature of heat sink of vapor chamber, ℃
T_{fin}	Temperature of the multi hollow fins heat sink, ℃
T_{hs}	Temperature of the evaporator of vapor chamber, ℃
h_{fin}	Coefficient of heat transfer for the fin, W/Km^2
R_{vc}	Thermal resistance of vapor chamber, K/W
R_{fin}	Thermal resistance of multi hollow fins heat sink, K/W
R_{total}	Total thermal resistance of vapor chamber with multi hollow fins heat sink, K/W
N_{fin}	Number of fin
D_{fin}	Diameter of fin, m
L_{fin}	Height or length of the fin, m
A_{fin}	Area of the fin, m^2
A_{base}	Base area of the fin, m^2
A_{plate}	Area of the copper plate
$\sum A$	Total area of condenser, m^2

CHAPTER 1

INTRODUCTION

1.1 Background of Experimental Study

Heat pipes are known as the heat transfer devices for transferring of huge amount of the heat efficiently. They are evacuated vessels with high effective thermal conductivity. The cross section is basically circular in shape, and filled up with small amount of the working fluid. This is due to the pipe which is able to transfer the heat effectively through long distances and had a minimal temperature variation between both the cold ends and hot ends of pipe, or to the isothermalize surfaces. The common material for making heat pipe is copper with an internal wick structure where the wick structure allows the working fluid to flow from condenser to evaporator through capillaries. The distilled water will be act as the fill liquid in the pipe itself. Basically, a heat pipe is divided into condenser and evaporator section which it demonstrate a closed evaporator-condenser system. The heating part in the system is called evaporator section while the cooling part is called condenser section. They are separated by an adiabatic section in between.

Compare to solid conductors like aluminum or copper, heat pipes can transfer heat more even as they have got lower total thermal resistance. This is due to the working fluid filled up in heat pipe is in saturation pressure where water will boil at 100^{o}c if it is at atmospheric pressure. During saturation pressure, the water in the heat pipe can boil at any temperature as long as it is above its freezing point. Heat pipes are mainly used in wide range of transferring heat application. For instance, electronic cooling, heat transfer on space application and others are where heat pipes can perform ideally. As such, they are reliable enough to use in many kind of applications due to no moving parts of the pipes. One of the examples of flat heat pipes is called vapor chamber. A vapor chamber (VC) consists of the bottom (evaporator) and upper (condenser) part. The bottom part will absorb heat while upper part which is the evaporator will dissipates heat to the surrounding which is the ambient. Heat transfer occurs from bottom to upper section where the fluid from bottom and then condense at the upper part. The working fluid is recycling in the system of VC.

Apart from that, a conventional fin heat sink (FHS) has fins attached at the top of flat metal where the metal is usually covered by aluminum or copper. A typical of FHS-VC heat sink device where the FHS is placed on top the VC as shown in Figure 1.

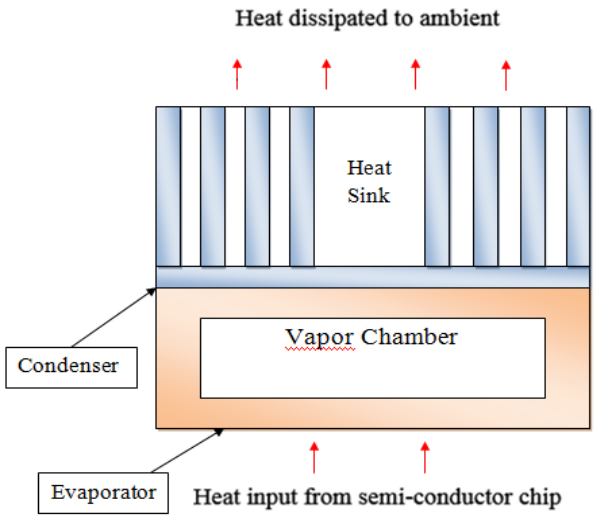

Figure 1: Cross section of a vapor chamber

With the aids of cooling fins, the heat will dissipate out efficiently to the ambient. The fins attached act as the large surface area which helps to have better contact with the surrounding air and transfer effectively. VC can improve the cooling of electronic devices better than the traditional design of heat sink from solid base plate attached with fins. The temperature distribution between the traditional solid base plate heat sink attached with fins and the conventional FHS-VC heat sink as shown in Figure 2 and 3.

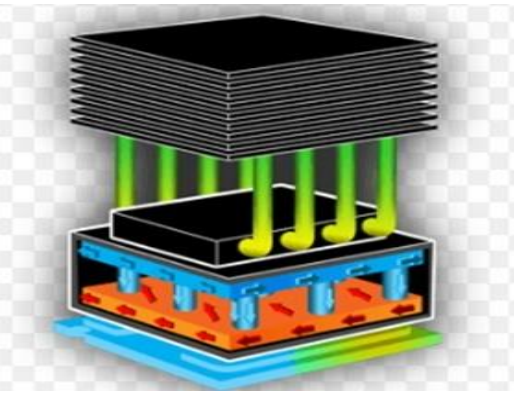

Figure 2: Temperature distribution of heat sink with vapor chamber base

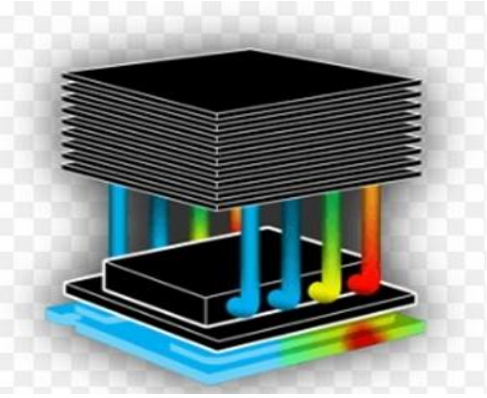

Figure 3: Temperature distribution of heat sink with solid metal base

Research of both heat sinks show the FHS-VC heat sink has better temperature distribution as they are more uniform than traditional solid base plate heat sink. When temperature distribution is more uniform, the overall thermal resistance will be improved. Thermal resistance exists between the bottom of FHS and VC. It is a heat property that resists the transferring of heat across a medium. For instance, during the process occurs in evaporator and condenser. The overall thermal resistance of VC-FHS includes the contact resistance (CR), spreading resistance, resistance of condenser and internal resistance. Likewise, the total thermal resistance created by the bottom part of VC will be minimized when it operate efficiently under the optimal conditions. The good performance of VC that minimizes the overall thermal resistance is used in the thermal management in electronic packaging nowadays. It helps to cool down the components and enhance the overall performance of the devices. In real life, thermal management is crucial especially in

electronic industry as high temperature in the electronic device will shorten the life cycle of the components and eventually causes the device failure and leads to degradation.

1.2 Problem Statement

Power transistors or Light Emitting Diodes (LEDs) are high power semiconductor devices. They generate a large amount of heat which means to be dissipated to the ambient surrounding.

The major problem encountered in thermal management of electronic device is to remove the heat of high power semiconductor devices more efficiently. Industries are searching for efficient and small heat sinks. Therefore, it is crucial to study and to provide a better solution to improve the heat dissipating rate. Thermal engineers are investigating two-phase cooling solutions with the aid of VCs and HPs. Conventional heat sinks with metal base plates do not have enough capacity to cool down the semiconductors. This is because of the hot spots generated on the base of the heat sink resulting high thermal heat spreading resistance. A VC used in conjunction with a conventional heat sink can achieve a better and more even heat flux distribution. This results in increased heat dissipation rate. Heat sink with fins is introduced with VC to increase in the total surface area of the cooling system. By incorporating the heat spreading effectiveness of VC and the heat transfer area of the fins, the overall thermal contact resistance between VC and FHS can be eliminated.

1.3 Aims and Objectives

The objective in this research is to study the thermal performance of VC with embedded multi hollow fins heat sink. Experiments are carried out under natural and forced convection air cooling.

1.4 Outline of Thesis

CHAPTER 1: INTRODUCTION

This chapter introduce about the conventional heat sink and vapor chamber fin heat sink and its working principles and applications. We discuss the problem arises in electronic industry and the objective of the study.

CHAPTER 2: LITERATURE SURVEY

This chapter is doing literature survey on:

- Thermal performance of Vapor Chamber Finned Heat Sink (VC-FHS).
- Heat transfer characteristics on Vapor Chamber.
- Experiment Study of Grooved Vapor Chamber
- Flat thermosyphon and system they work.

CHAPTER 3: THEORETICAL INVESTIGATION

This chapter discussed on:

- Theoretical model of Vapor Chamber Fin Heat Sink
- Theoretical calculations to determine the performance of VC-FHS.

CHAPTER 4: EXPERIMENTAL INVESTIGATION

This chapter discussed on:

- Apparatus used in the experiment.
- Experimental Procedure and the preliminary investigation.
- Experimental Results.

CHAPTER 5: DISCUSSION OF RESULTS

This chapter discussed on:

- Effect of Fill Ratio
- Effect of Natural and Forced convection
- Effect of Power
- Comparison of Vapor Chamber #1 and #2

- Thermal resistance and coefficient of heat transfer
- FHS with VC-FHS

CHAPTER 6: SUGGESTION FOR FURTHER STUDIES

This chapter discussed on the suggestions that can be done for further improvements in future.

CHAPTER 7: CONCLUSION

This chapter finalizes the whole project by concluding the results of investigation.

CHAPTER 2

LITERATURE REVIEW

2.1 Thermal Performance of Vapor Chamber Finned Heat Sink (VC-FHS)

(Attia et al, 2012) carried out experiment investigation on VC with the variation of working fluids by varies the charge ratio. The experiment is tested out to evaluate thermal performance of 2mm high and 50mm diameter VC with methyl alcohol and water with difference of the charge ratios. Furthermore, Propylene Glycol as well as water with two different concentrations which are 15% and 50% was carry out experiment to examine the effect of surfactant to treat as enhancement agent of working fluid. Total thermal resistances to study in this experiment are divided into three parts. They are junction, internal and condenser resistance in order to indentify which part of thermal resistance will give the better effect on the VC thermal resistance. Based on the experiment study shown, water is better compare to methyl alcohol. This is because the total thermal resistance when water as working fluid is lower. When using propylene glycol as the water surfactant, the VC total thermal resistance reduces to about 50% compare to using only pure water. Besides, the 30% charge ratio shows the most significant for all of the working fluids that used to test. Furthermore, the junction resistance shows the greatest value of total thermal resistance which is around 90%.

(Jeng, 2015) proposed a novel fin heat sink designed with motor fan and many vertical passages that could be applied for heat dissipation of LED lamp. There was a total 6 models of finned heat sink being built with different specifications in order to investigate the effects of motor fan, multiple vertical passages and separation on the chamber of the heat sink on heat transfer rate of fin heat sink. Based on Table 1, it shows different specifications of fin heat sink.

Model	Motor fan	Fan's maximum air flow rate (CFM)	Multiple vertical passages	Separation
A	-	-	-	-
B	-	-	✓	-
C1	✓	3.5	✓	-
C2	✓	3.5	✓	Complete
D	✓	5.3	✓	Complete
E	✓	17.16	✓	Complete

Table 1: Specifications of finned heat sinks

In this study, the Nusselt number (Nu) was took to analyze overall thermal performance of heat sinks. Different models of heat sinks were compared with the power input of 15.48W. The Nu values obtained for models A, B and C1 are similar and significantly lower than model C2 by 22-29% and 41-50% lower than model D and E. The presence of motor fan illustrates the internally forced convection of transferring of heat for the heat sink. The study showed that forced convection has high impact on overall thermal performance of heat sink with fins.

(Li et al., 2010) investigate that with the use of VC compare to the conventional heat sink, heat transferred rate to the bases of heat sink for VC is more uniform. They carried out experiment by study the performance of VC with plate fins heat sink with the method of infrared thermography. They use vary number of fin, width and height of the fin as well as Reynolds number to investigate on overall thermal performance of VC heat sink. After the experiment, data was computed and compare with the conventional aluminum heat sink. They found out that it is true that VC as base plate can transferred heat evenly more than the conventional type. Overall thermal resistance also shows a decreasing value. At a fixed Reynolds number, with increased fins height, fins width and number of fins, the VC heat sinks would have larger heat transfer area for convection which gradually reduces thermal resistance of conduction across it. In brief, lower Reynolds number shows greater results with the various dimensions of fin.

(Luo et al., 2010) presented a differently VC with coupled fin heat sink. In their research, this particular type VC is carry out experiment and allows to input to high power of the LED light source (20W)for determining the overall performance of VC coupled fin heat sink on heat dissipation for higher power of the LED device. In order to get a better significant of the results, they compare the results with another fin heat sink device fabricated. The experiment was carried out with two prototypes and results were computed. 20 thermocouples were put and used do the measurement of temperature of PCB board. Results show that VC coupled fin heat sink can get the better heat dissipation rate and the temperature distribute more evenly. The thermal resistance of VC is only 0.05KW. The overall thermal resistance get is 0.654K/W when surrounding temperature reached 27^{o}c. The solution presented are computed and used to solve the hotspot problems of LED appliances to apply in the LED industry.

(Michels, Milanez and Mantelli, 2012) presented a prototype of VC heat sink with hollow fins with thin copper tubes to replace the conventional solid fins in order to maximize the fins efficiency. The hollow fins makes the heat transfer is to be larger and will not easily dry out. The experiment was study with forced convection and different fill ratio was being used. They have found that with higher filling ratios which are 25%, 35% and 60%, the thermal resistance values obtained will be significantly lower with increasing heat source output. The lower filling ratio of 15% and 20%, the overall thermal resistance values is larger. With higher heat source output, the heat transfer coefficient will be higher and the higher vapor of mass flow will results in lower thermal resistance. However, with heat source output above 150W, there is a signature of dry-out occurs where condensation is inefficient enough to transfer the condensate to back to VC. Therefore, overall thermal resistance is high. Result shows that the best filling ratio is 25% with lowest thermal resistance which start from 0.12K/W to 0.20K/W. In brief, the prototype presented showed that the VC heat sink with hollow fins could achieve 20% less overall thermal resistance when we compared with conventional solid fins.

(Naphonand Wiriyasart, 2015) carry out experiment to determine the thermal performance and heat transfer characteristics of VC in presence and absence of the micro-channel under fixed of the heat flux. Based on the experiment, the model that they are using for VC is attached a two-phase VC along with wick structure. The method they use to carry out experiment is by finite volume method. They computed the temperature distribution of VC with the effect of micro-channel presence or absence. They compared the results obtained and make a conclusion. The conclusion of the experiment obtained is discussed. They found out that the VC with micro-channel shows a greater result on temperature distribution as well as the thermal performance of VC. With the results, designer could be use to improve the design of VC for cooling systems of electronic devices for a better cooling performance in future.

(Shih, 2011) invent a heat sink embedded with VC to see the performance of the heat sink. The equipment includes a VC and heat conduction plate. For the heat conduction plate, it has one side formed of radiation fins while two lateral edges formed in another side. The objective of the invention model is to find out a better heat transfer model to increase the cooling effect. In order to save material, they reduce the weight and in order to pull up rate of heat transfer by fabricates particular model with a smaller thickness. However, result shows that with a smaller thickness, the fastening force apply will cause distortion and deform the whole model and this affects the heat transfer effect. Apart from that, there will be a gap between the plate and VC if deformation occurs. This will also affects the performance of the VC. The drawing of invention was use as reference of the drawing for future.

(Shukla et al, 2013) investigate the thermal performance of VC without wick with different working fluids. The working fluids used in this experiment is nano fluids. A VC with 64mm width and 78mm length was used to fabricate on thickness of 5mm then it was used to test with aluminum-water as well as the copper-water nano fluids. 30% of the nano fluids were filled in the VC. It is tested with the power input of 90-150W. The motive on the experiment is to present on thermal resistance of VC with 2 of the working fluids. The results of the experiment showed that nano fluids charge of VC perform a better performance than the de-ionized water charge of VC. Based on results obtained in the experiment, the total thermal resistance was reduced about 5% when there was an increase of weight percentage of nano particles. This investigation proves that the VC-heat sink with the filling of nano fluids can collaborate with the components to carry out the function of heat dissipating and use widely in the application of cooling of electronics.

(Wang et al, 2011) tested on thermal performance of a vapor chamber with the used of window program VCTM V1.0 and apply findings to a high-performance server. The experiment used a method from a novel formula to investigate the effective thermal conductivity of a VC to determine the thermal performance. Throughout findings in the experiment, it can be summarized that copper and aluminum heat spreader has poorer effective thermal conductivities than VC. 100W/cm^2 was the maximum heat flux of VC. The thermal conductivity affected by the power input. There are error for the experiment which is not more than ±3%. For one or two dimensional VC, the thermal conductivity is around 100 W/m^oc which is less than the single solid phase metals. Besides, the thermal conductivity based on three dimensional VC is about 870W/m^oc which is many times more than copper base plate.

(Wong et al, 2010) investigate a novel vapor chamber and carried out experiment using the vapor chamber. The conventional wick on top plate was replaced by parallel grooves with inter-grooves openings which place at the plate inner surface. While the layer of porous wick place was placed at bottom part of plate as evaporator. The vapor chamber for this experiment was 10cm x 8.9cm. The heating area used was a 0.021m x 0.021m or a 0.011m x 0.011m. The resistance of VC was measured ranging from 80W-300W. From the results obtained for the heating area of 0.21m x 0.21m, VC thermal resistance ranged from 0.08 K/W to 0.04 K/W for the heating power ranged from 80W to 460W. The resistance decreased while the heat source power increased. For the heating area of 0.011m x 0.011m, the VC performance on an area base is 0.14Kcm^2/W and the heat flux is 120W/cm^2. Based on the experiment, evaporator resistance of VC resistance was a dominator. Based on the investigation, the heat transfer coefficients associated with the evaporation was a few times larger than that associated with the condensation.

2.2 Heat Transfer Characteristics of VC

(Kang et al, 2012) study on the uniformity of temperature and the heating rate of heat spreader with multi- well. It is simulate and analyze by CFD software on natural convection. In the study, they used the multi-well heat spreader that made up of copper, aluminium, silver and VC. The four types of multi-well heat spreader are used to simulate and the results was used to compare. They used dual and six heat sources to apply to the heating power of 1200W. For six heat sources which is at heating power of 188W, 300W, 600W and 1200W, the heating rate are used to study. Based on the results of simulation, the lower heating power will greatly effect on the surrounding temperature. Hence, the temperature will rise in curve line. With higher heating power there was little effect on the surrounding temperature. The results also prove that six heating sources are better than dual sources as the temperature uniformity is better. From the study, the results obtained from the simulation are vapor chamber multi-well heat spreader shows the greater uniformity, follow by silver, copper and aluminum.

(Reyes, Alonso, Arias and Velazquez, 2012) carried out experiment to study the performance of a vertically placed VC based heat spreader with the dimension of 190mm x 140mm x 15mm. It is used in avionics applications. They also study the effect of natural convection as to act as the failure mode of the aircraft supply system to be use in the actual design. In the experiment, they use various heat spreader geometries, with a metal rectangular shape fins heat sink to be the reference model. The result shows that VC heat spreader has the highest performance which they are efficiently spread the heat even though they have a higher weight. It is better compare to the metallic heat sinks counterparts. The surface temperature found was in the range of 80^{o}c to 100^{o}c, and the suitable power input is ranged from 95W to 145W. Apart from that, they also get a conclusion that natural convection shows good performance with the use of VC heat spreader. The results are computed and use to find out the minimum weight that is most suitable to use in the actual design of heat spreader.

(Tan et al, 2010) study about the wick structure on FPHP to investigate the performance of liquid flows inside. They used various sources of heat to carry out study which are line, discrete, strip heaters. The Green' function approach are used to simulate. The results were then used to simulate the different heat source used to carry out experiment on the heat pipe. In the research, the analytical liquid flow model in this study was about to show quantitatively on the pressure and velocity distribution on the model with the various heating conditions. The result on the analytical model is able to use to obtain the optimum position of IC chip on PCB so that designer can provide a better position of the chips.

(Tsai, Kang and Vieira de Paiva, 2013) have presented a model of a VC heat spreader two-phase heat transfer device. This is because the increasing heat dissipation in electronic packaging that has to be solved for a better future. They have built a prototype of VC with a dimension of 90mm x 90mm x 3.5mm to study its thermal performance by determining the thermal resistances under five different orientations. By analyzing the results obtained, the inclination did not show a clear impact on the temperature uniformity. However, it was found that the VC had the highest resistance of spread which is $0.718\,K/W$ while total thermal resistance is $0.89K/W$ with the inclination of 90^{o} due to the effect of gravity on the VC mechanism. Research shows that spreading resistance that exists between the heater and the bottom surface of the VC was affecting the thermal resistance in big portion. Besides that, they also varied the power input from 5W to 50W and it was found that with increasing power input, the overall thermal resistance of VC will be reduced. Likewise, result indicates that spreading resistance act as a crucial role for the overall thermal resistance as it will affect the higher or lower value of thermal resistance.

(Wang et al, 2011) carried out experiments on FPHP to determine the effect of the length on evaporator and condenser that will affect the performance of their model. Experiments were used a FPHP with a heat transfer length and width of 25.5cm and 2.5cm. The working fluid used is water. The results were used to compare with vapor chamber and the traditional heat pipe. From the results obtained, FPHP could achieve a long distance of heat transfer than vapor chamber. It had a big contact area on heat sources when compare with traditional heat pipe. The length of evaporator is proportionally to the heat transfer limit while inversely proportional to thermal resistance. Besides, FPHP will dry out at low heating power when condenser length increases. The closer to the length of condenser and evaporator, the easier to achieve the thermal performance of FPHP.

(Wiriyasart et al, 2013) study on the characteristic of transferring of heat on VC that has no Micro-channel to cool the computer processing unit (CPU). The mathematical model of a VC in the investigation is on two-phase closed chamber of presence on wick column and sheet. In their research, pressure as well as temperature distributions of VC was presented using equation of momentum, energy, and continuity to solve. The CPU in the experiment is replaced by two heaters as heat source. The input of power is 80W for heater. The result was compared with the measured data. It was found that the predicted results and the measured data had a difference in 1.4% which is acceptable. The good agreement obtained from the numerical results can be used in future for designer to design a better thermal performance of a VC while remove the trial and error test in future.

(Yang et al, 2015) carried out investigation on a new design of flat polymer heat pipe. The purpose of the investigation was to determine how much heat can be eliminating based on the heat source with various conditions. The design of the heat pipe is 1mm of thickness for the copper frame which in between the up and down of FR4 polymer for getting a VC. Table 2 showed the five of the flat heap pipes specifications.

Case	Thermal via	Filling ratio (%)	Weight (g)
A	-	36	6.87
B	✓	0	8.37
C	✓	20	8.57
D	✓	28	8.65
E	✓	36	8.73

Table 2: Specifications of flat heat pipes

The heat pipe overall thermal resistance was used a TDIM method to measure which known as transient dual interface method. Based on experiment results obtained, the heat pipe containing working fluid will minimize the thermal resistance compared to the heat pipe with the absence of working fluid. With input power of 6-16W, the thermal resistance of filling ratio of 28% is the lowest. Overall using the system to measure the total thermal resistance, a reduction of 57% achieved.

(Yu et al, 2012) study the performance of a FPHP heat spreader by using different wick structures. The experiment was conducted with various parameters ranging from 5W to 20W. Eight varieties of wick were used during the experiment to determine the optimum wick. A variety of liquids was used to carry out the experiment as working fluids. For instance, water, acetone, ethanol, TiO_2 nanofluids. The results obtained shows that TiO_2nanofluids was the best working fluid as it showed the best heat spreading performance of FPHP heat spreader. The best filling ratio was about 50% to 60%. By using the present study of experiment, a simulation was conducted. In brief, simulation results give a strong agreement with present research.

2.3 Experiment Study of Grooved Vapor Chamber

(Zhang et al, 2009) study on a new design of grooved VC. VC with grooves structure helps to achieve better radial as well as axial heat transfer. Besides, the study shows that the structure can form capillary loop between the condenser and evaporator surfaces. In the experiment, effect of fill ratio, heat flux as well as the performance of VC was studies. The working fluid used in the experiment was water. The faces for condenser and evaporator have a diameter and thickness of 8.5cm and 0.3cm. The depth and width of the grooves are 0.03cm and 0.02cm. Based on results obtained, VC achieves better performance from fill ratio of working fluid with the weight of 1 to 2g where the optimal amount is 1.43g where the liquid was filled for 40.4%. The heat flux attached with the particular working fluid ratio was 3.05 x $10^5 W/m^2$. The experimental results were used to compare with numerical simulation results to show reliability.

2.4 Thermal Performance of Flat Thermosyphon

(Zhang et al, 2008) do research to investigate thermal performance of flat thermosyphon. In the study, they used a transparent two phase thermosyphon to study and observe. The area of study in this experiment was characteristics of phase change of heat transfer, performance with various fill ratios and the surface of evaporator to groove. Based on the experiment, it was found that the water shows the best results compare to ethanol. Thermal resistance when using ethanol as working fluid is higher than using of water. Moreover, the thermal resistance will decrease when the heating flux increases. Besides, the presence of grooved surface shows better transferring of heat compare with the absence of grooved. In brief, the two phase thermosyphon gives a good result of leveling the temperature at condenser surface.

CHAPTER 3

THEORETICAL INVESTIGATION

3.1 Theoretical Model

The model that investigates in this thesis is vapor chamber with multi hollow fins heat sink. VC with multi hollow fins heat sink is a type of 2 dimensional flows VC which the bottom part of the VC acts as the evaporator and the fins act as the condenser. The distilled water that filling up the VC will undergoes evaporation and evaporates through the evaporator to the fins as water vapor. When the water vapor reaches the fins which are the condensers, they will condense back to the evaporator in liquid. This causes the recycling occurs. The power input from the heating element to the base of the VC with an aluminum block place between them. VC will acts as the heat spreader to spread out the heat to the fins when power input. During the heat spreading process, there are thermal resistance exist. The thermal resistances includes are resistance of the fins (R_{fin}) and resistance of VC (R_{vc}) as shown in Figure 4. The overall thermal resistance is the sum of the two resistances and it has to be reduced or minimize in order to maximize the efficiency of VC so that the heat transfer process happens more effective.

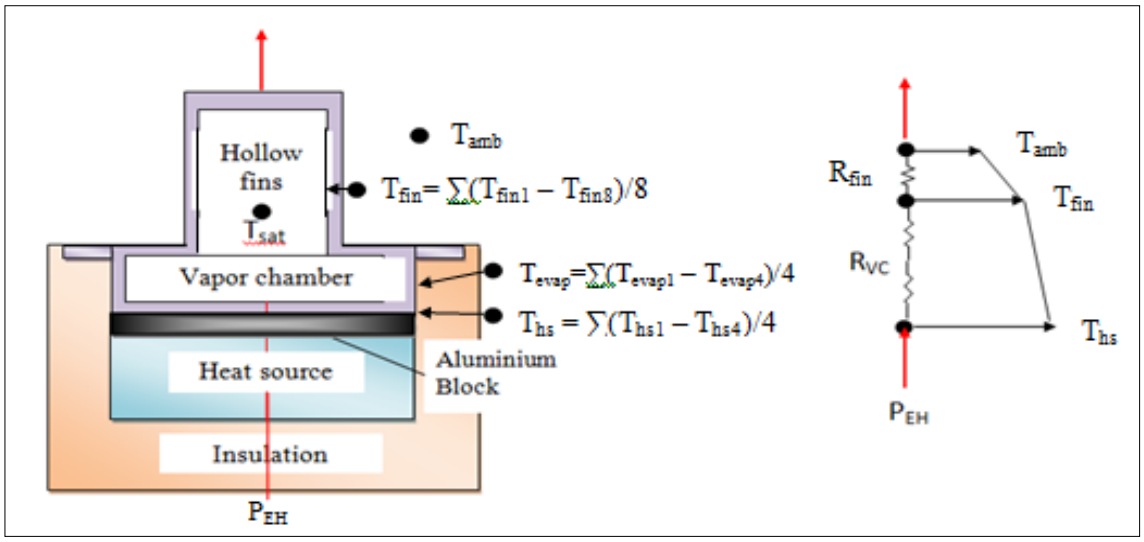

(a) Cross-section of VC. (b) Resistance network of VC.

Figure 4: Thermal Resistance Network

Besides, during the heat spreading process, we also discovered about the convection heat transfer coefficient. It is a quantitative characteristic of convection occurs in heat transfer between a fluid medium and the wall surface flowed over by fluid. It depends mainly on the thermal properties of a medium and the thermal boundary conditions. The SI unit for overall heat transfer coefficient is W/m^2K. There are numerous methods and formulas that can be used to calculate h_a. In the study of this case, we only used two formulas for the calculation of h_{fin} which are the heat transfer coefficient of the fins. The formulas are discussed later on.

3.2 Theoretical Calculations

Power input to the electric heater, P_{EH} is calculated by using Ohm's Law Formula.

$$P_{EH} = VI \qquad (1)$$

Where V is the voltage input, V

I is the current input, I

The formulas to compute thermal resistance of the VC with multi hollow fins heat sink are as shown:

$$R_{VC} = \frac{T_{hs} - T_{fin}}{P_{EH}} \quad (2)$$

$$R_{fin} = \frac{T_{fin} - T_{amb}}{P_{EH}} \quad (3)$$

$$R_{total} = R_{VC} + R_{fin} \quad (4)$$

Where R_{vc} is the resistance of the VC, K/W

R_{fin} is the resistance of the multi hollow fins heat sink, K/W

R_{total} is the total thermal resistance, K/W

T_{hs} is the temperature of evaporator, ℃

T_{evap} is the temperature of VC heat sink, ℃

T_{fin} is the temperature of the multi hollow fins heat sink (condenser), ℃

T_{amb} is the ambient temperature, ℃

The formulas to compute the heat transfer coefficient of fin, h_{fin} of VC with multi hollow fins heat sink are as shown:

$$A_{fin} = N_{fins}(\pi D_{fin} L_{fin}) \quad (5)$$

$$A_{base} = \frac{\pi D2}{4}(N_{fins}) \quad (6)$$

$$A_{plate} = 2\left(1 + \sqrt{2}\right)a^2 \quad (7)$$

$$\sum A = A_{plate} - A_{base} + A_{fin} \quad (8)$$

$$h_{fin} = \frac{1}{R_{fin}\sum A} \quad (9)$$

$$h_{fin} = \frac{P_{EH}}{\sum A(T_{fin} - T_{amb})} \quad (10)$$

Where N_{fins} is the number of fin

D_{fin} is the diameter of the fin, m

L_{fin} is the height or the length of the fin, m

A_{fin} is the area of the fin, m^2

A_{base} is the base area of the fin, m^2

A_{plate} is the area of the copper plate, m^2

$\sum A$ is the total area of condenser, m^2

CHAPTER 4

EXPERIMENTAL INVESTIGATION

4.1 Experimental Set Up

The experiment investigation carried out by using two VCFHSs fabricated from 55 mm O/D x 1 mm thick x 35 mm long copper transition sockets capped with 1 mm thick copper plates on top. An array of 1 mm thick x 10 mm OD copper tubes were brazed on the copper plate in a radial symmetrical pattern to act as fins. There are eight tubes each 25 mm long in VC#1 and four tubes each 35 mm long in VC#2. Attachments were provided at the top of the central tube in each of the VC to fit vacuum gauges and to provide connections to a vacuum pump. Figure 5 shows the VC #1 and VC#2 with hollow copper tubes that built to help to determine the result.

Figure 5: Vapor chamber with embedded hollow condenser tube heat sink

The apparatus set up in the experiment is to determine the influence of different fill ratio of water in the copper ring on natural and forced convection, different power input on the heating element on natural and forced convection. We determine the suitable fill ratio and power input that minimize the overall thermal resistance. The same VC is used when carried out the experiment with different fill ratio of water. The fill ratio that used in this experiment is fill ratio of 1 and 0.5 respectively.

The equipments that used to conduct the experimental setup are thermocouples, control valve, pressure gauge, aluminum block, aluminum string, thermal paste, insulation wool, heating element, voltmeter, ammeter, voltage regulator, data logger and cooling fan. The VC with multi hollow fins heat sink attached to the aluminum block and then to heating element with thermal paste applied in between. Thermal paste is a heat conductive paste that able to provide a better surface contact by minimizing the air trapped in between two surfaces. In order to minimize the heat loss to the surrounding during the experiment, the VC heat sink is insulated with insulating wool with only the multi-hollow-fins heat sink and the octagonal shape copper plate being exposed. The voltage regulator is connected to the heating element and the power input is determined by measuring the voltage and current input using voltmeter and ammeter respectively according to the formula (P=VI). A pressure gauge is used to measure the vapor pressure inside the VC heat sink and a control valve attached is closed during the experiment to prevent air flow and keep the VC heat sink held in vacuum state. Data logger is used to record the temperature of thermocouples attached on the VC. The VCFHS was heated with a 50 mm diameter electric heating element. A 50 mm diameter x 10 mm thick aluminium block inserted in between the heating element and the VCFHS ensured uniform heating. Power input was measured with ac voltmeter and ammeter. Insulation was provided all around as shown. Figure 6 shows the schematic diagram of the experimental setup.

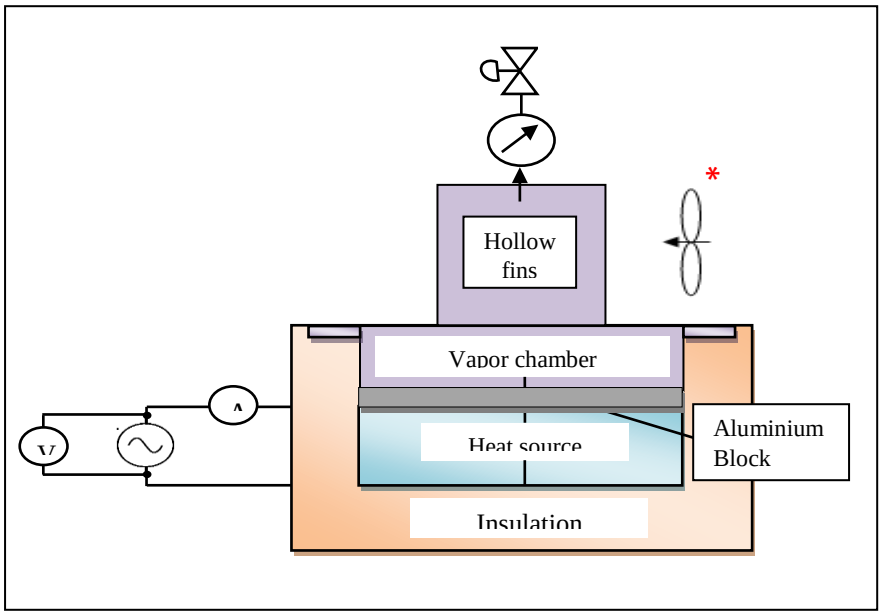

Figure 6: Schematic Diagram of the Experimental Setup

Natural convection of the experiment carries out with normal air flow in the air conditional room. A cooling fan is used for the forced convection experiment with different power input and fill ratio of water. It is to enhance the convective heat transfer process throughout the VC heat sink. When the boiling and evaporating rate of the VC is greater than the condensing, dry out condition will occurs and results in lower composition of distilled water after a long run due to the trapping of water in the hollow copper tubes that unable to flow back to the vapor chamber of the evaporator section. Figure 7 and 8 shows the experimental setup for natural and forced convection.

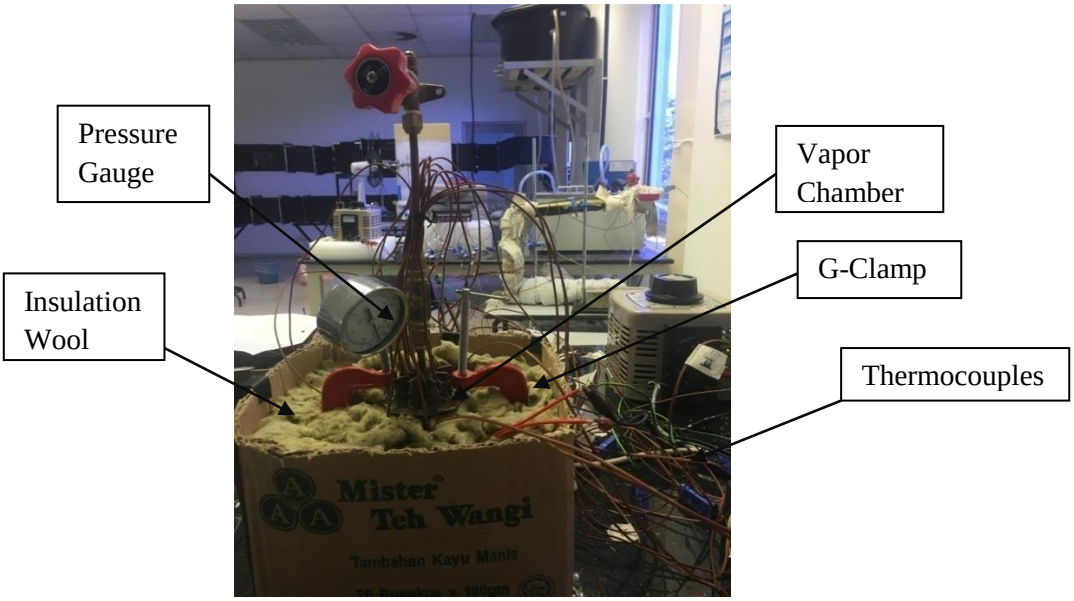

Figure 7: Photograph of experimental set up (Natural convection)

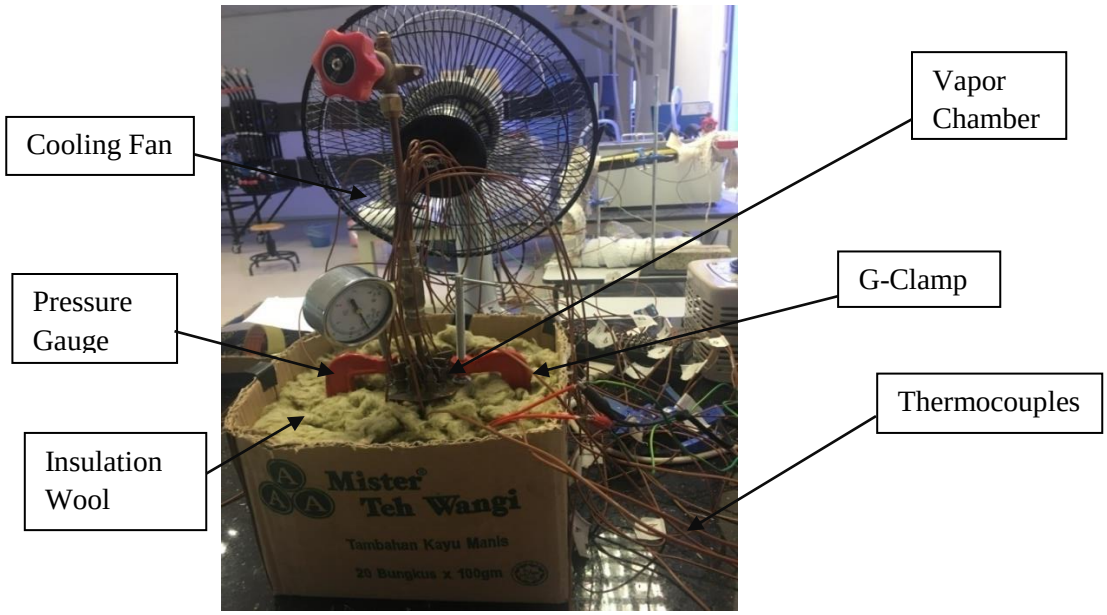

Figure 8: Photograph of experimental set up (Forced convection)

For VC #1, the experiment carried out used a total of 20 thermocouples placed in different position in order to measure the temperature. For VC #2, the experiment carried out using 16 thermocouples. Figure 9 shows the schematic diagram for the locations of the thermocouples for VC#1. Type T (copper-constanten) thermocouples ($\pm$ 0.5^{o}C accuracy) were employed to measure temperatures. Four temperature probes were inserted into grooves machined on the aluminum block to measure the heating surface temperatures (T_{hs}). Other thermocouples were mechanically attached with binding wire and thermal paste to measure the surface temperatures. Ambient temperature (T_{amb}) and insulation surface temperatures (T_{ins}) were measured by other thermocouple probes as shown. Ambient temperature was not controlled and varied by about $\pm$ 1.0^{o}C. All thermocouple readings were recorded on a Graphtec multi-point millivolt recorder.

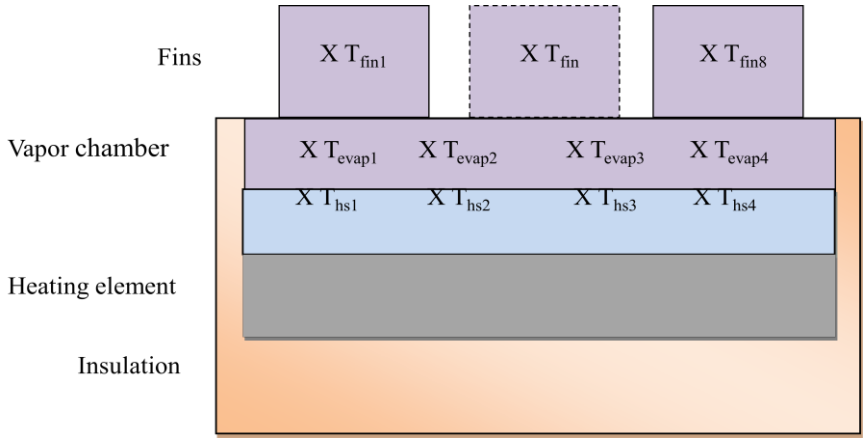

Figure 9: Schematic diagram showing the locations of thermocouples

4.2 Experimental Procedure

Experiments were carried out to determine the thermal resistance across the VC (R_{VC}) and the thermal resistance of the multi hollow fins heat sink (R_{fin}) under natural convection with low and high power. The experiments were conducted by using the same VC but with different fill ratio of water, which is fill ratio 1.0 and 0.5.

1. VC was filled with 100% of distilled water using syringe with needle.
2. VC was vacuumed for 1 hour using vacuum pump to ensure it is kept in vacuum condition.
3. VC was left inside the lab for a day to ensure that no leakage occurs.
4. VC is being insulated using insulation wool to minimize the heat loss to the surrounding during the experiment.
5. Data logger was switched on to check the initial temperature of all the thermocouples (T1-T20).
6. Voltage regulator was being switched on to provide power input of 10W to the heating element attached to the VC.
7. The voltage input, current input, actual power input and initial pressure were recorded.
8. The apparatus was left under natural convection for 2.5 hours.
9. After 2.5 hour, the thermocouples' temperature shown in the data logger was recorded (T1-T20).
10. The thermal resistance of VC (R_{VC}) and the thermal resistance of the multi hollow fins heat sink (R_{fin}) were calculated.
11. Steps 6 to 10 were repeated with power input of 20W.
12. Steps 1 to 11 were repeated by using fill ratio of 0.5.
13. Steps 1 to 12 were repeated by using VC #2.

Experiments were carried out to determine the thermal resistance across the VC (R_{VC}), and the thermal resistance of the multi hollow fins heat sink (R_{cond}) under forced convection with low and high power. The experiments were conducted by using the same VC but with different fill ratio of water, which is fill ratio 1.0 and 0.5.

1. VC was filled with 100% of distilled water using syringe with needle.
2. VC was vacuumed for 1 hour using vacuum pump to ensure it is kept in vacuum condition.
3. VC was left inside the lab for a day to ensure that no leakage occurs.
4. VC is being insulated using insulation wool to minimize the heat loss to the surrounding during the experiment.
5. Data logger was switched on to check the initial temperature of all the thermocouples (T1-T20).
6. Voltage regulator was being switched on to provide power input of 10W to the heating element attached to the VC.
7. A fan was positioned with an angle of 10^{o} to the plane to maximize the efficiency of heat transfer process.
8. The voltage input, current input, actual power input and initial pressure were recorded.
9. The apparatus was left under forced convection for 2 hours.
10. After 2 hour, the thermocouples' temperature shown in the data logger was recorded (T1-T20).
11. The thermal resistance of VC (R_{VC}) and the thermal resistance of the multi hollow fins heat sink (R_{fin}) were calculated.
12. Steps 6 to 11 were repeated with power input of 20W.
13. Steps 1 to 12 were repeated by using fill ratio of 0.5.
14. Steps 1 to 13 were repeated by using VC #2.

4.3 Experimental Results

Experiments were performed with power inputs (P_{EHs}) of 10 and 20 W under both natural convection (NC) and forced convection (FC) air cooling modes. At each power setting, temperatures were recorded until steady state was reached. Experiments were repeated three times to determine repeatability of results. Results were found to be repeatable to be better than $\pm$ 1.0^{o}C. A summary of the experimental runs conducted and the operating conditions are tabulated in Table 1. Mean average evaporator (T_{evap}), fin (T_{fin}) and heating surface (T_{hs}) temperatures are shown in Table 3. Insulation surface temperature (T_{ins}) varied from 20 - 27^{o}C, depending upon cooling modes and power input.The summary of the results is tabulated in Table 4. The graphs were plotted on the temperature and resistance distribution to show the effect of input power, natural and forced convection and fill ratio of water for both VC. Besides, we plotted graphs which compare the thermal performance of both VC to determine which to choose

There are a total of 42 graphs for this experimental investigation.

Figure 10: Transient Temperature of T_{fin} for VC#1 under NC and FR=1.0 (Runs#1&2)
Figure 11: Transient Temperature of T_{evap} for VC#1 under NC and FR=1.0 (Runs#1&2)
Figure 12: Transient Temperature of T_{hs} for VC#1 under NC and FR=1.0 (Runs#1&2)
Figure 13: Transient Temperature of T_{fin} for VC#1 under FC and FR=1.0 (Runs #3&4)
Figure 14: Transient Temperature of T_{evap} for VC#1 under FC and FR=1.0 (Runs#3&4)
Figure 15: Transient Temperature of T_{hs} for VC#1under FC and FR = 1.0 (Runs#3&4)
Figure 16: Transient Temperature of T_{fin} for VC#1 under NC and FR=0.5 (Runs#5&6)
Figure 17: Transient Temperature of T_{evap} for VC#1 under NC and FR=0.5 (Runs#5&6)
Figure 18: Transient Temperature of T_{hs} for VC#1 under NC and FR=0.5 (Runs#5&6)

Run #	VC	FR	NC/FC	P_{eh}(W)	P_{sat}(psi)	T_{sat}(°c)	T_{amb}(°c)	T_{ins1}(°c)	T_{ins2}(°c)	T_{evap}(°c)	T_{fin}(°c)	T_{hs}(°c)	R_{fin}(K/W)	R_{vc}(K/W)	∑R(K/W)	h_{fin}
1. a	1	1	NC	10	2.5	56.5	22.1	25.3	26.6	69.6	61.6	73.5	4	1.2	5.2	
b							22	24.8	26.2	68.6	60.5	72.6	3.9	1.2	5.1	
c							21.6	23.2	25.2	68.2	60.8	72.5	3.9	1.2	5.1	
Avg							21.9	24.4	26	68.8	61	72.9	3.9	1.2	5.1	26
2. a				20	11	92.1	22.3	26.4	28	106.2	92.5	112.8	3.5	1.0	4.5	
b							22.4	26.3	27.5	105.3	92.6	112	3.5	1.0	4.5	
c							22.2	26	26.7	105.8	93	112.5	3.5	1.0	4.5	
Avg							22.2	26.2	27.4	105.8	92.7	112.4	3.5	1.0	4.5	29
3.			FC	10	0.5	26.4	21.3	21.5	23.4	36.8	29.7	40.6	0.8	1.1	1.9	127
4.				20	1	38.7	21.3	21.9	24.7	49.8	37.8	57.3	0.8	1.0	1.8	127
5.		0.5	NC	10	2	52.2	21.9	24.1	25	65.8	58.4	69.6	3.7	1.1	4.8	27
6.				20	10	89.5	22	25.6	27.7	98.4	85.1	105.5	3.2	1.0	4.3	32
7.			FC	10	0.5	26.4	21.4	22.4	24.3	42.9	35.3	46	1.4	1.1	2.5	73
8.				20	1	38.7	21.9	23.4	24.9	62.5	49.9	70.7	1.4	1.0	2.4	73
9. a	2	1	NC	10	2.2	54.2	19.5	20.7	23.6	65.3	61	69.7	4.2	0.9	5.1	
b							19.4	20.8	23.5	64.2	60.8	69.6	4.1	0.9	5	
c							21	22.9	24.4	66.2	62.6	70.9	4.2	0.8	5	
Avg							20	21.5	23.8	65.2	61.5	70	4.2	0.9	5.1	30
10. a				20	9.5	88.2	19.6	21.7	26.6	108.4	99.2	114.8	4	0.8	4.8	
b							19.4	21.8	26.5	108.1	98.4	114.7	3.9	0.8	4.8	
c							21	22.9	27.4	107.9	99.2	115.2	3.9	0.8	4.7	
Avg							20	22.1	26.8	108	98.9	114.9	3.9	0.8	4.7	32
11.			FC	10	0.5	26.4	20.2	20	21.7	35.7	30.9	39.7	1.1	0.9	2	114
12.				20	1	38.7	20.8	21.4	22.9	53.9	42	61.1	1.1	0.9	2	114
13.		0.5	NC	10	2	52.2	22.6	23.6	25.2	64.4	61.4	69.4	3.9	0.8	4.7	33
14.				20	9	86.8	22.2	23.2	26.8	104.9	96.1	112.9	3.7	0.8	4.5	34
15.			FC	10	0.5	26.4	20.5	20	23.4	36.3	29.9	42	0.9	1.2	2.1	140
16.				20	1	38.7	20.5	20	23.7	53.2	40.7	63.9	1.0	1.1	2.1	126
13(2)			NC	10	2	52.2	22.4	23.4	25.1	67.2	61.5/63.4*	71.8	3.9/4.1*	1/0.8*	4.9/4.9*	32/31*
14(2)				20	9	86.8	22.5	23.3	25.9	105.3	96.7/99.8*	113.4	3.7/3.9*	0.8/0.7*	4.5/4.6*	34/32*

Table 3: Experimental Results

Run#	VC#	FR	NC/FC	P_{EH}(W)	T_{amb}(°c)	T_{ins1}(°c)	T_{ins2}(°c)	T_{fin}(°c)	T_{evap}(°c)	T_{hs}(°c)	R_{fin}(K/W)	R_{VC}(K/W)	∑R(K/W)	h_{fin}
1	1	1	NC	10	21.9	24.4	26	61	68.6	72.9	3.9	1.2	5.1	26
2				20	22.2	26.2	27.4	92.7	105.8	112.4	3.5	1.0	4.5	29
3			FC	10	21.3	21.5	23.4	29.7	36.8	40.6	0.8	1.1	1.9	127
4				20	21.3	21.9	24.7	37.8	49.8	57.3	0.8	1.0	1.8	127
5		0.5	NC	10	21.9	24.1	25	58.4	65.8	69.6	3.7	1.1	4.8	27
6				20	22	25.6	27.7	85.1	98.4	105.5	3.2	1.0	4.3	32
7			FC	10	21.4	22.4	24.3	35.3	42.9	46	1.4	1.1	2.5	73
8				20	21.9	23.4	24.9	49.9	62.5	70.7	1.4	1.0	2.4	73
9	2	1	NC	10	20	21.5	23.8	61.5	65.2	70	4.2	0.9	5.1	30
10				20	20	22.1	26.8	98.9	108	114.9	3.9	0.8	4.7	32
11			FC	10	20.2	20	21.7	30.9	35.7	39.7	1.1	0.9	2	114
12				20	20.8	21.4	22.9	42	53.9	61.1	1.1	0.9	2	114
13		0.5	NC	10	22.6	23.6	25.2	61.4	64.4	69.4	3.9	0.8	4.7	33
14				20	22.2	23.2	26.8	96.1	104.9	112.9	3.7	0.8	4.5	34
15			FC	10	20.5	20	23.4	29.9	36.3	42	0.9	1.2	2.1	140
16				20	20.5	20	23.7	40.7	53.2	63.9	1.0	1.1	2.1	126

Table 4: Summary of the Experimental Results

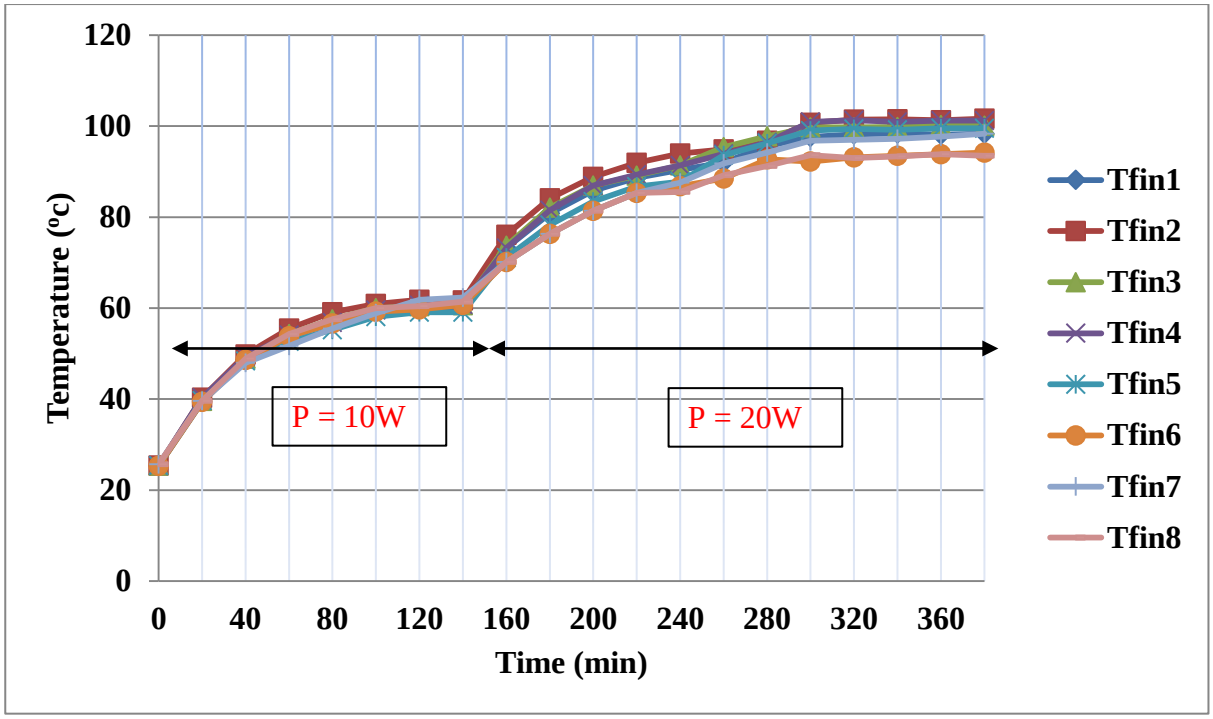

Figure 10: Transient Temperature of T_{fin} for VC#1 under NC and FR = 1.00 (Runs #1 & 2).

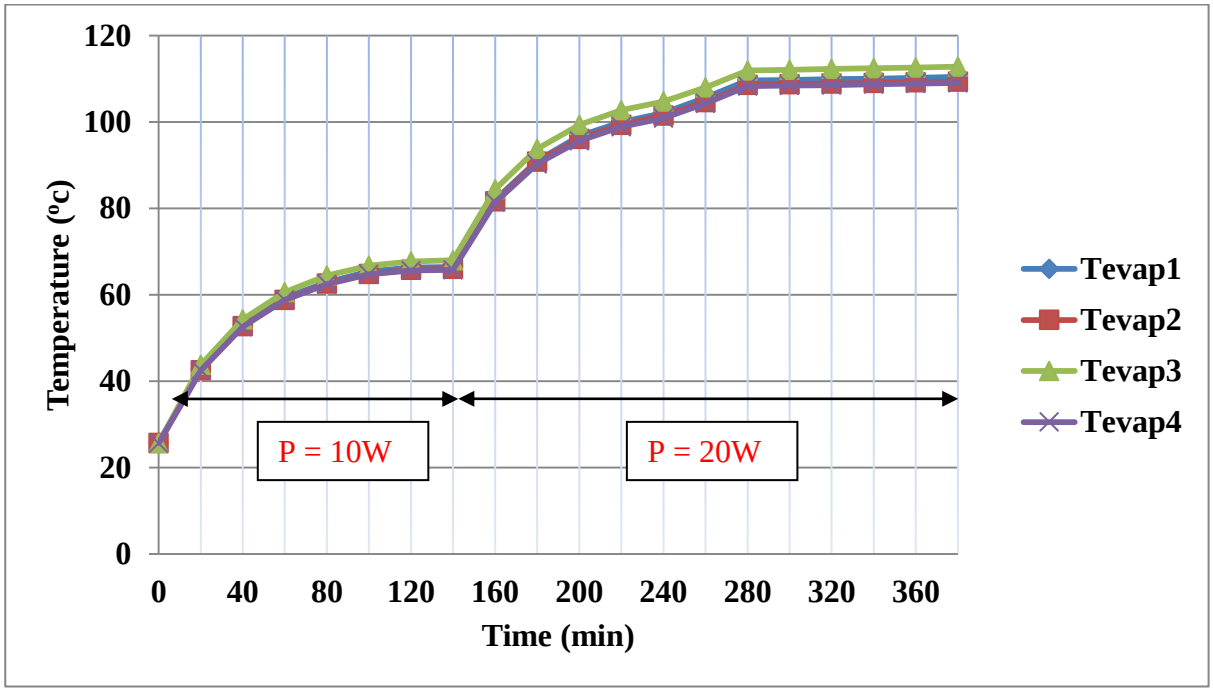

Figure 11: Transient Temperature of T_{evap} for VC#1 under NC and FR=1.0 (Runs #1 & 2).

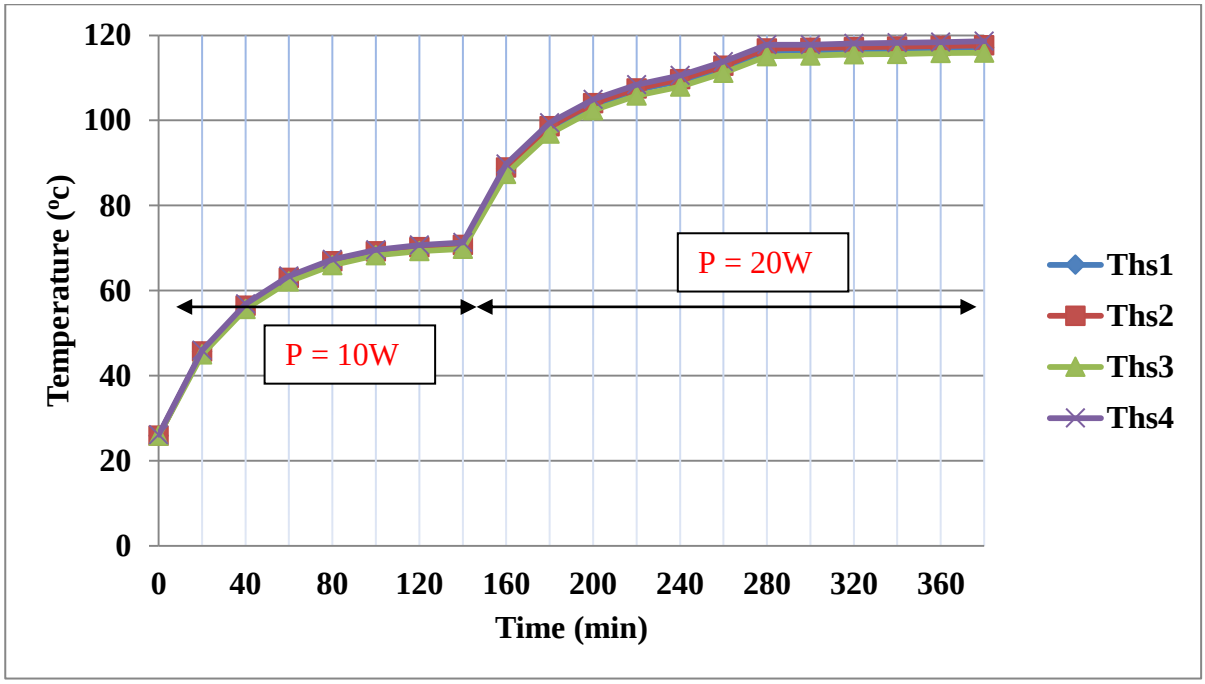

Figure 12: Transient Temperature of T_{hs} for VC#1 under NC and FR=1.0 (Runs #1 & 2).

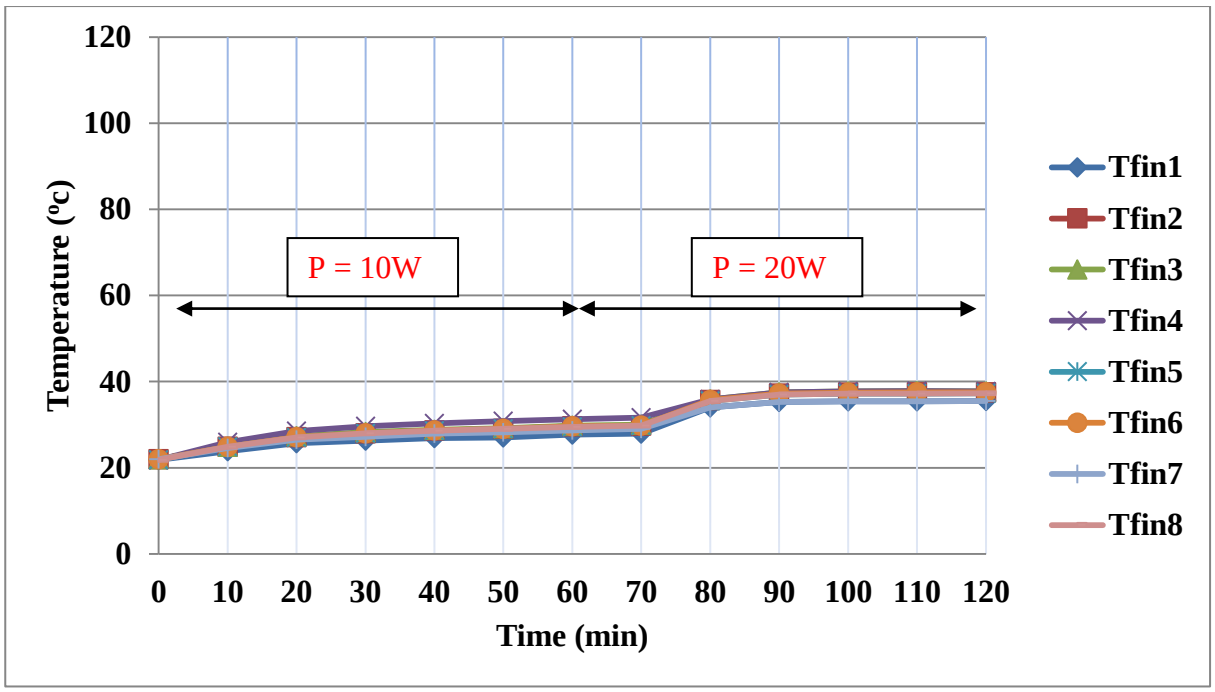

Figure 13: Transient Temperature of T_{fin} for VC#1 under FC and FR = 1.0 (Runs #3 & 4).

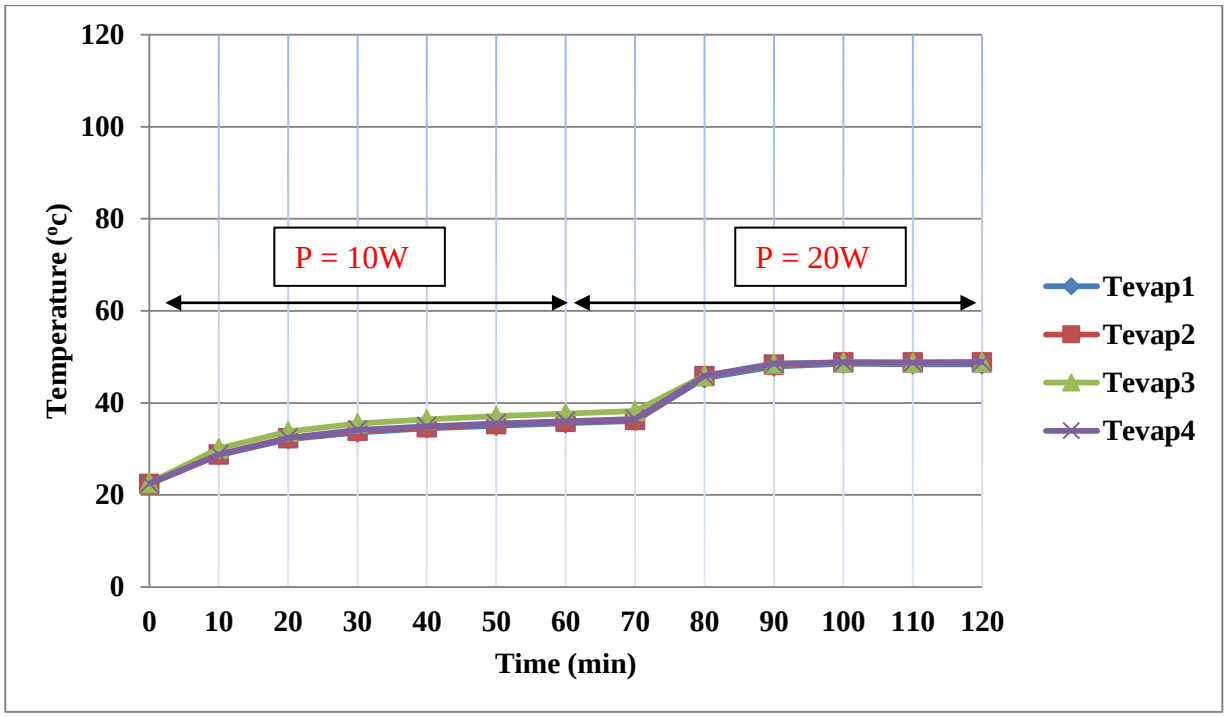

Figure 14: Transient Temperature of T_{evap} for VC#1 under FC and FR=1.0 (Runs #3 & 4).

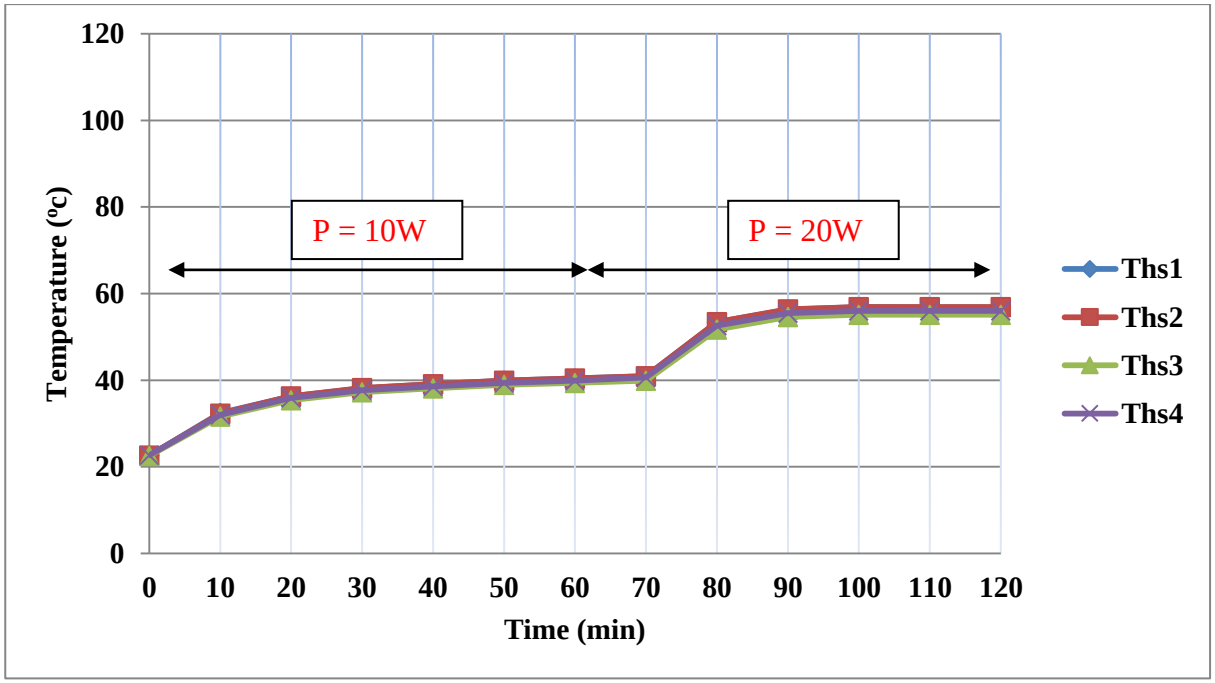

Figure 15: Transient Temperature of T_{hs} for VC#1 under FC and FR=1.0 (Runs #3&4)

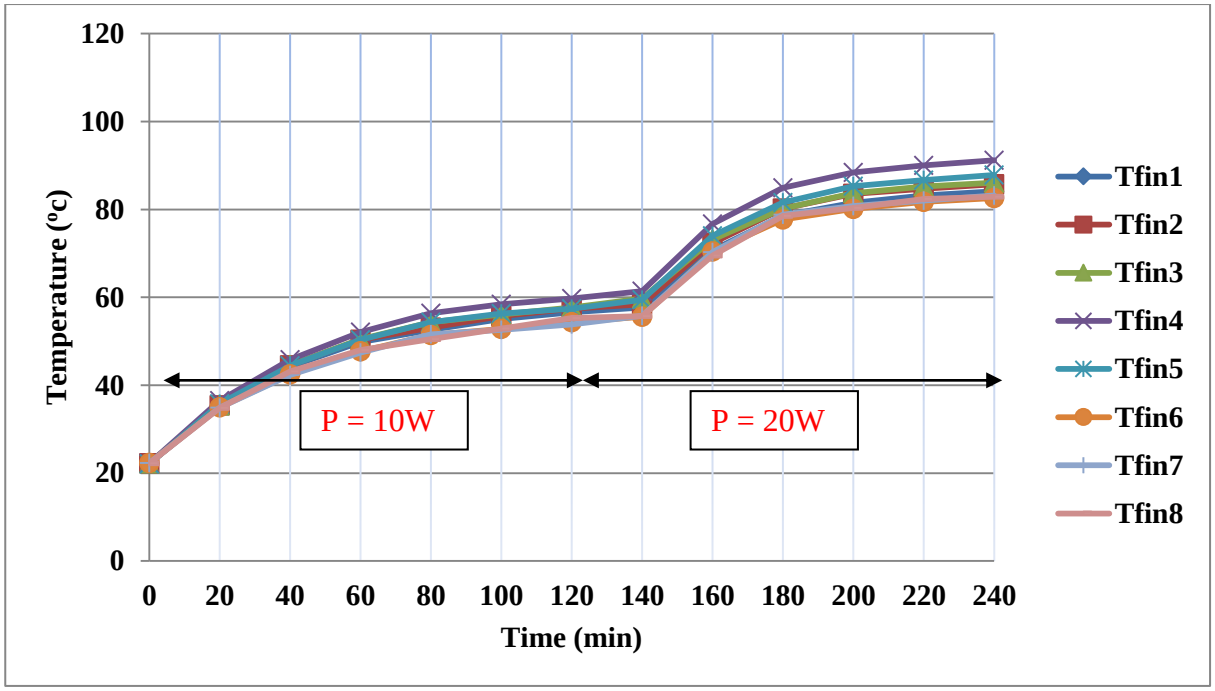

Figure 16: Transient Temperature of T_{fin} for VC#1 under NC and FR=0.5 (Runs#5&6)

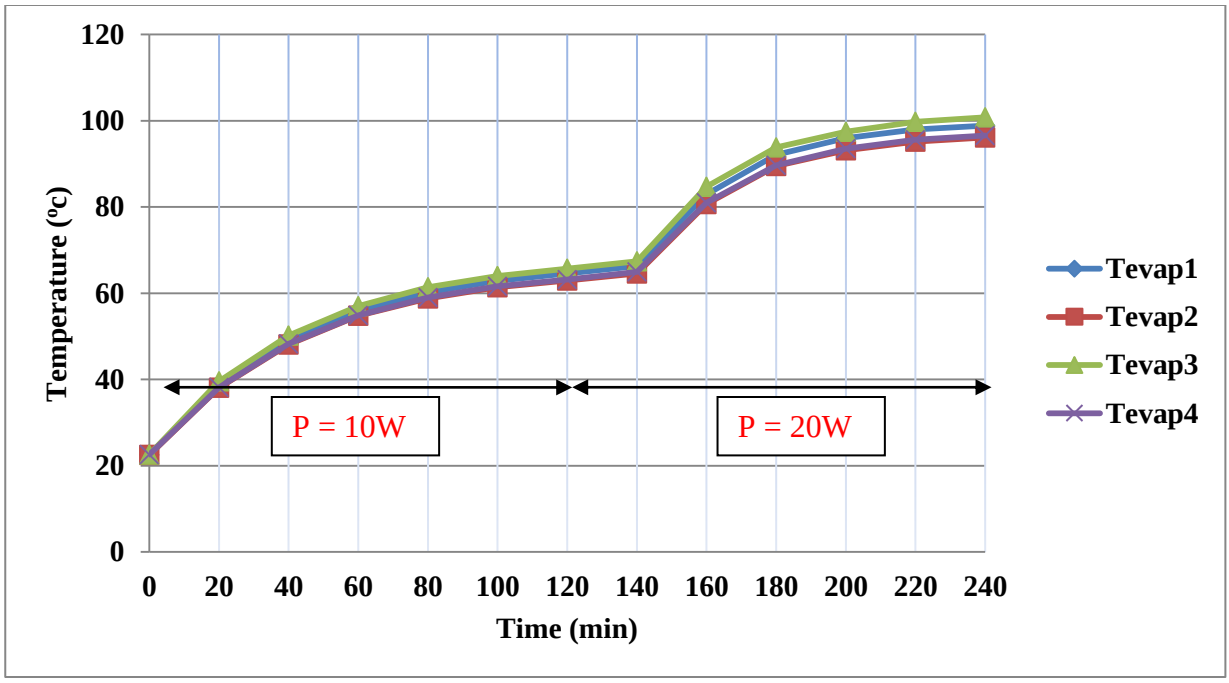

Figure 17: Transient Temperature of T_{evap} for VC#1 under NC and FR=0.5 (Runs #5 & 6).

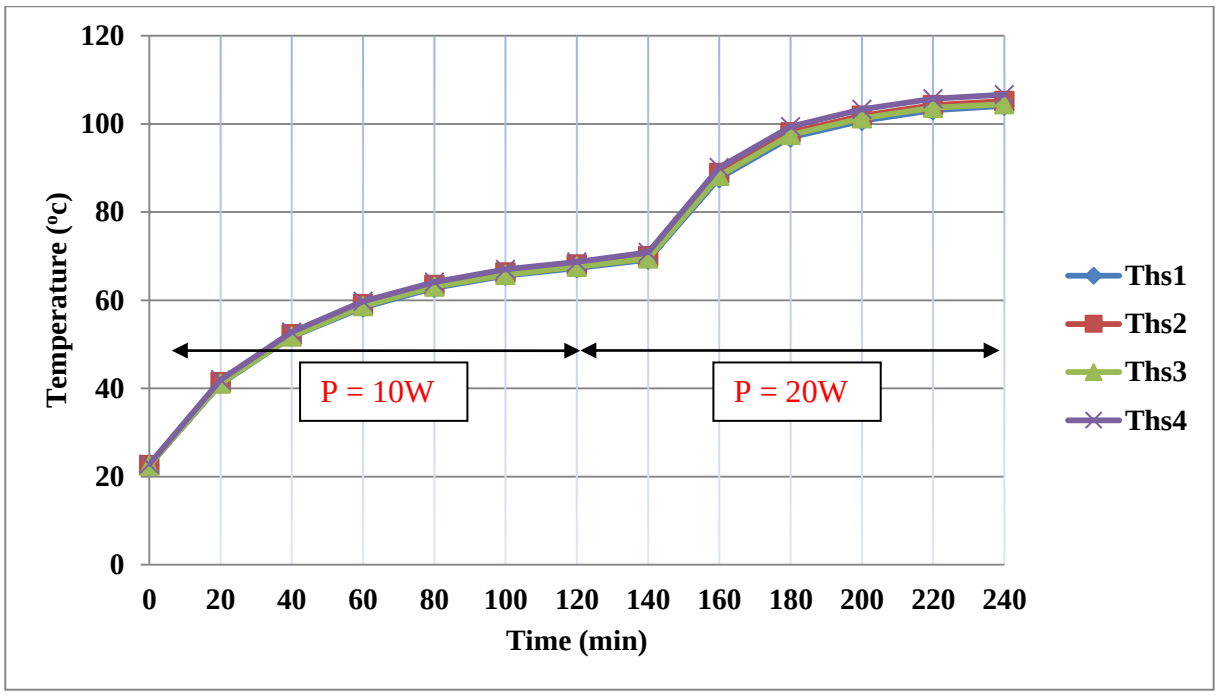

Figure 18: Transient Temperature of T_{hs} for VC#1 under NC and FR=0.5 (Runs #5&6)

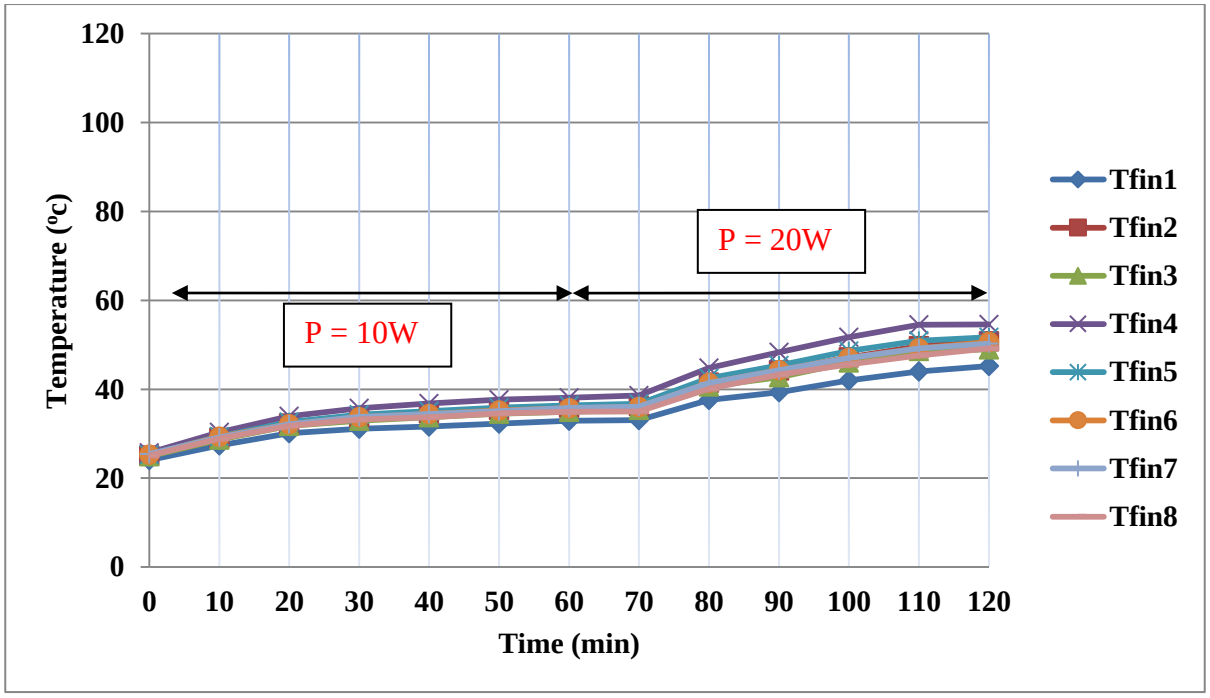

Figure 19: Transient Temperature of T_{fin} for VC#1 under FC and FR = 0.5 (Runs #7 & 8).

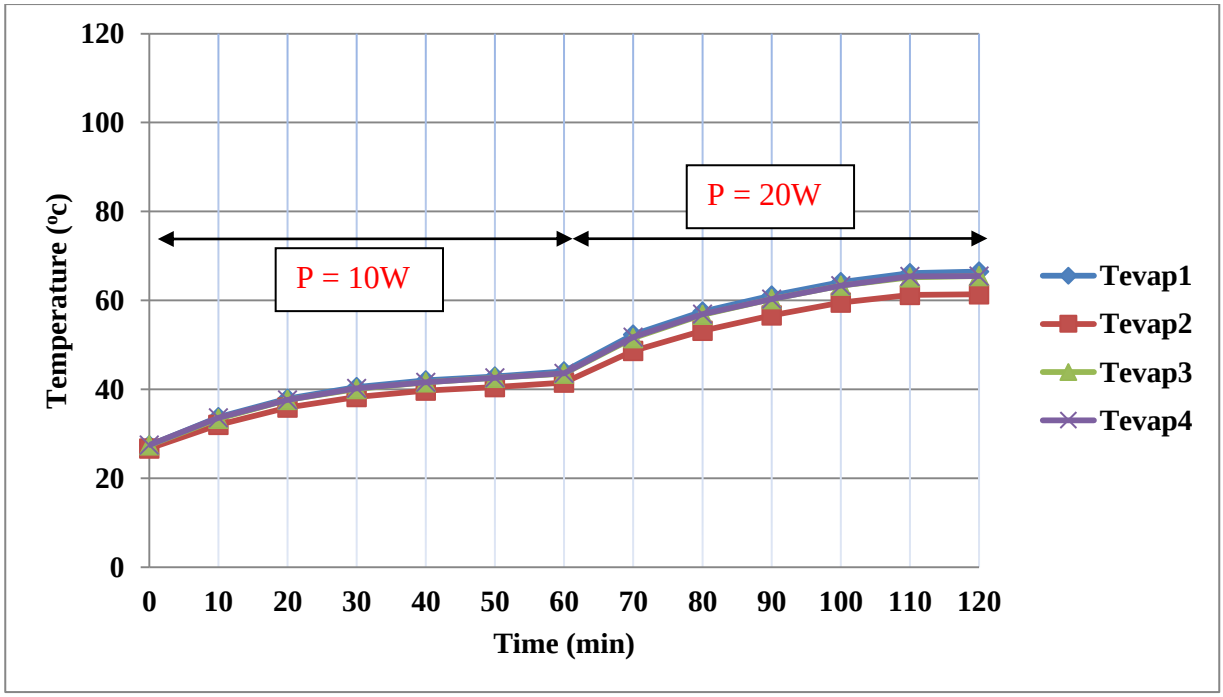

Figure 20: Transient Temperature of T_{evap} for VC#1 under FC and FR=0.5 (Runs #7 & 8).

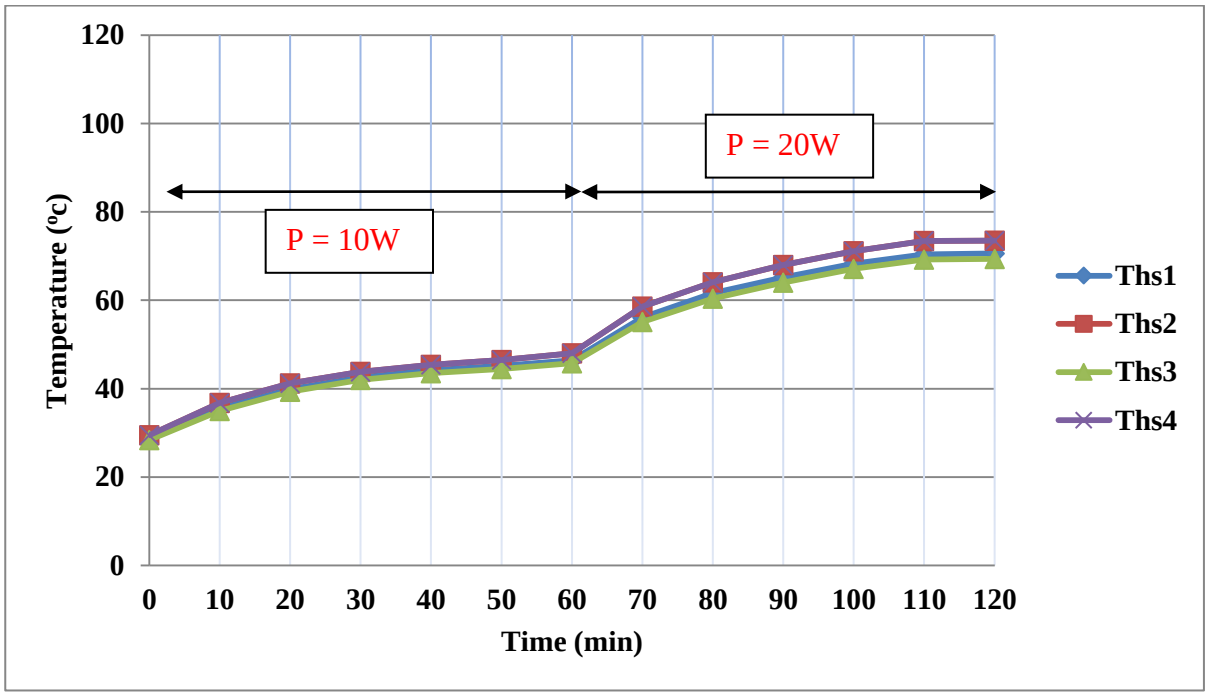

Figure 21: Transient Temperature of T_{hs} for VC#1 under FC and FR =0.5 (Runs #7 & 8).

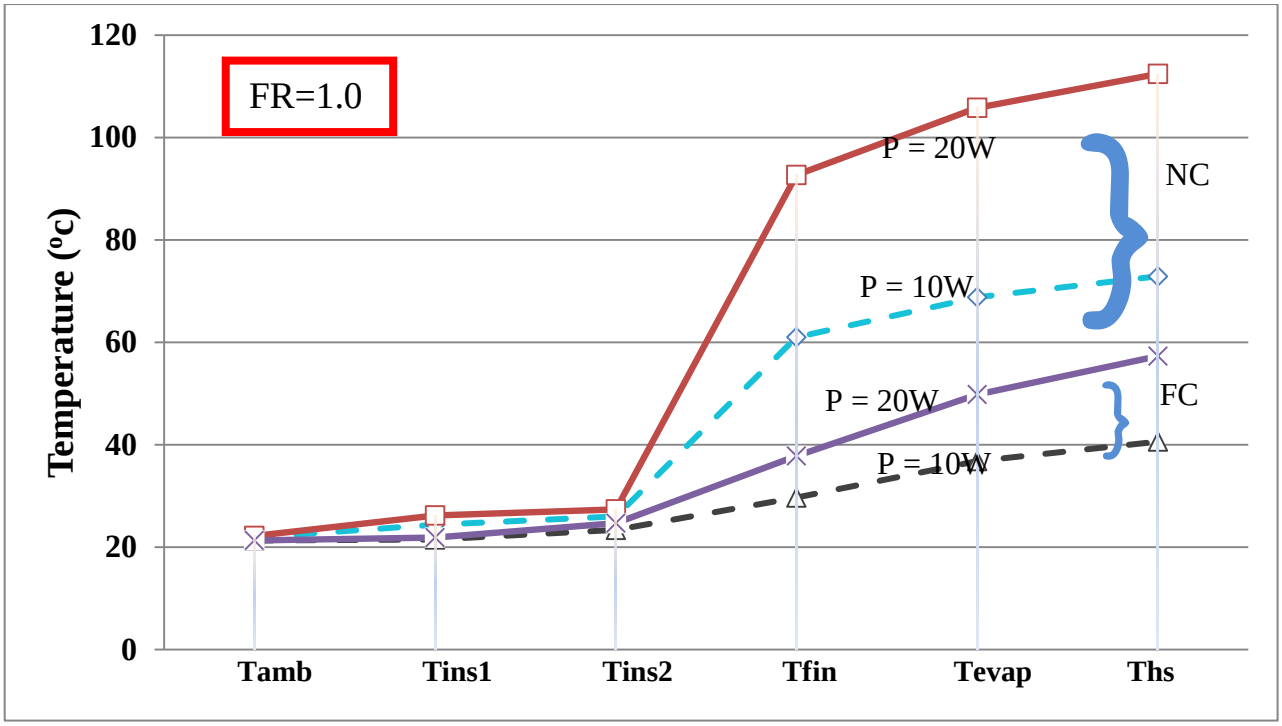

Figure 22: Temperature distribution showing effect of Power Input (P_{EH}) and Convection (NC/FC) for FR = 1.0

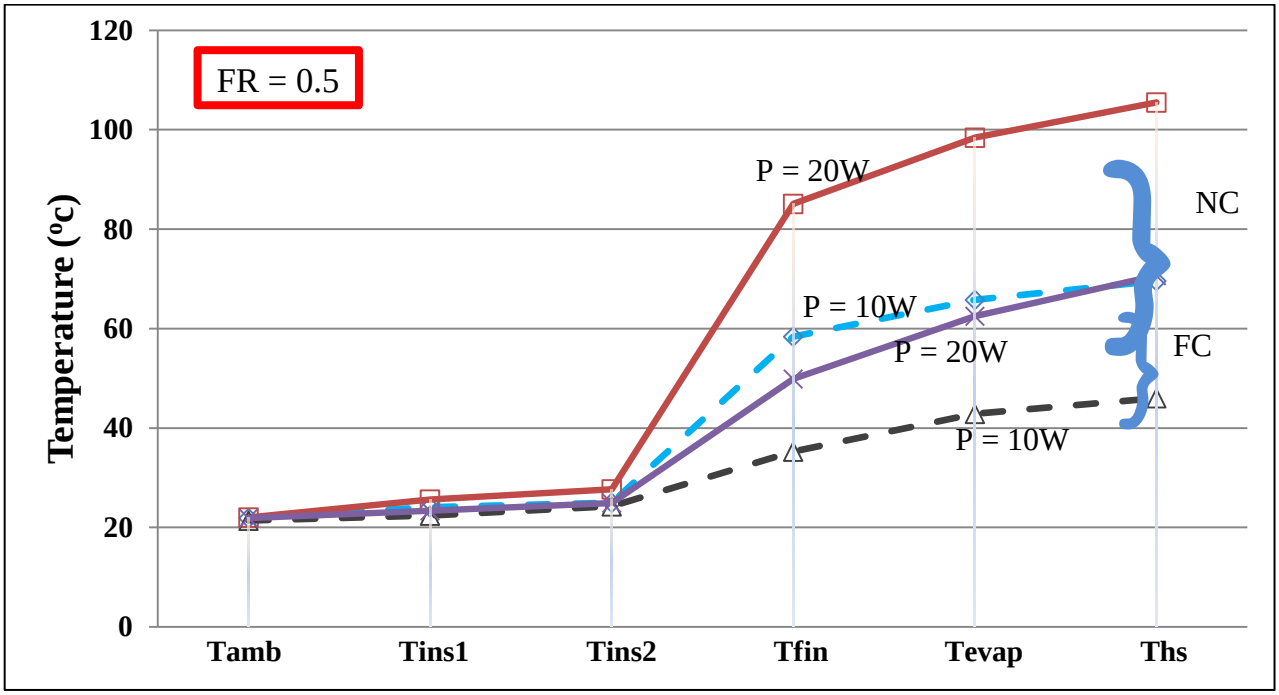

Figure 23: Temperature distribution showing effect of Power Input (P_{EH}) and Convection (NC/FC) for FR = 0.5

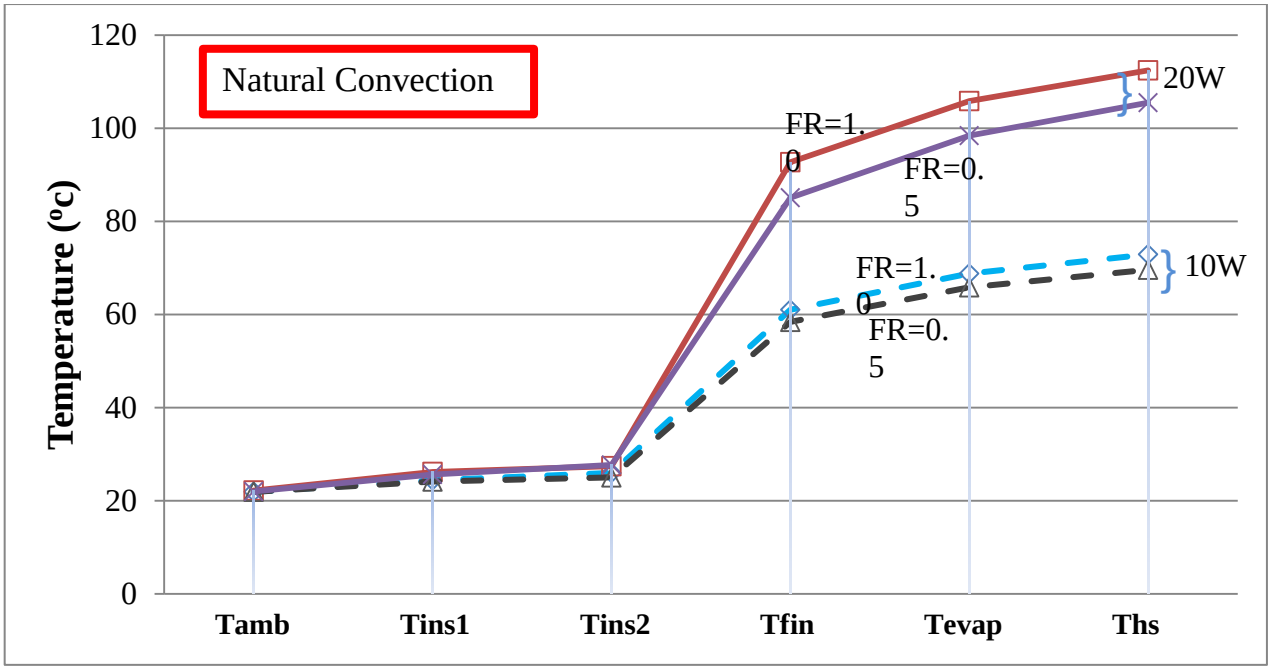

Figure 24: Temperature distribution showing effect of Power Input (P_{EH}) and Fill Ratio (FR) for Natural Convection

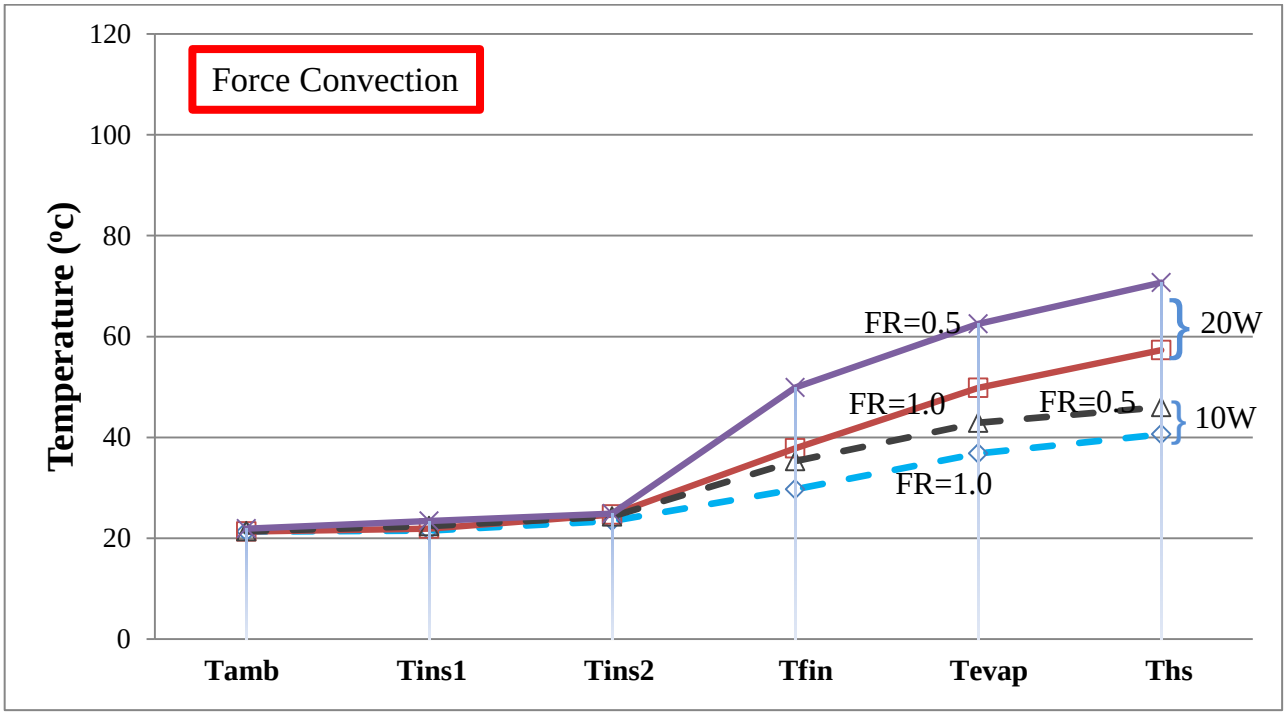

Figure 25: Temperature distribution showing effect of Power Input (P_{EH}) and Fill Ratio (FR) under Force Convection

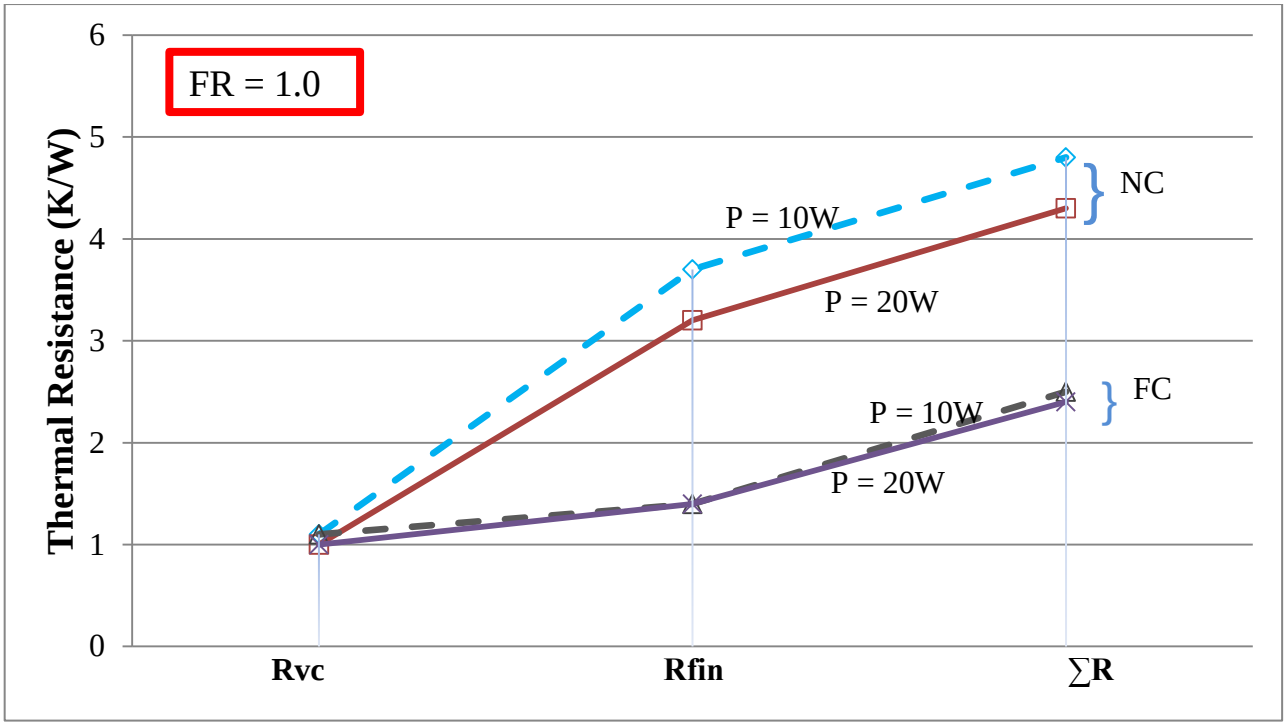

Figure 26: Effect of Power Input (P_{EH}) and Convection (NC/FC) on Thermal Resistance for FR=1.0

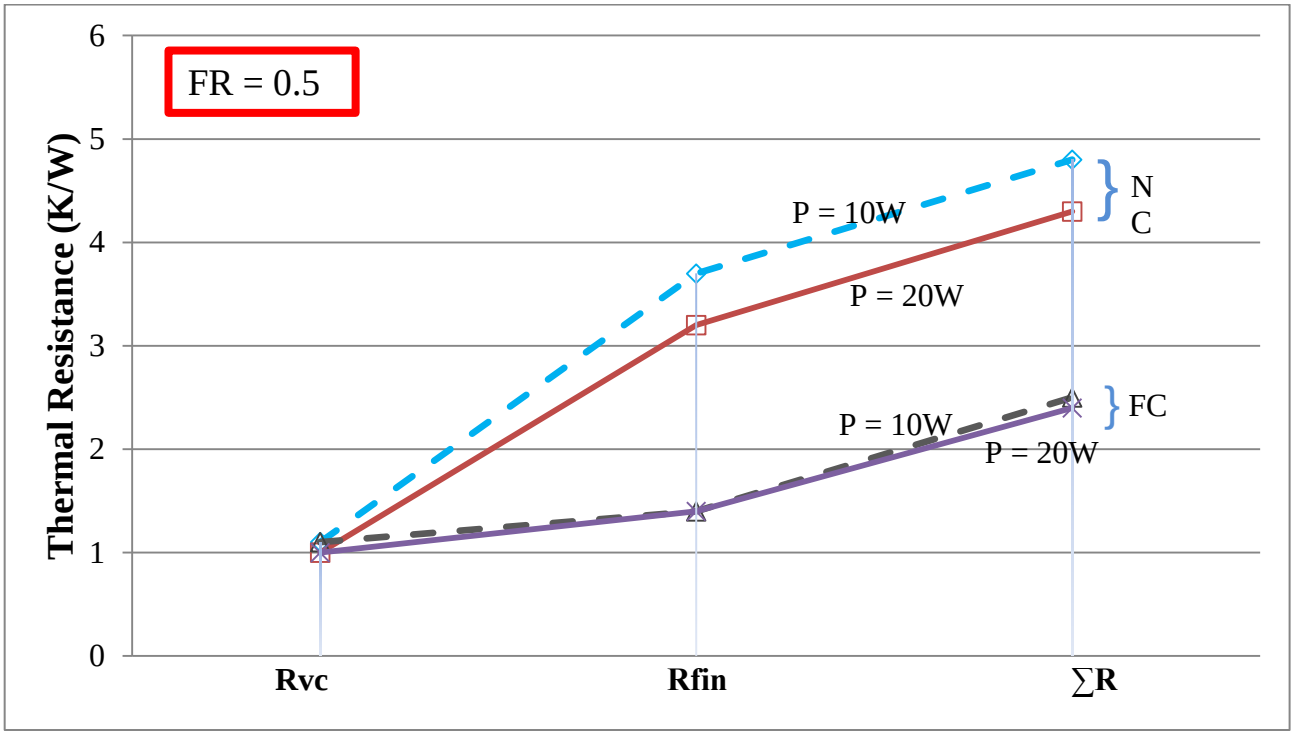

Figure 27: Effect of Power Input (P_{EH}) and Convection (NC/FC) on Thermal Resistance for FR=0.5

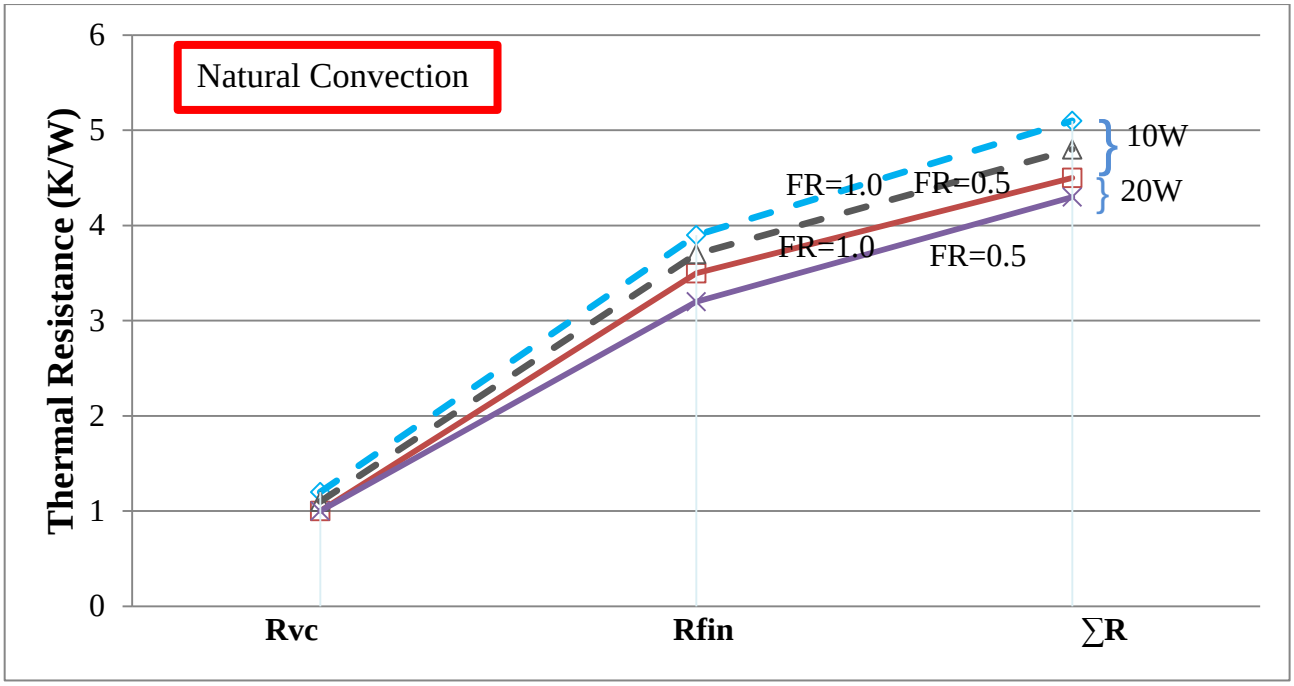

Figure 28: Effect of Power Input (P_{EH}) and Fill Ratio (FR) on Thermal Resistance on NC

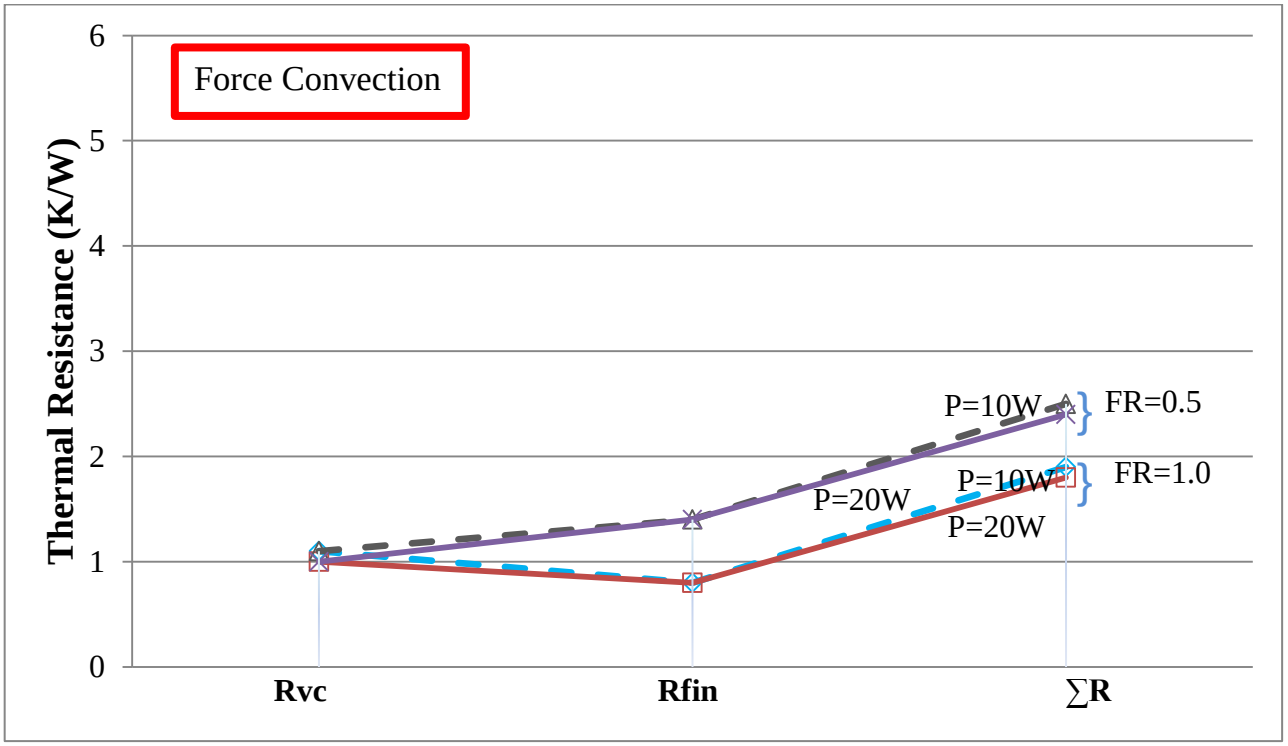

Figure 29: Effect of Power Input (P_{EH}) and Fill Ratio (FR) on Thermal Resistance on FC

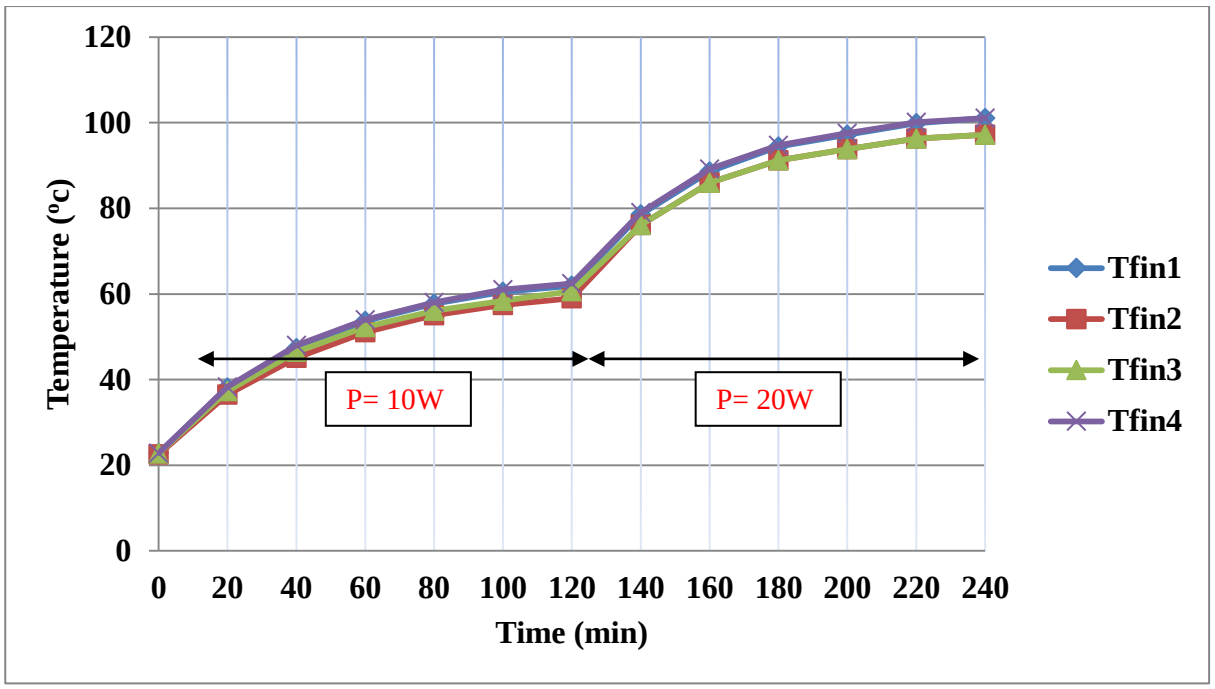

Figure 30: Transient Temperature of T_{fin} for VC#2 under NC and FR =1.0 (Runs #9& 10).

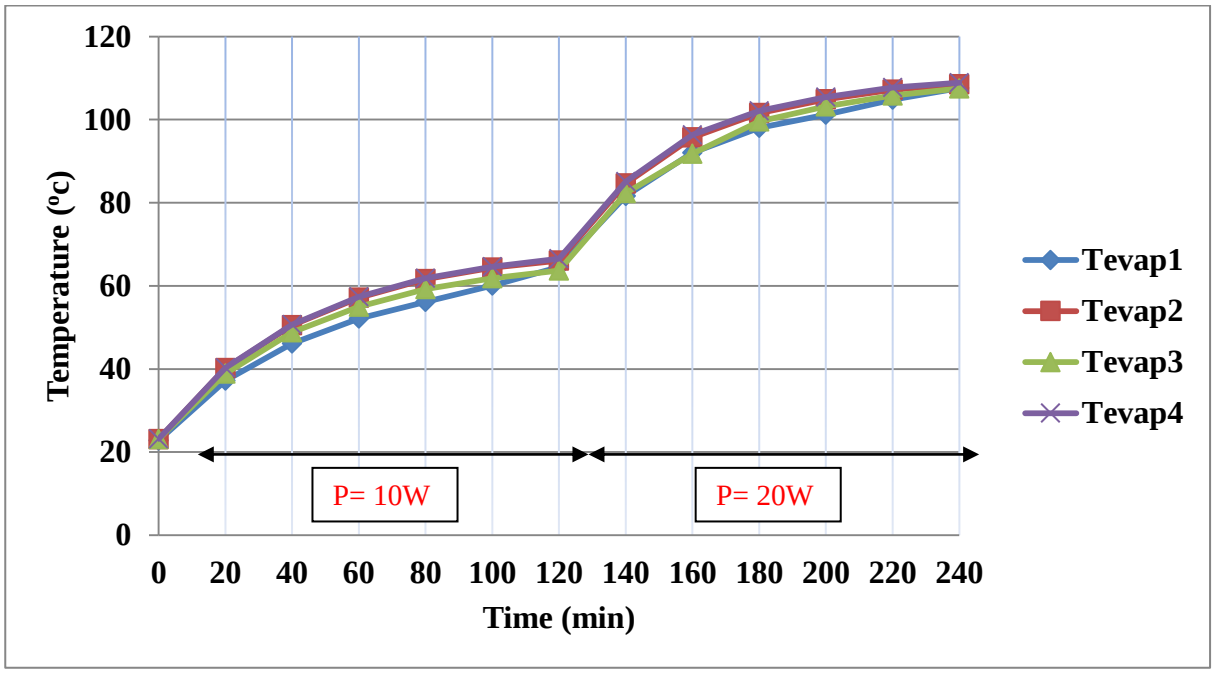

Figure 31: Transient Temperature of T_{evap} for VC#2 under NC and FR=1.0 (Runs #9&10).

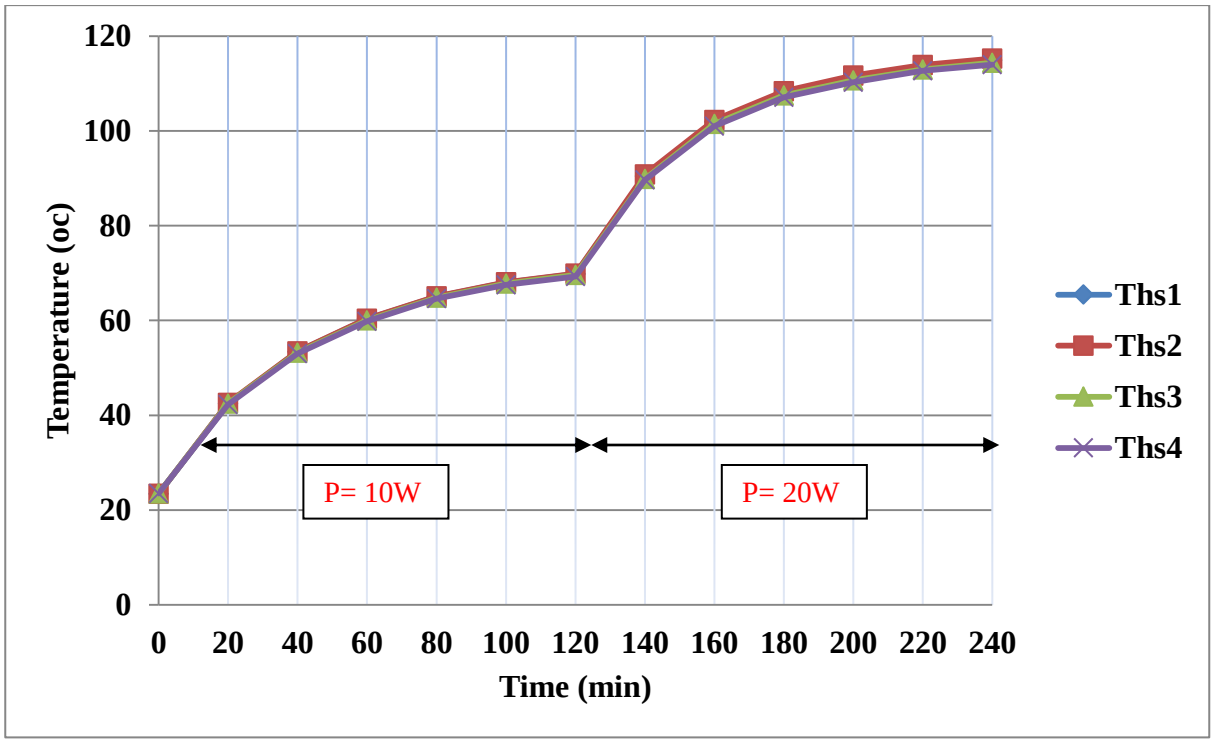

Figure 32: Transient Temperature of T_{hs} for VC#2 under NC and FR = 1.0 (Runs #9&10).

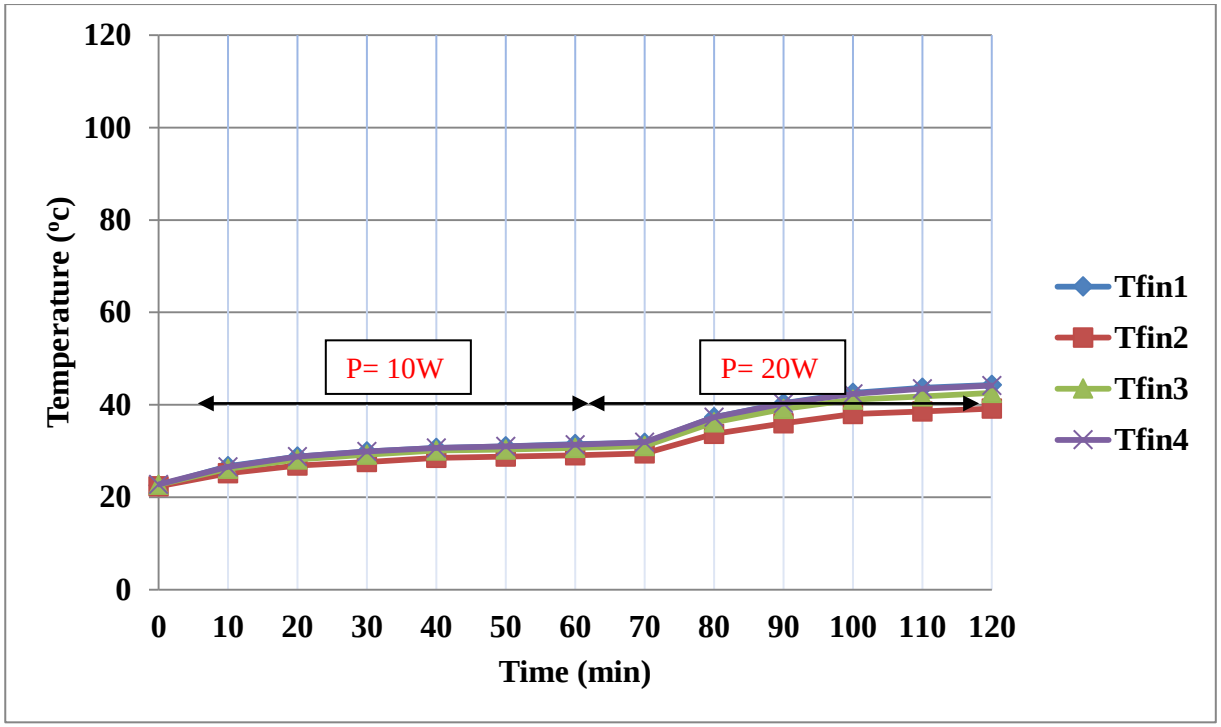

Figure 33: Transient Temperature of T_{fin} for VC#2 under FC and F =1.0 (Runs #11 & 12).

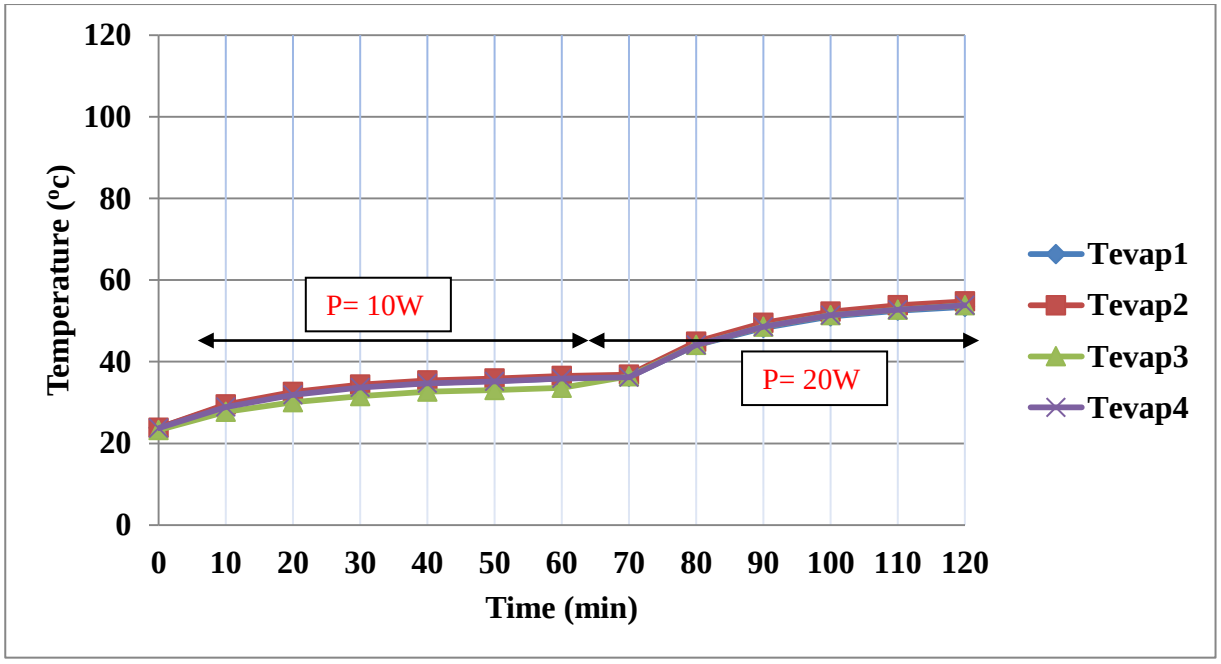

Figure 34: Transient Temperature of $T_{evap}$for VC#2 under FC and FR = 1.0 (Runs #11 & 12).

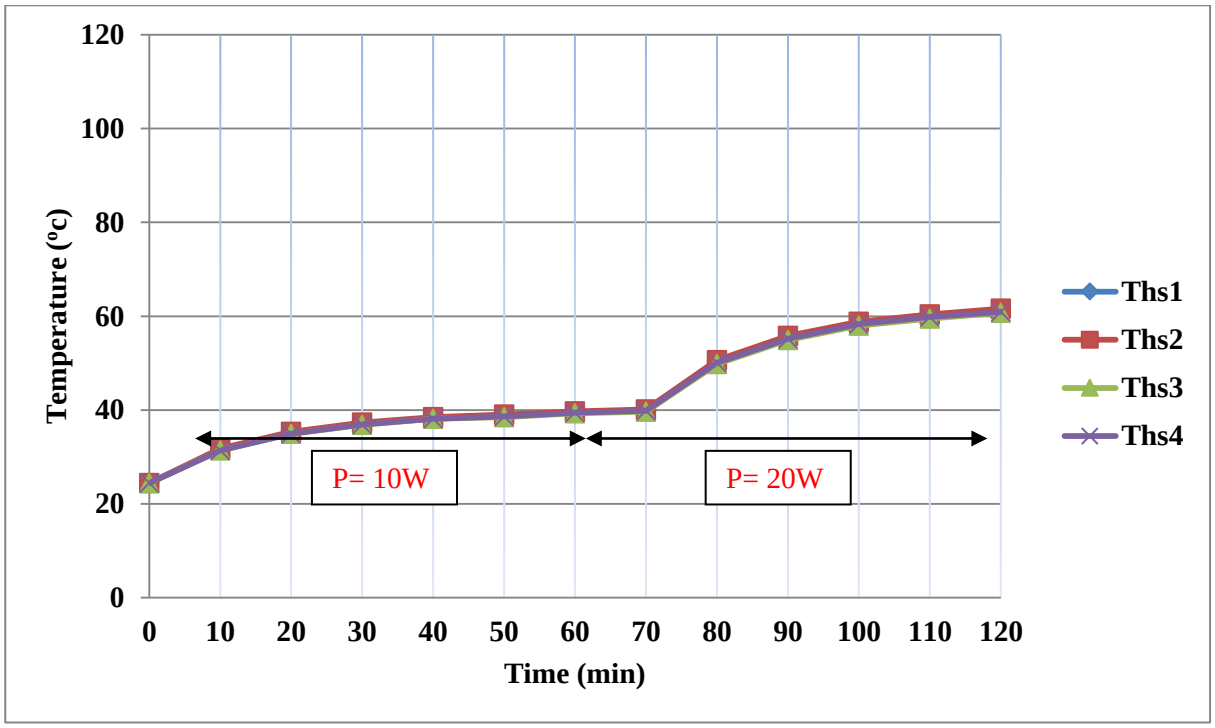

Figure 35: Transient Temperature of T_{hs} for VC#2 under FC and FR=1.0 (Runs #11&12).

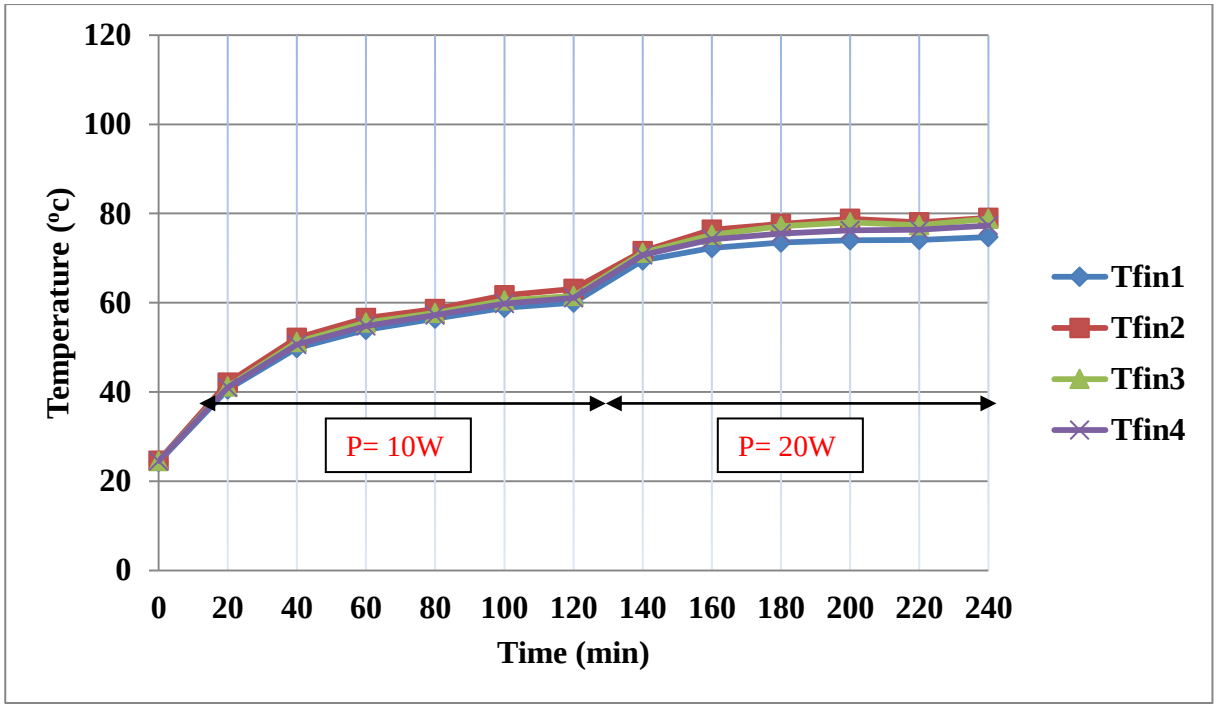

Figure 36: Transient Temperature of T_{fin} for VC#2 under NC and FR=0.5 (Runs #13&14).

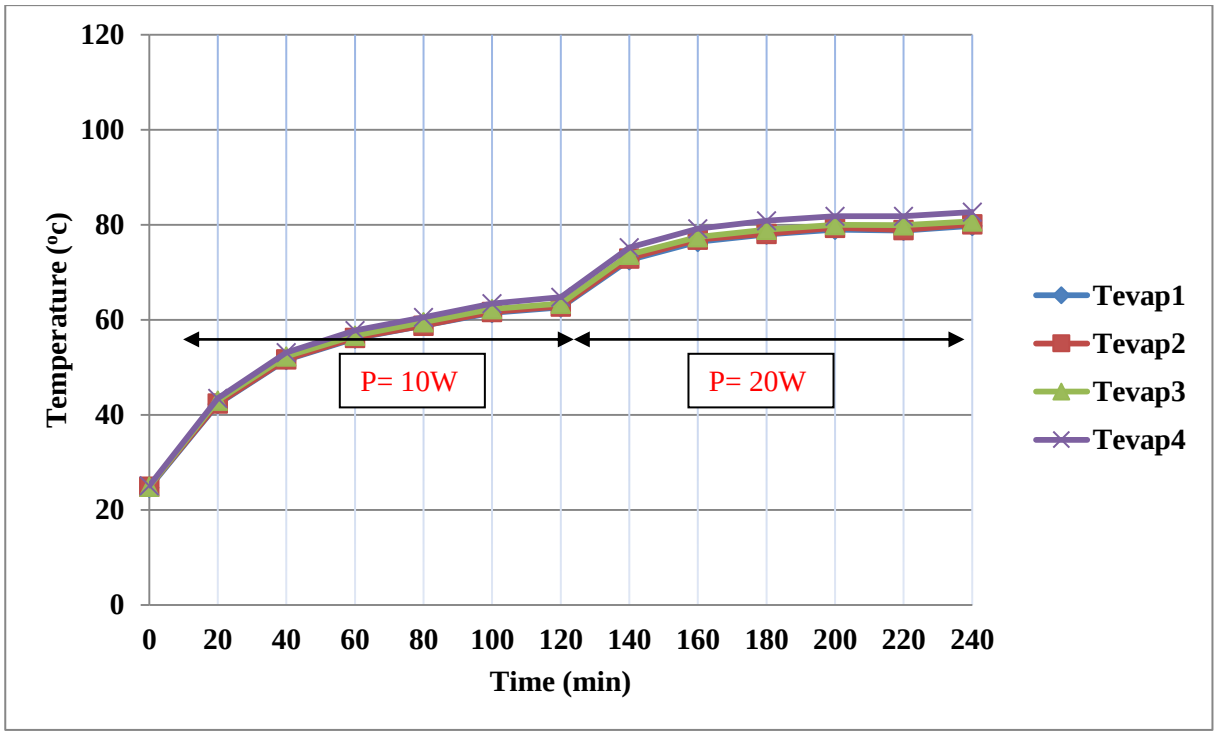

Figure 37: Transient Temperature of T_{evap} for VC#2 under NC and FR=0.5(Runs#13&14)

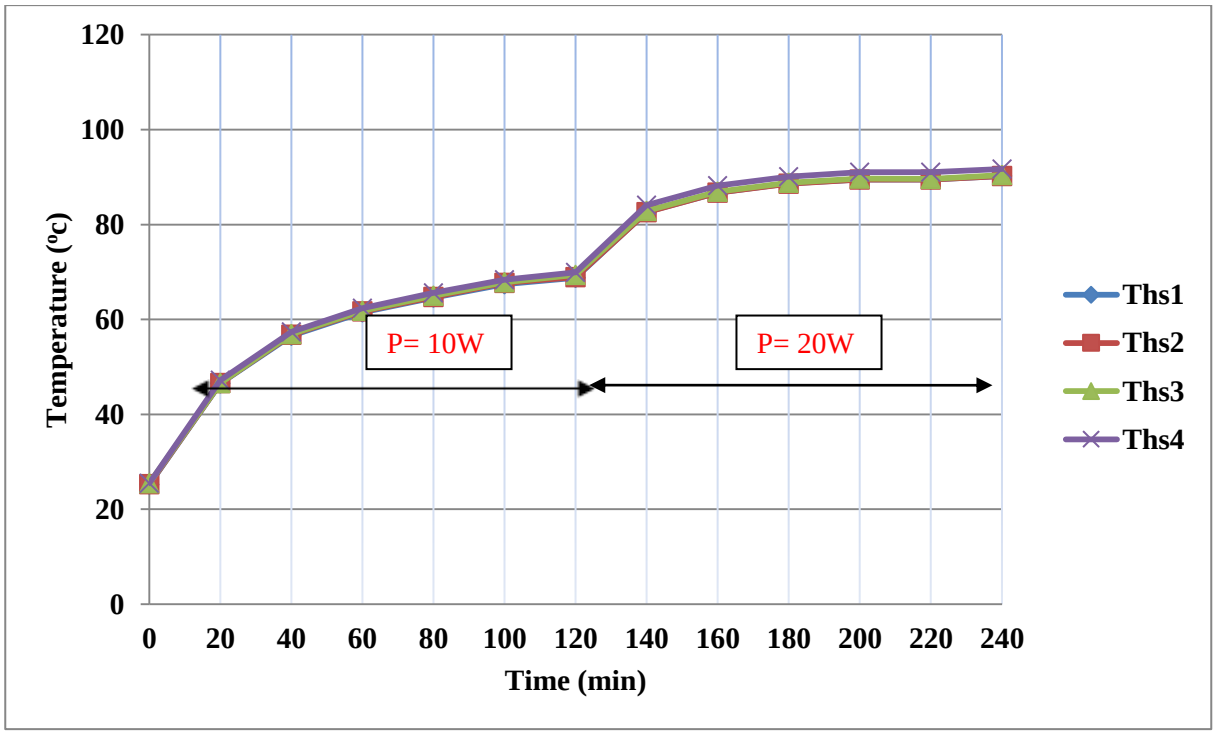

Figure 38: Transient Temperature of T_{hs} for VC#2 under NC and FR=0.5 (Runs #13&14).

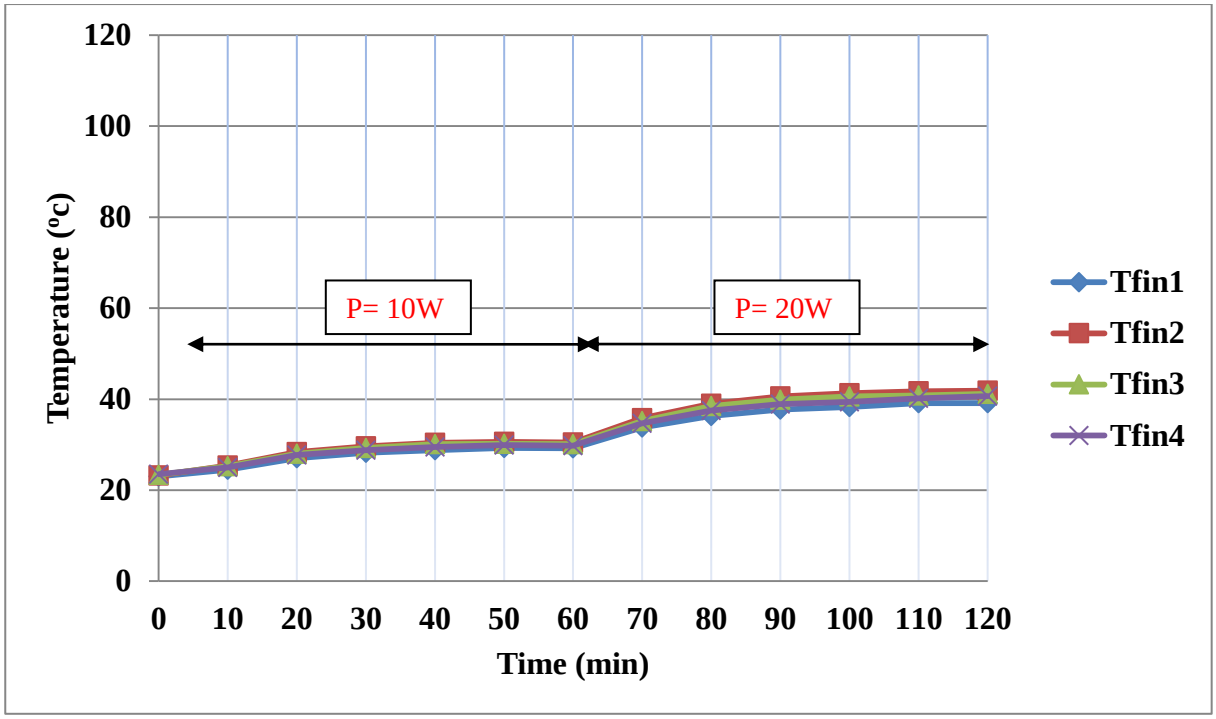

Figure 39: Transient Temperature of T_{fin} for VC#2 under FC and FR=0.5 (Runs #15&16).

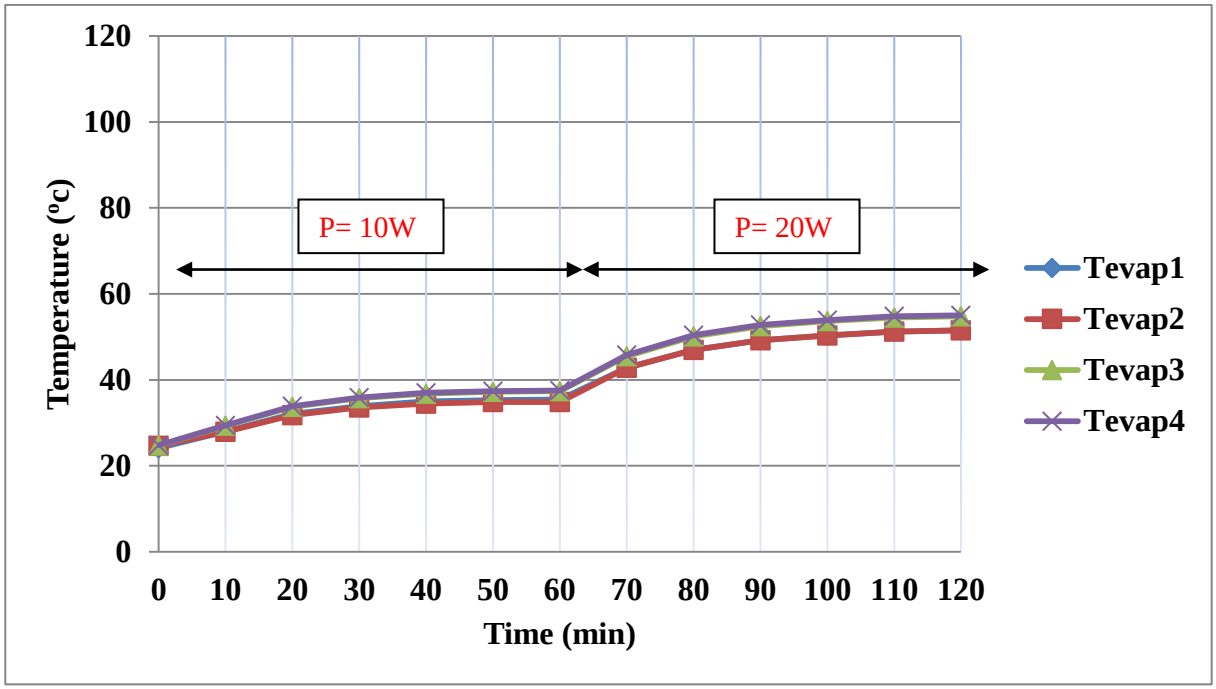

Figure 40: Transient Temperature of $T_{evap}$for VC#2 under FC and FR=0.5 (Runs#15&16).

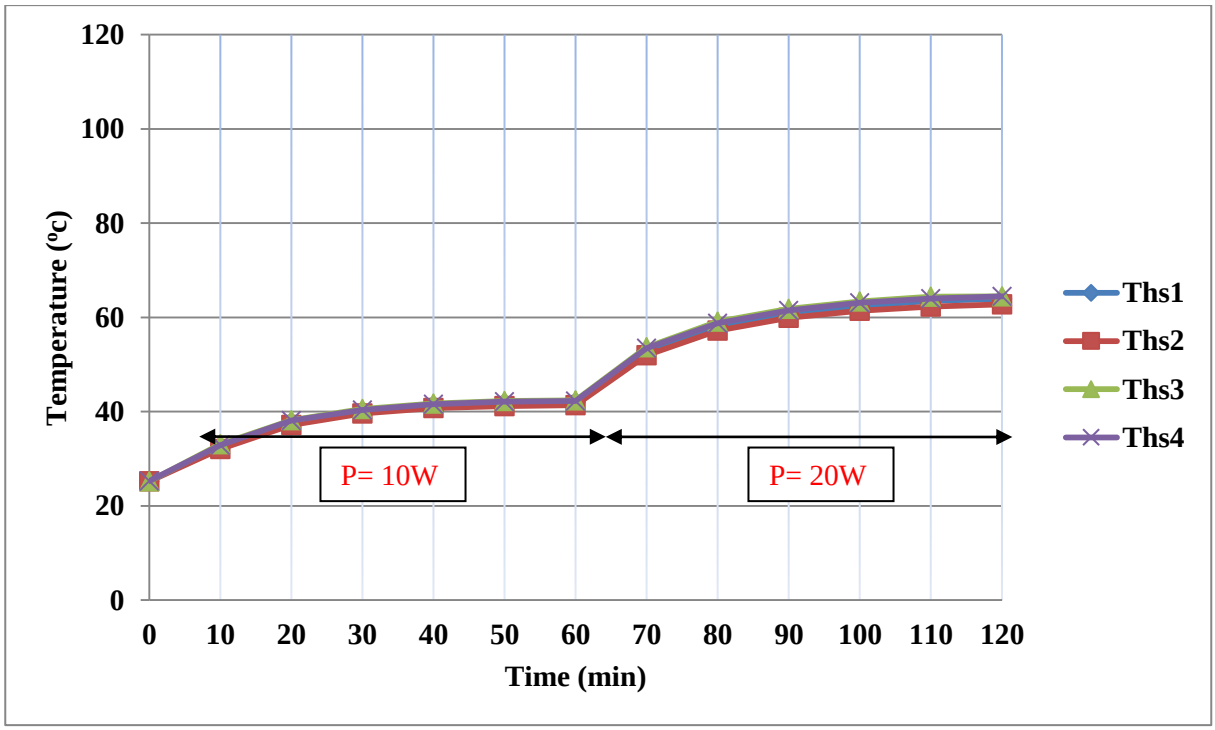

Figure 41: Transient Temperature of T_{hs} for VC#2 under FC and FR=0.5 (Runs #15&16).

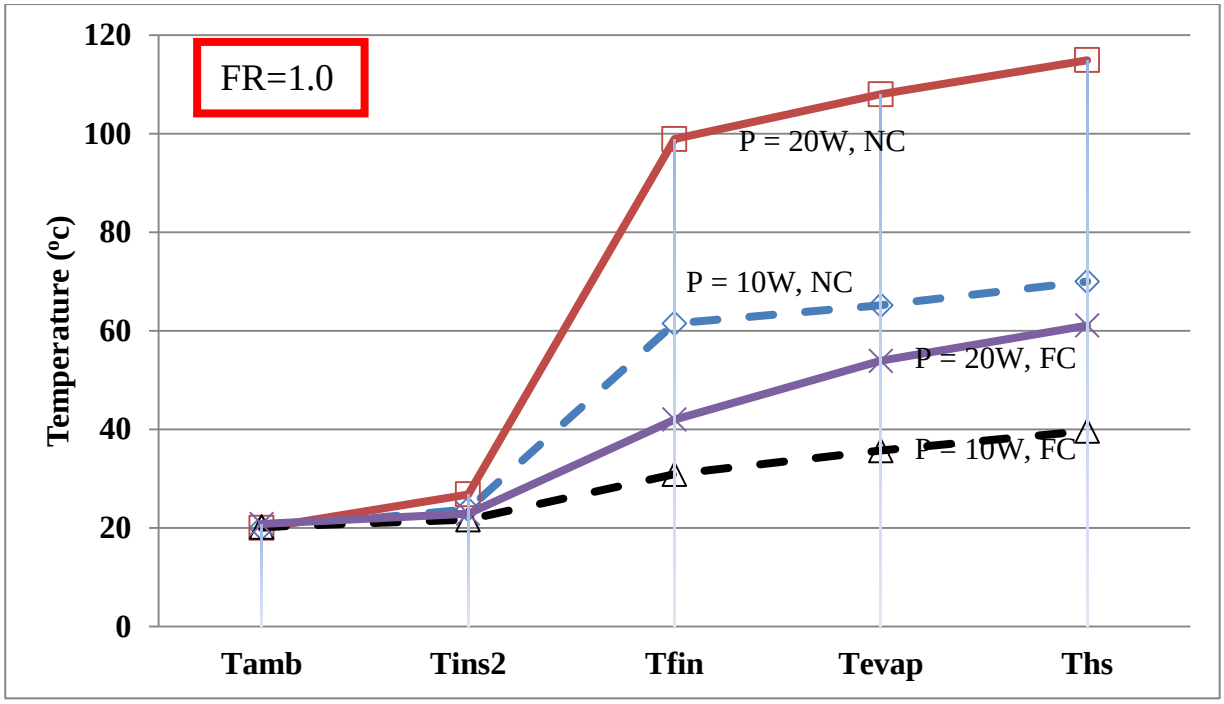

Figure 42: Temperature distribution showing effect of Power Input (P_{EH}) and Convection (NC/FC) for FR = 1.0

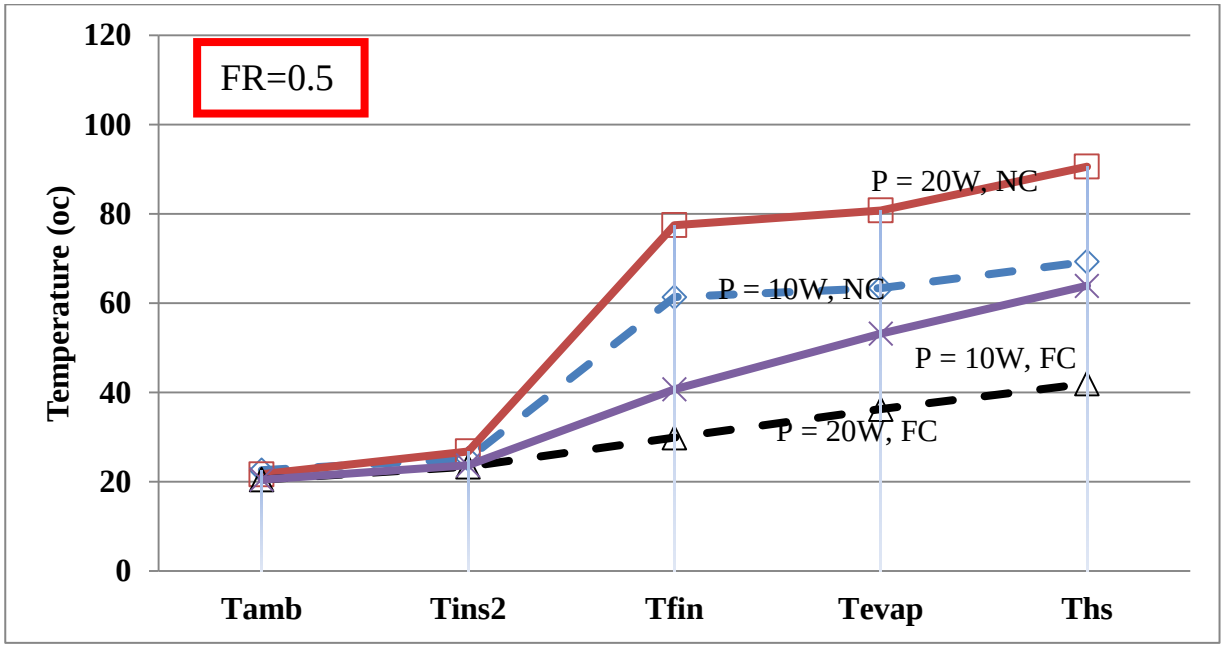

Figure 43: Temperature distribution showing effect of Power Input (P_{EH}) and Convection (NC/FC) for FR = 0.5

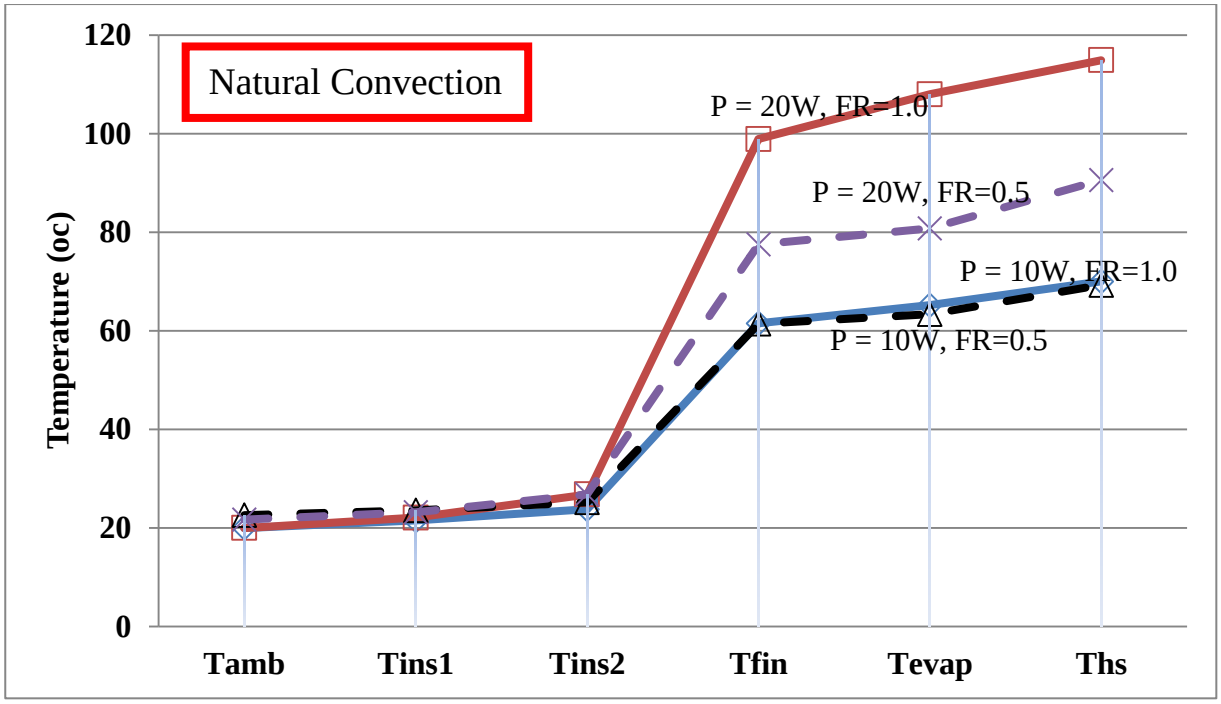

Figure 44: Temperature distribution showing effect of Power Input (P_{EH}) and Fill Ratio for Natural Convection

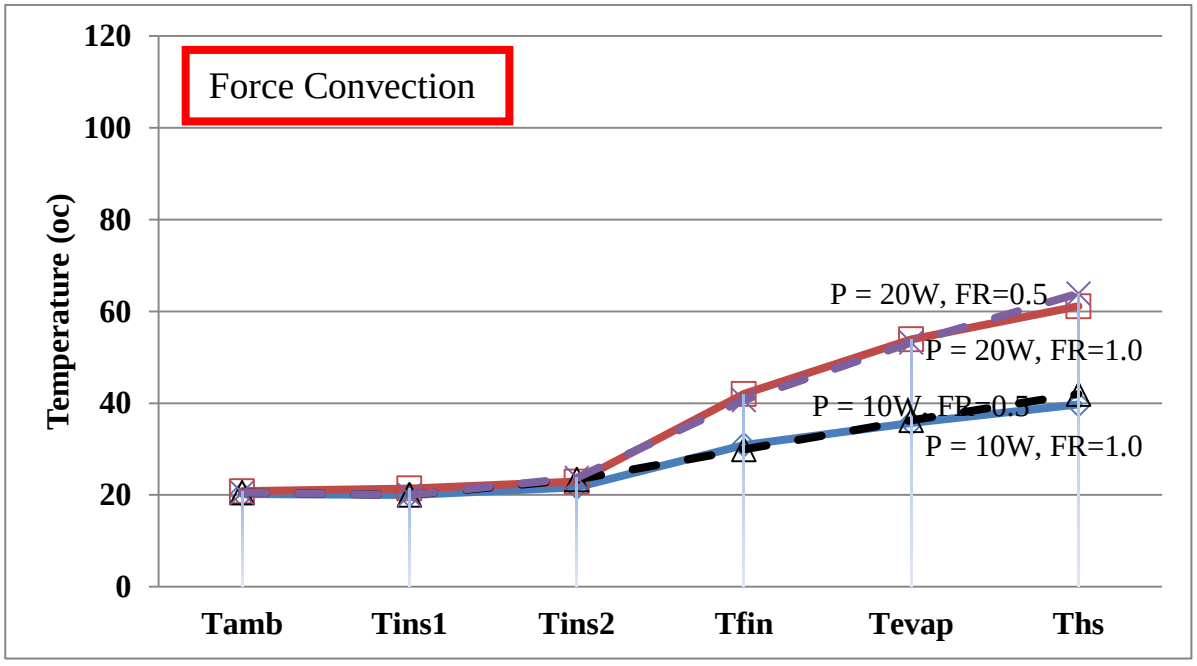

Figure 45: Temperature distribution showing effect of Power Input (P_{EH}) and Fill Ratio for Force Convection

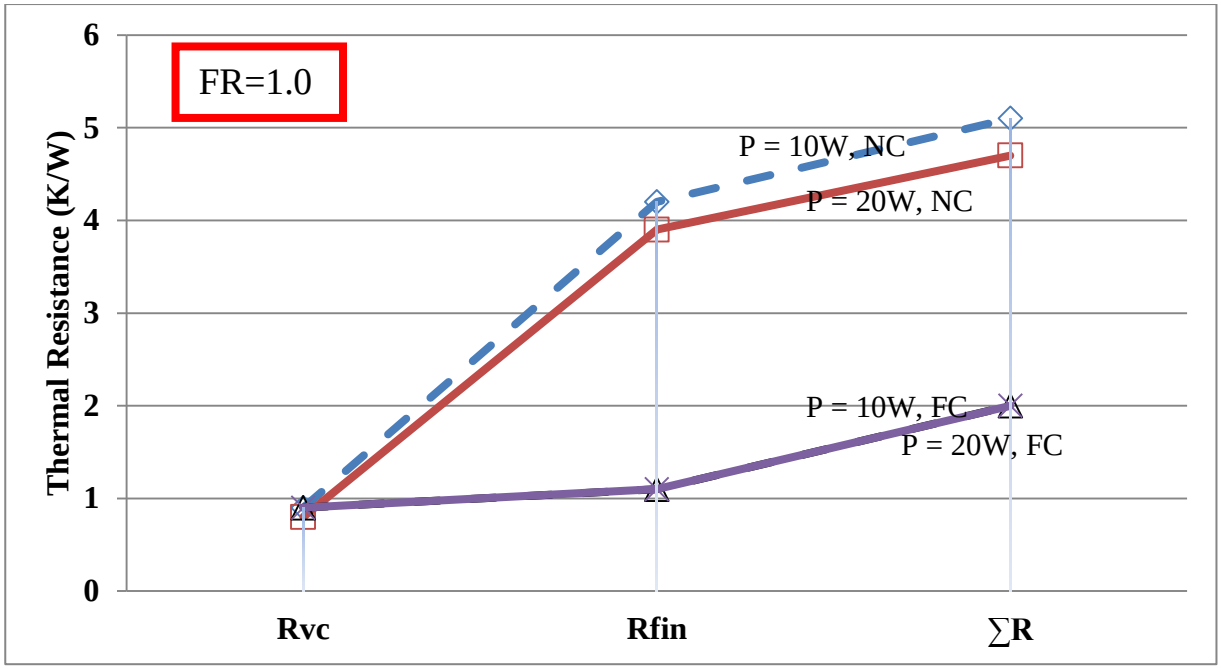

Figure 46: Effect of Power Input (P_{EH}) and Convection (NC/FC) on Thermal Resistance for FR = 1.0

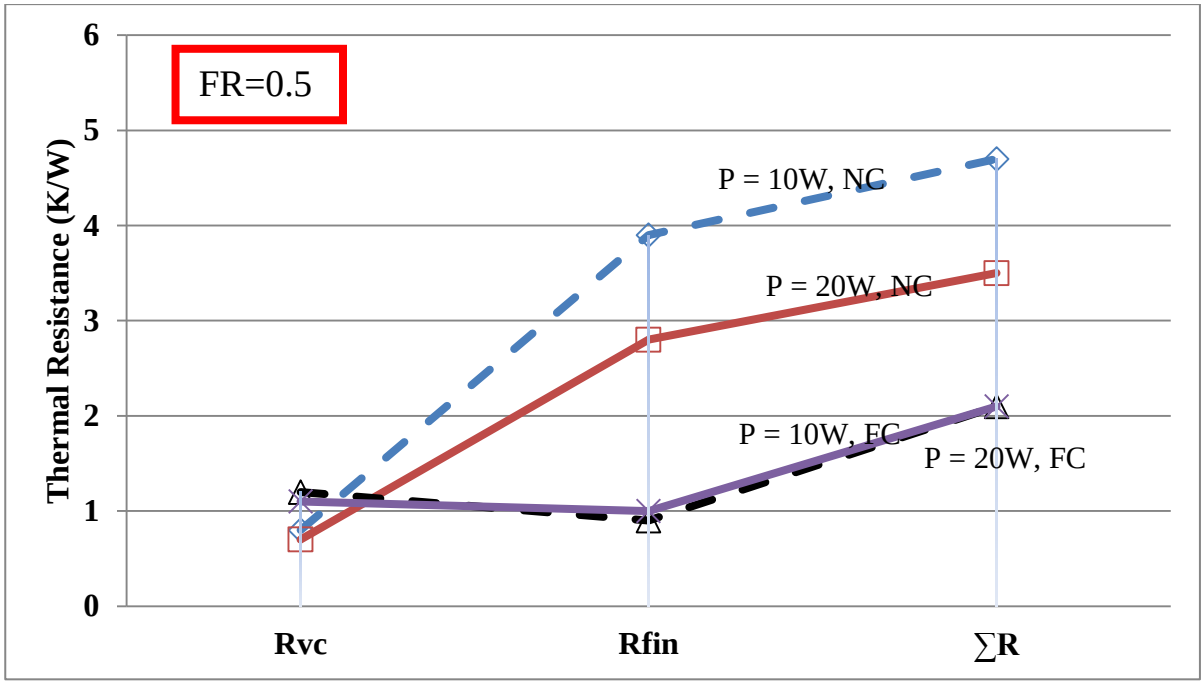

Figure 47: Effect of Power Input (P_{EH}) and Convection (NC/FC) on Thermal Resistance for FR = 0.5

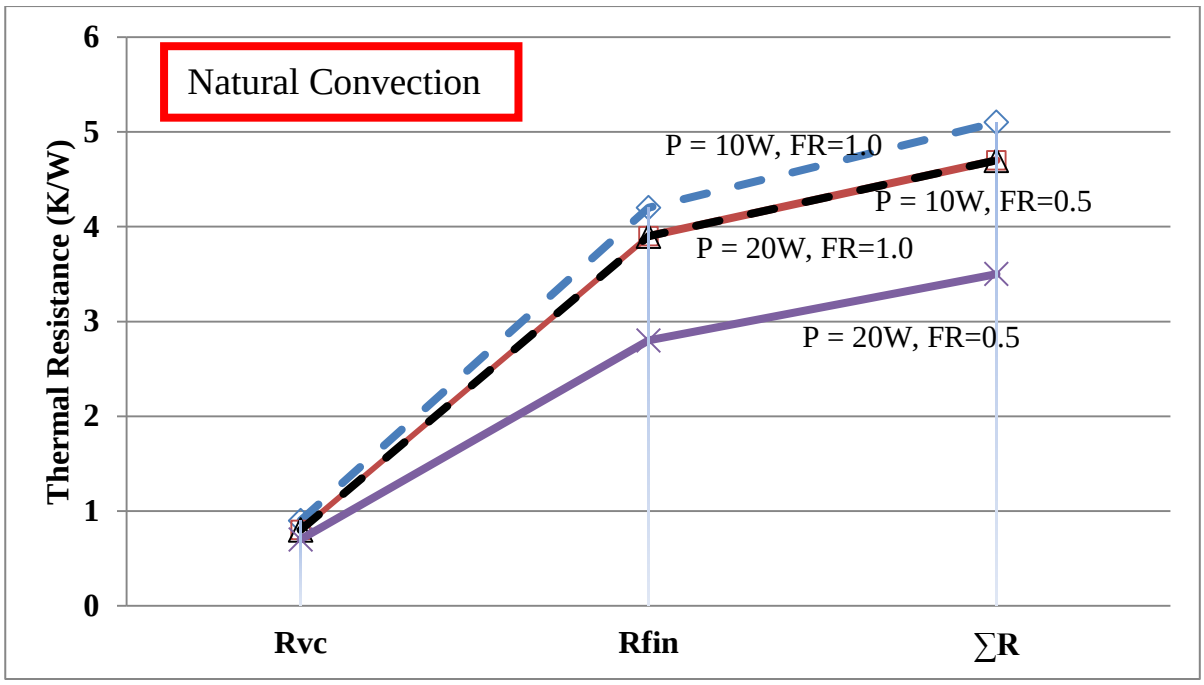

Figure 48: Effect of Power Input (P_{EH}) and Fill Ratio on Thermal Resistance for Natural Convection

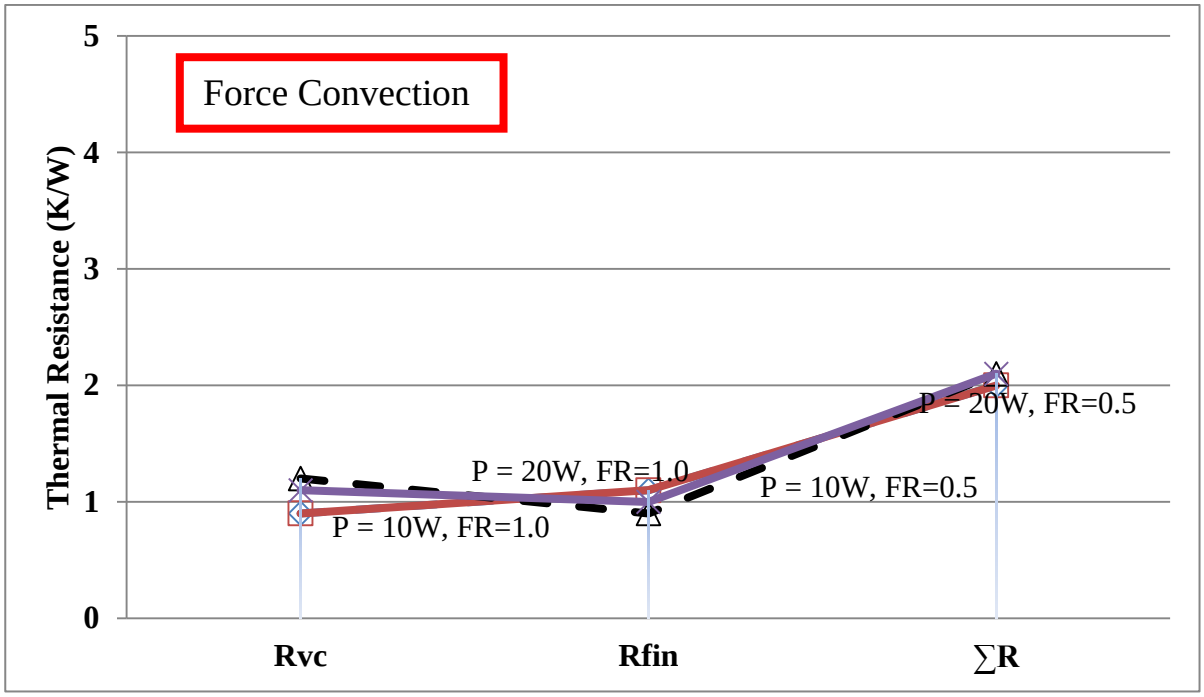

Figure 49: Effect of Power Input (P_{EH}) and Fill Ratio on Thermal Resistance for Force Convection

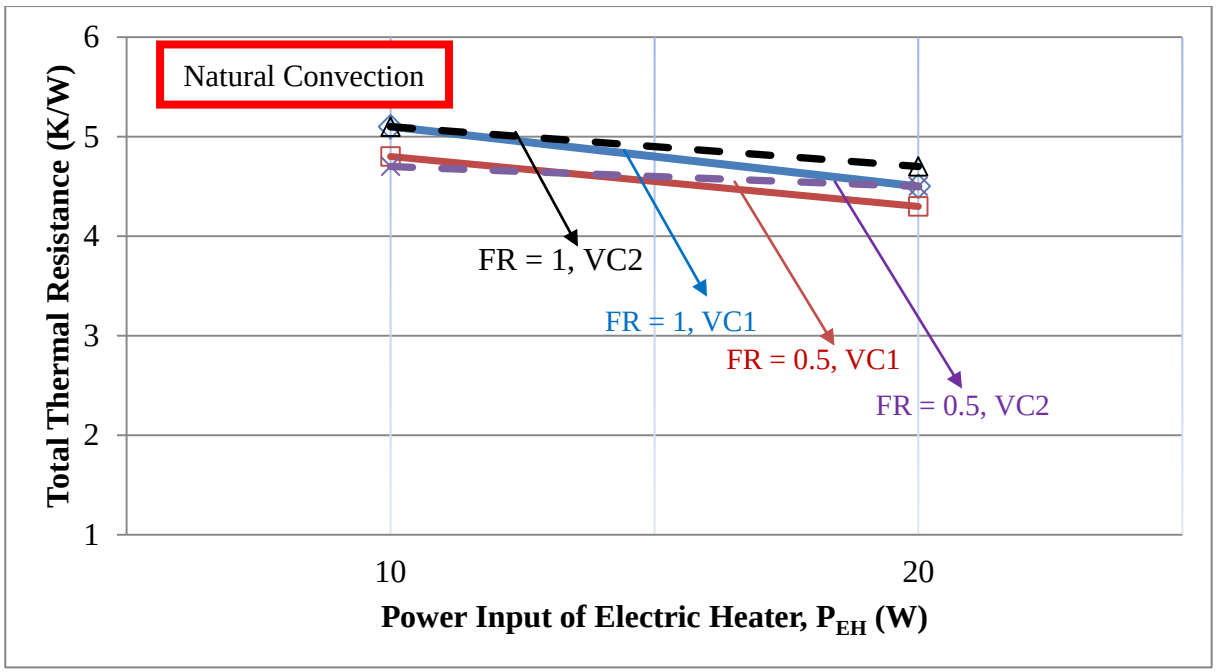

Figure 50: Total Thermal Resistance showing effect of Fill Ratio for VC1 & VC2 under Natural Convection

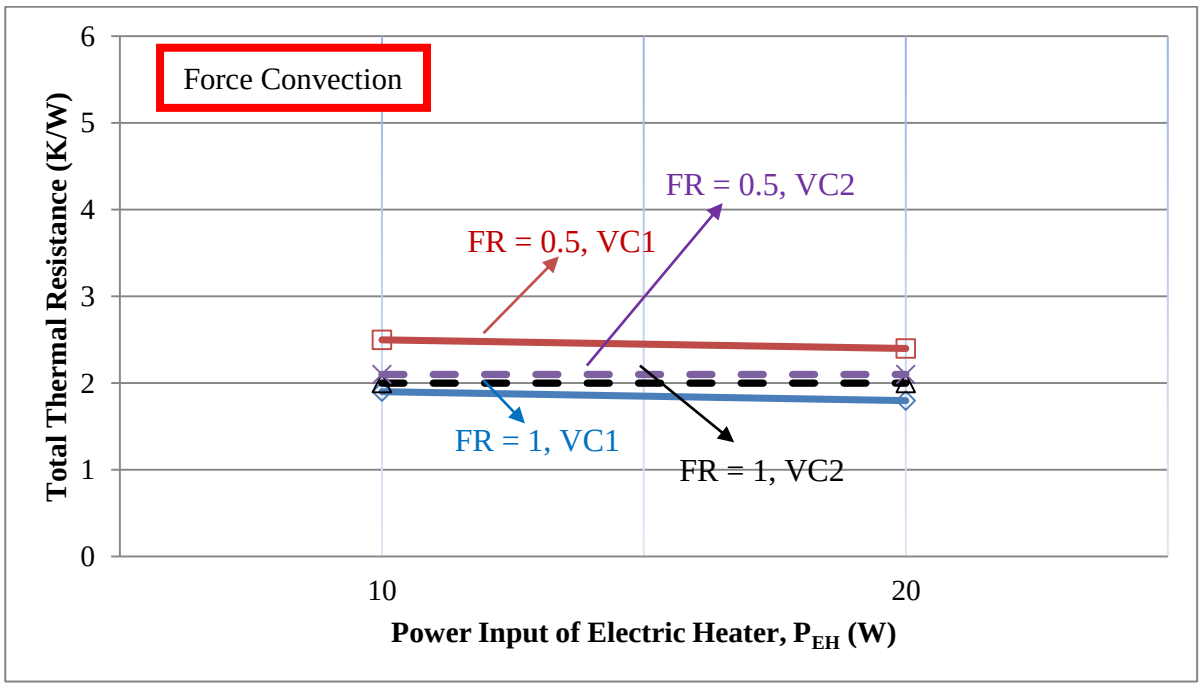

Figure 51: Total Thermal Resistance showing effect of Fill Ratio for VC1 & VC2 under Force Convection

CHAPTER 5

DISCUSSION OF RESULTS

5.1 Repeatability test of the results (Runs #1, 2, 9, 10)

Based on the experiment of study, same test were run repeatedly with the same working fluid and fill ratio. For run #1 and 2 which are using the VC #1,same test were repeated for three times on the four runs under natural convection with fill ratio of 1.0 for water. From the results obtained for run #1 which the power input was 10W, the temperatures for the run were found to be repeatable within ±1.0^{o}C in 120 minutes or7200 seconds. For run #2 which the power input for 20W, the temperatures for the run were found to be repeatable within ±0.5^{o}C in 280 minutes or 16800 seconds. For run #9 and 10 which are using the VC #2, same test were repeated for three times on the four runs under natural convection with the fill ratio of 1.0 for water. Based on the results obtained for run #9, the power input of 10W has the repeatability of temperature within ±1.0^{o}C in 120 minutes. For run #10 which the power input for 20W, the temperatures for the run were found to be repeatable within ±0.5^{o}C in 120 minutes. In order to calculate the average transient temperature of the repeated experiment for computing the total thermal resistance and heat transfer coefficient, we take the average of the value for the three repeated results. Figure 10 to 12 present on the transient temperature for run #1 and 2 where Figure 30 to 32 present on the transient temperature for run #9 and 10.

5.2 Transient Temperature Results (Runs #1 to 16)

The transient temperature results were plotted in Figure 10 to 21 and Figure 30 to 41. In the Figures, the results of temperatures along the fins and evaporator were also plotted. From the Figures, the temperature of the VC was increasing from the room temperature due to the heat transfer from the power input to the VC. The power input used for the study was 10W and 20W where each power input of the experiment will heat up the VC until it achieved steady state. Under natural convection for power input of 10W on VC #1 and 2, it was noticed that all the temperature achieved its steady state around 120 minutes of heat up. For power input of 20W on VC #1 and 2, the temperature achieved its steady state at around 120 to 150 minutes. Under force convection for power input of 10W on VC #1 and 2, it was noticed that the temperature achieved its steady state at around 60 minutes. For power input of 20W on VC #1 and 2, the temperature achieved its steady state at around 50-60 minutes. At higher power input, the temperature of the VC will be higher. This is because when the power input is higher, more heat will transfer to the device. Under natural convection, the highest temperature was up to 114.9^{o}C which was on run #10 VC #2. Under force convection, the highest temperature was up to 70.7^{o}C which was on run #10 VC #1. By comparison of the natural convection and force convection, the surface temperature of VC on natural convection is higher. This is because the condensing rate is expected to be slower under NC as it is using the natural air flow speed. This would result in less condensate return to the evaporator section of the VC. Hence the larger pool of un-evaporated liquid in the evaporator section would result in poorer performance of the NC.

5.3 Effect of Fill Ratio on Vapor Chamber

5.3.1 Effect of Fill Ratio on VC #1

In order to compare the effect of fill ratio and power input under natural and force convection, the temperature distribution of the VC #1 were plotted in Figure 24 and 25. In Figure 24, result showed that the fill ratio of 0.5 performed better than the fill ratio of 1.0 under natural convection. On power input of 20W, the surface temperature of aluminum block reached about 112^{o}C in FR of 1.0, where in FR of 0.5 the temperature reached about 106^{o}C. On power input of 10W, the surface temperature of aluminum block reached about 73^{o}C in FR of 1.0, where in FR of 0.5 the temperature is slightly lower which is about 70^{o}C. The reason of the poorer performance of the high fill ratio in natural convection might be due to the higher rate of evaporation than the rate of condensation. With high fill ratio, the working fluid was "stuck" at the fins causes the rate of condensation return to be lesser. Hence, the evaporator was to be "starved".

On the other hand, Figure 25 showed that the fill ratio of 1.0 performed better than the fill ratio of 0.5 under force convection. On the power input of 10W, the surface temperature of aluminum block reached about 41^{o}C in high fill ratio, where in low fill ratio the temperature reached about 46^{o}C. On power input of 20W, the surface temperature of aluminum block was about 57^{o}C in high fill ratio where the temperature increase to about 71^{o}C in low fill ratio. The fin temperature for high fill ratio is around 38^{o}C where the low fill ratio is about 50^{o}C. This showed that there are better cooling effect on high fill ratio. The reason for the better performance of high fill ratio in force convection might be due to the rate of condensation of working fluid return to the evaporator section is high enough. Therefore, the high fill ratio of working fluid will be better to transfer the heat with higher rate to the condenser section.

5.3.2 Effect of Fill Ratio on VC #2

In order to compare the effect of fill ratio and power input under natural and force convection, the temperature distribution of the VC #2 were plotted in Figure 44 and 45. In Figure 44, result showed that the fill ratio of 0.5 performed better than the fill ratio of 1.0 under natural convection. On power input of 10W, the surface temperature of aluminum block reached about 70^{o}C in FR of 1.0, where in FR of 0.5 the temperature is slightly lower which is about 69^{o}C. The decrease in temperature is not significant on both of the fill ratio. On power input of 20W, the surface temperature of aluminum block reached about 115^{o}C in FR of 1.0, where in FR of 0.5 the temperature reached about 113^{o}C. Again, the temperature difference was not much. But as overall, the performance of low fill ratio performed better in natural convection because it has a lower temperature at the heat source. The lower temperature obtained was due to the higher heat transfer rate in the VC. The possible reason behind had been explained earlier in part 6.3.1 which isthe higher rate of evaporation than the rate of condensation that causes “stuck up” at the condenser section.

Meanwhile for the force convection on Figure 45, the result showed that the fill ratio of 1.0 performed better than the fill ratio of 0.5 as the temperature distribution of high fill ratio is lower. On the power input of 10W, the surface temperature of aluminum block reached about 40^{o}C in high fill ratio, where in low fill ratio the temperature reached about 42^{o}C, with a 2^{o}C of difference. On power input of 20W, the surface temperature of aluminum block was about 61^{o}C in high fill ratio where the temperature increase to about 64^{o}C in low fill ratio. The result showed that better cooling effect on high fill ratio. The heat transfer occurs faster in liquid than in solid state. Therefore, when the fill ratio is higher and the rate of condensation return to the evaporator is high enough, more working fluid filled in the VC will transfer the heat faster, hence results in better cooling and higher heat transfer coefficient.

5.4 Effect of Convection on Vapor Chamber

5.4.1 Effect of convection on VC #1

In order to compare the effect of convection and power input respective with the fill ratio of VC #1, Figure 22 and 23 were plotted for the temperature distribution. Convection is the flow of heat or heat transfer from a hot to cold region. Based on Figure 22, the temperature distribution of natural convection shows a higher temperature than the force convection for high fill ratio. The surface temperature of aluminum block for natural convection for power input of 10W to 20W ranged from 73^{o}C to 112^{o}C. On the other side, the surface temperature of aluminum block for force convection ranged from 41^{o}C to 57^{o}C. In higher power for both natural and force convection results in higher temperature. The temperature distribution for natural convection on high fill ratio with low power input is from 61^{o}C to 73^{o}C. For high power input the temperature distribution is from 93^{o}C to 112^{o}C. Meanwhile, the temperature distribution for force convection on high fill ratio with low power input is from 30^{o}C to 41^{o}C. For high power input the temperature distribution is from 38^{o}C to 57^{o}C. The probable reason for such results might be there is external agent involved on the fluid motion in force convection. In natural convection, the fluid motion is natural. Therefore, the heat transfer rate in lower which results in higher temperature and poorer cooling effect.

Moreover, in Figure 23 shows the temperature distribution on convection with high and low input power in low fill ratio. The result obtained was similar to the concept of the temperature distribution in high fill ratio. Natural convection results in higher temperature compare to force convection. The temperature distribution for natural convection on low fill ratio with low power input is from 58^{o}C to 70^{o}C. For high power input the temperature distribution is from 85^{o}C to 106^{o}C. Meanwhile, the temperature distribution for force convection on low fill ratio with low power input is from 35^{o}C to 46^{o}C. For high power input the temperature distribution is from 50^{o}C to 71^{o}C.

5.4.2 Effect of convection on VC #2

In order to compare the effect of convection and power input respective with the fill ratio of VC #2, Figure 42 and 43 were plotted for the temperature distribution. Natural convection occurs on the flow of fluid motion with buoyancy effect while force convection occurs with the flow of fluid motion with external device input on it. For instance, cooling fan. No difference with the VC #1, the temperature distribution of natural convection shows a higher temperature than the force convection. In higher power for both natural and force convection results in higher temperature. The temperature distribution for natural convection on high fill ratio with low power input is from 62^{o}C to 70^{o}C. For high power input the temperature distribution is from 99^{o}C to 115^{o}C. Meanwhile, the temperature distribution for force convection on high fill ratio with low power input is from 31^{o}C to 40^{o}C. For high power input the temperature distribution is from 42^{o}C to 61^{o}C. The heat transfer process occurs in force convection is faster. The faster the heat transfer process, the higher heat transfer coefficient will be acquired. In forced convection, the process was accelerated by a fan. Hence the increase in temperature of the working fluid occurs faster in the VC and higher heat transfer coefficient.

Figure 43 shows the temperature distribution on convection with high and low input power in low fill ratio. Based on the result obtained, the higher power of natural and force convection have a higher temperature. This is because higher energy produced in every second to the device when the power increases. Besides, natural convection results in higher temperature compare to force convection. The temperature distribution for natural convection on low fill ratio with low power input is from 61^{o}C to 69^{o}C. For high power input the temperature distribution is from 96^{o}C to 113^{o}C. Meanwhile, the temperature distribution for force convection on low fill ratio with low power input is from 30^{o}C to 42^{o}C. For high power input the temperature distribution is from 41^{o}C to 64^{o}C.

5.5 Effect of Fill Ratio on Total Thermal Resistance

5.5.1 Total Thermal Resistance on VC #1

In order to compare the effect of fill ratio and power input on total thermal resistance for convection on VC #1, Figure 28 and 29 were plotted to investigate. Thermal resistance is defined as the resistance of a system or medium to the heat flow through the boundaries and dependent upon the thermal properties of the system. For instance, this is thermal conductivity of the material. Under natural convection, Figure 28 shows the total thermal resistance for low power is higher than the high power. The resistance that included in the study is resistance of fin which is the condenser and the resistance of VC. The total thermal resistance is calculated using the summation of the R_{fin} and R_{VC}. The total thermal resistance for high fill ratio under natural convection ranged from 4.5K/W to 5.1K/W where for low fill ratio it ranged from 4.3K/W to 4.8K/W. Based on the results, the total thermal resistance of high fill ratio is higher than low fill ratio. This is because the heat transfer rate in natural convection is slower. Therefore with the high fill ratio, the possibility that the working fluid to “stuck up” at the fin is higher. When there is less condensate return to the evaporator section, the heat transfer coefficient will be smaller results in higher total thermal resistance.

Under force convection, Figure 29 shows the total thermal resistance for low power is higher than the high power. The total thermal resistance for high fill ratio under force convection ranged from 1.8K/W to 1.9K/W where for low fill ratio it ranged from 2.4K/W to 2.5K/W. The variation of total thermal resistance on both fill ratios is small. Based on the results obtained, the total thermal resistance for high fill ratio is lower than low fill ratio which is opposed to the natural convection experiment. In force convection, the rate of condensate to return to the evaporator is high due to the external force apply at the condenser part. Therefore, high filled working fluid will helps to transfer the heat faster from the heat source. Hence, result in the lower thermal resistance.

5.5.2 Total Thermal Resistance on VC #2

In order to compare the effect of fill ratio and power input on total thermal resistance for convection on VC #2, Figure 48 and 49 were plotted to investigate. The evaporator and condenser resistances are calculated based on the outer surface area of the wall. Under natural convection, Figure 48 shows the total thermal resistance for low power is higher than the high power. The mainpurpose of the study is to reduce the overall thermal resistance by increasing the rate of heat transfer to get a better cooling device for electronic industry. The total thermal resistance for high fill ratio under natural convection ranged from 4.7K/W to 5.1K/W where for low fill ratio it ranged from 4.5K/W to 4.7K/W. Based on the results, the total thermal resistance of high fill ratio is higher than low fill ratio. The heat transfer of working fluid that pass through the wick structure of the wall of VC from condenser to evaporator is slower under natural convection as been described earlier in part 6.3.1.

Under force convection, Figure 49 shows the total thermal resistance is same for both high and low powers. The total thermal resistance for high fill ratio under force convection is 2K/W where for low fill ratio it is 2.1K/W. The total thermal resistance on both fill ratios is the same. Based on the results obtained, the total thermal resistance for high fill ratio is slightly lower than low fill ratio which is opposed to the natural convection experiment. The variation of overall thermal resistance is only 0.1K/W. In force convection, the rate of condensate to return to the evaporator is high due to the external force apply at the condenser part. Therefore, working fluid of fill ratio of 0.5 to 1.0 can give a good performance which helps to transfer the heat faster from the heat source. However, the results obtained showed that the optimum fill ratio is 1.0.

5.6 Effect of Convection on Total Thermal Resistance

5.6.1 Total Thermal Resistance on VC #1

In order to compare the effect of convection and power input respective with the fill ratio for VC #1, Figure 26 and 27 were plotted for the overall thermal resistance. Convection is the flow of heat or heat transfer of a medium from a hot to cold region. Based on Figure 26, the power input of natural convection shows a higher thermal resistance than the force convection for high fill ratio. The overall thermal resistance for natural convection for power input of 10W to 20W ranged from 4.5K/W to 5.1K/W. On the other side, the total thermal resistance for force convection ranged from 1.8K/W to 1.9K/W which is only 0.1K/W of variation. In higher power for both natural and force convection results in lower thermal resistance. This is because during high power, the energy pass through per second was higher to overcome the resistance to become smaller. When the power increases, there is more heat transfer through the device resulting in higher heat transfer coefficient. As for force convection on high fill ratio, the overall thermal resistance is not much variation due to the external sources forcing on the condenser part resulting in better cooling effect.

Based on Figure 27, the thermal resistance for natural convection is higher than for force convection. When the power increase, the thermal resistance is reduce. The overall thermal resistance for natural convection for power input of 10W to 20W ranged from 4.3K/W to 4.8K/W. Besides, the total thermal resistance for force convection ranged from 2.4K/W to 2.5K/W which is also with 0.1K/W of variation. As for natural and force convection for low fill ratio, the resistance of fin is higher than the resistance of VC. As for force convection, the variation of thermal resistance is small indicating the rate of heat transfer for high and low power is almost equal.

5.6.2 Total Thermal Resistance on VC #2

In order to compare the effect of convection and power input respective with the fill ratio for VC #2, Figure 46 and 47 were plotted for the overall thermal resistance. Based on Figure 46, the power input of natural convection shows a higher thermal resistance than the force convection for high fill ratio. This is because the air flow for natural convection is slower compare to force convection with external force on the air flow. The cooling effect is poorer results in rate of heat transfer is slower. The overall thermal resistance for natural convection for power input of 10W to 20W ranged from 4.7K/W to 5.1K/W. On the other side, the total thermal resistance for force convection for high and low power is the same which is 2K/W. In higher power for natural convection tends to result in lower thermal resistance. This is because during high power, the energy pass through per second was higher to overcome the resistance to become smaller. While on the other hand for force convection, the total thermal resistance did not change shows that 10 and 20W of power did not affect much for the thermal resistance due to the external air used to cool down the VC.

Based on Figure 47, the same theory get in previous part where the thermal resistance for natural convection is higher than for force convection. When the power increase, the thermal resistance is reduce. The overall thermal resistance for natural convection for power input of 10W to 20W ranged from 4.5K/W to 4.7K/W. Besides, the total thermal resistance for force convection is the same which is 2.1K/W. As for natural for low fill ratio, the resistance of fin is higher than the resistance of VC. As for force convection, the resistance of VC is higher than the resistance of fin. This can be mean by the heat transfer rate at the condenser is lower than the evaporator part for natural convection. While for force convection, the fin has lower thermal resistance indicates the heat transfer rate is higher than the evaporator part.

5.7 Thermal Performance of VC #1 and VC #2

In order to compare the thermal performance of the two VC, Figure 50 and 51 were plotted on the thermal resistance to show the effect of fill ratio and input power under natural and force convection. The variation of both VC is the number of fins where VC #1 has eight fins meanwhile VC #2 has four fins.

5.7.1 Natural Convection

Based on Figure 50, the total thermal resistance for VC #1 and VC #2 with the fill ratio of 1.0 at power of 10W is the highest which is 5.1K/W under natural convection. During the power of 10W, the VC #2 of fill ratio of 0.5 has the lowest thermal resistance which is 4.7K/W. This concludes that under natural convection, the fill ratio of 0.5 performed better than the fill ratio of 1.0 with the power of 10W. Compared with the fill ratio of 0.5 for VC #1 and VC #2 with power of 10W, VC #2 performs better than VC #1. This may be due to less condensate return to the evaporator section and more "stuck" of working fluid at the condenser for VC #1, therefore with the increase in the number of fins, the condensate that "stuck" at the fins will be greater. Hence the un-evaporated liquid from the evaporator session will lower down the heat transfer rate from the condenser to evaporator.

Meanwhile, when we see for the power input of 20W, the highest total thermal resistance is on the VC #2 with fill ratio of 1.0 which is 4.7K/W. Besides, the thermal resistance for VC #1 with fill ratio of 1.0 and VC #2 with fill ratio of 0.5 are the same which is 4.5KW. The lowest total thermal resistance is VC #1 with the fill ratio of 0.5 which is 4.3K/W. The total thermal resistance for VC #1 and VC #2 with fill ratio of 0.5 has a variation of only 0.2K/W which is not significant enough to make any conclusion. The probable reason for such results might be due to the power for 20W is strong enough to perform better to transfer the heat from the evaporator to the condenser. Hence, with the increase of surface area by increasing the number of fins, the heat transfer rate is higher for VC #1 with fill ratio of 0.5.

5.7.2 Force Convection

Based on Figure 51,the total thermal resistance for VC #1 with the fill ratio of 0.5 at power of 10W is the highest which is 2.5K/W under force convection. During the power of 10W, the VC #1 of fill ratio of 1.0 has the lowest thermal resistance which is 1.9K/W. Besides, the second highest total thermal resistance is VC #2 with the fill ratio of 0.5 which is 2.1K/W. This concludes that under force convection, the fill ratio of 1.0 performed better than the fill ratio of 0.5 with the power of 10W. Compared with the fill ratio of 1.0 for VC #1 and VC #2 with power of 10W, VC #1 performs better than VC #2. This is because during force convection experiment carried out with the cooling fan, the surface of the fin will have a better cooling effect, the condensate return to the evaporator section with me more. The number of fins increase will results in the increasing of total surface area of condenser. The larger the total surface area, the more surface it exposed to the air to cool down the evaporated liquid in the fin heat sink. In brief, the heat transfer coefficient of the force convection will be larger than in the natural convection.

If we look into the power of 20W, the ranking of the highest and lowest thermal resistance is the same with the ranking of power 10W. The total thermal resistance for force convection on power 10W and 20W has not much variation. The highest thermal resistance for power 20W is 2.4K/W where the lowest total thermal resistance is 1.8K/W. Whereas for the VC #2 with the fill ratio of 0.5, the total thermal resistance remains the same with the power of 10W and 20W. Therefore, if we were to use force convection on the cooling of electronic device, the fill ratio is the better choice compare to the half fill ratio.

In brief, if we compare the Figure 50 and 51, the overall thermal resistance for natural convection is higher than force convection. The concept that shows the results obtained has been explain earlier. Based on the experiment study, there is heat loss to the surrounding by convection and radiation. In order to investigate the error form with the heat loss, another experiment of run #13(2) and #14(2) were repeated with the same power and fill ratio on VC #2. In the experiment, insulation was added on

the thermocouples head on the fins in order to investigate the temperature difference with and without the insulation. Results were tabulated in Table 3.

5.8 Heat transfer Coefficient of VC

Heat transfer is the process of exchanging of the thermal energy between the systems. Heat can be travel through three ways which are conduction, convection as well as radiation. When the heat is transfer between a surface wall and a working fluid at a variation of temperature is known as convective heat transfer. Based on the study of VC-FHS, the working fluid of water is transferring heat by convection to the surface wall of the flat plate heat pipe with capillary tube. Heat is transfer from the high temperature end to the low temperature end. Heat loss to the surrounding from the VC-FHS to the surrounding air is by conduction and radiation. The convective heat transfer coefficient is based on the working fluid properties such as velocity, viscosity and temperature. The heat transfer coefficient that can be measured in this study is the convective heat transfer coefficient.

In this study, heat transfer coefficient of the fin, h_{fin} had been calculated to investigate the performance of both VC to determine the optimum fins to use on VC-FHS system. Based on the results that had been calculated, the heat transfer coefficient of force convection is higher than in natural convection. This applied to both of the VC. The reason is because natural convection is solely caused by the buoyancy force due to the variation of density with different temperatures in the working fluid. Natural convection is never induced by external force which applies free convection for the transferring of heat through the system. The highest heat transfer coefficient is 140W/m^2K which is force convection on VC #2 with the fill ratio of 0.5. The higher the heat transfer coefficient, the higher the rate of heat transfers through the system. The lowest heat transfer coefficient is 26W/m^2K on natural convection on VC #1 with the fill ratio of 1.0. The range of heat transfer coefficient for natural convection is from 26W/m^2K to 34W/m^2K. Meanwhile, the range of heat transfer coefficient for force convection is from 73W/m^2K to

140W/m^{2}K. This shows that the thermal resistance will be lower for force convection process as the heat transfer rate is higher through the working fluid.

The study of experiment has been neglect the issue of heat loss to surrounding by convection and radiation. In order to determine the accuracy of the results, another experiment of run #13(2) and #14(2) were tested by apply insulation to the fin. Based on the results, the fin temperature increase about 3% for both the power inputs. The resistance of fin is believed to be increased by around 5%. This is because when insulation applies to the fin, heat loss to the surrounding will be limited and hence the heat was trapped inside the fins that increase the temperature of fin. With this result, the reduction of the resistance of VC is about 12.5% to 20%. When the thermal resistance of the fin is increased, the heat transfer coefficient will be smaller. The higher the thermal resistance, thus the smaller the heat transfer coefficient. The heat transfer coefficient is about to reduce from 3% to 6%. The results obtained for this experiment can be assume to use in other runs of experiment in earlier stage with the correction of error.

5.9 Comparison of VC-FHS with FHS

Based on the research study, simulation was carried out in order to compare the thermal performance of VC-FHS and FHS. The simulation was done with the MATHCAD program. Different model of VC-FHS and FHS with different dimension were used to compare. Based on the simulation results of FHS, the RF1D obtained for natural convection is around 11-12K/W. From the results obtained in my research, the total thermal resistance is around 4-5K/W. This proved that with the VC embedded in the FHS, the overall performance will be improved. This is because VC is the flat heat pipe provide wick structure which will distribute the temperature of the working fluid in the pipe evenly through capillary, thus the rate of condensation and evaporation will be higher in order to results in better cooling. When the temperature is lower, the cooling effect is better. Thus, lower thermal resistance we get.

CHAPTER 6

SUGGESTIONS FOR FUTURE STUDIES

- Carry out experiment study on FR of 0.25 or 0.75.
- Change the working fluid with another liquid like acetone.
- Varied the fins height and width.
- Varied the size of the VC heat sink.
- Used a better insulator in order to prevent the likelihood of heat loss to the surroundings.

CHAPTER 7

CONCLUSIONS

The conclusions of the study are as shown:

- ✓ FC performs better with lower thermal resistance compared to NC.
- ✓ Under NC, lower FR (FR=0.5) performs better.
- ✓ Under FC, higher FR (FR=1.0) performs better.
- ✓ Under NC, lower FR does not affect the performance of VC1&VC2.
- ✓ Under FC and at low FR, VC2 performs better than VC1.

REFERENCES

- Attia, A. A., & El-Assal, B. T. (2012). Experimental investigation of vapor chamber with different working fluids at different charge ratios. *Ain Shams Engineering Journal*, *3*(3), 289-297.

- Jeng, T. (2015). Combined convection and radiation heat transfer of the radially finned heat sink with a built-in motor fan and multiple vertical passages. *International Journal of Heat and Mass Transfer*, 80, pp.411-423.

- Kang, S. W., Chen, Y. T., Hsu, C. H., & Lin, J. Y. (2012). Temperature Uniformity Analysis of a Multi-well Vapor Chamber Heat Spreader. *Frontiers in Heat Pipes (FHP)*, *3*(1).

- Li, H., Chiang, M., Lee, C. and Yang, W. (2010). Thermal performance of plate-fin vapor chamber heat sinks. *International Communications in Heat and Mass Transfer*, 37(7), pp.731-738.

- Luo, X., Hu, R., Guo, T., Zhu, X., Chen, W., Mao, Z. and Liu, S., (2010), June. Low thermal resistance LED light source with vapor chamber coupled fin heat sink. In *2010 Proceedings 60th Electronic Components and Technology Conference (ECTC)* (pp. 1347-1352). IEEE.

- Michels, V., Milanez, F. and Mantelli, M. (2012). Vapor chamber heat sink with hollow fins. *J. Braz. Soc. Mech. Sci. & Eng.*, 34(3), pp.233-237.

- Ming, Z., Zhongliang, L., &Guoyuan, M. (2009). The experimental and numerical investigation of a grooved vapor chamber. *Applied Thermal Engineering*, *29*(2), 422-430.

- Naphon, P. and Wiriyasart, S., (2015). On the Thermal Performance of the Vapor Chamber with Micro-channel for Unmixed Air Flow Cooling. *Engineering Journal*, *19*(1), pp.125-137.

- Reyes, M., Alonso, D., Arias, J.R. and Velazquez, A., (2012). Experimental and theoretical study of a vapour chamber based heat spreader for avionics applications. *Applied Thermal Engineering*, *37*, pp.51-59.

- Shih, D., (2011). *Heat sink equipped with a vapor chamber*. U.S. Patent Application 13/029,878.

- Shukla, K., Solomon, A., & Pillai, B. (2013). Thermal Performance of Vapor Chamber with Nanofluids. *Frontiers in Heat Pipes (FHP)*, *3*(3).

- Tan, B. K., Wong, T. N., &Ooi, K. T. (2010). A study of liquid flow in a flat plate heat pipe under localized heating. *International Journal of Thermal Sciences*, *49*(1), 99-108.

- Tsai, M.C., Kang, S.W. and de Paiva, K.V., (2013). Experimental studies of thermal resistance in a vapor chamber heat spreader. *Applied Thermal Engineering*, *56*(1), pp.38-44.

- Wang, R. T., Wang, J. C., & Chang, T. L. (2011). Experimental analysis for thermal performance of a vapor chamber applied to high-performance servers. *Journal of Marine Science and Technology*, *19*(4), 353-360.

- Wang, S., Chen, J., Hu, Y., & Zhang, W. (2011). Effect of evaporation section and condensation section length on thermal performance of flat plate heat pipe. *Applied Thermal Engineering*, *31*(14), 2367-2373.

- Wiriyasart, S., &Naphon, P. (2013). Study on the Heat Transfer Characteristics of a Vapor Chamber without Micro-channel for Cooling an Electronic Component. *Thammasat International Journal of Science and Technology*, *18*(3), 16-22.

- Wong, S. C., Hsieh, K. C., Wu, J. D., & Han, W. L. (2010). A novel vapor chamber and its performance. *International Journal of Heat and Mass Transfer*, *53*(11), 2377-2384.

- Yang, K. S., Yang, T. Y., Tu, C. W., Yeh, C. T., & Lee, M. T. (2015). A novel flat polymer heat pipe with thermal via for cooling electronic devices. *Energy Conversion and Management*, *100*, 37-44.

- Yu, I. S., Rhi, S. H., & Cha, K. I. (2012). Micro and nano thermal flow characteristics of a flat plate heat pipe heat spreader. *International Journal of Physical Sciences*, *7*(11), 1762-1772.

- Zhang, M., Liu, Z., & Ma, G. (2008). The experimental investigation on thermal performance of a flat two-phase thermosyphon. *International Journal of Thermal Sciences*, *47*(9),1195-1203.

APPENDICES

Thermal conductivity aluminium (W/mK):

$k_{fin} := 200$

Fin dimensions (m):

$H_{fin} := 0.03 \quad S_{fin} := 0.01 \quad t_{fin} := 0.0035 \quad \Delta x_{base} := 0.005 \quad W_{fin} := 0.049$

Assume: Natural convection coefficient (W/m^2K):

$h_a := 5$

$N_{fin} := \frac{W_{fin}}{S_{fin}} = 4.9 \qquad A_{fin} := \left(2.H_{fin} + t_{fin}\right)W_{fin}\cdot 5 = 0.016$

$x := \left(\frac{W_{fin}}{5}\right) - t_{fin} = 6.3 \times 10^{-3} \qquad A_t := A_{fin} + 0.0024 = 0.018$

Fin efficiency:

$$m_{fin} := \left[\frac{h_a \cdot \left(2W_{fin} + 2 \cdot t_{fin}\right)}{k_{fin} \cdot W_{fin} \cdot t_{fin}}\right]^{0.5} = 3.912$$

$$H_{finc} := H_{fin} + \frac{t_{fin}}{2} = 0.032$$

$$\eta_{fin} := \frac{\tanh\left(m_{fin} \cdot H_{finc}\right)}{m_{fin} \cdot H_{finc}} = 0.995 \qquad \eta_o := 1 - \frac{N_{fin} \cdot A_{fin}}{A_t} \cdot \left(1 - \eta_{fin}\right) = 0.978$$

Fin resistance (K/W):

$$R_{fin} := \frac{1}{h_a \cdot A_t \cdot \eta_o} = 11.384 \qquad R_{base} := \frac{\Delta x_{base}}{k_{fin} \cdot W_{fin} \cdot S_{fin} \cdot N_{fin}} = 0.01$$

$$R_{f1D} := R_{fin} + R_{base} = 11.395$$

Thermal conductivity aluminium (W/mK):

$k_{fin} := 200$

Fin dimensions (m):

$H_{fin} := 0.03 \quad S_{fin} := 0.01 \quad t_{fin} := 0.0035 \quad \Delta x_{base} := 0.005 \quad W_{fin} := 0.049$

Assume: Force convection coefficient (W/m^2K):

$h_a := 40$

$N_{fin} := \frac{W_{fin}}{S_{fin}} = 4.9$

$A_{fin} := \left(2.H_{fin} + t_{fin}\right) W_{fin} \cdot 5 = 0.016$

$x := \left(\frac{W_{fin}}{5}\right) - t_{fin} = 6.3 \times 10^{-3}$

$A_t := A_{fin} + 0.0024 = 0.018$

Fin efficiency:

$m_{fin} := \left[\frac{h_a \cdot \left(2W_{fin} + 2 \cdot t_{fin}\right)}{k_{fin} \cdot W_{fin} \cdot t_{fin}}\right]^{0.5} = 11.066$

$H_{finc} := H_{fin} + \frac{t_{fin}}{2} = 0.032$

$\eta_{fin} := \frac{\tanh\left(m_{fin} \cdot H_{finc}\right)}{m_{fin} \cdot H_{finc}} = 0.961$

$\eta_o := 1 - \frac{N_{fin} \cdot A_{fin}}{A_t} \cdot \left(1 - \eta_{fin}\right) = 0.834$

Fin resistance (K/W):

$R_{fin} := \frac{1}{h_a \cdot A_t \cdot \eta_o} = 1.67$

$R_{base} := \frac{\Delta x_{base}}{k_{fin} \cdot W_{fin} \cdot S_{fin} \cdot N_{fin}} = 0.01$

$R_{f1D} := R_{fin} + R_{base} = 1.681$

FACULTY OF ENGINEERING AND GREEN TECHNOLOGY
UNIVERSITI TUNKU ABDUL RAHMAN

Date: _____

PERMISSION SHEET

It is hereby certified that **GOH WEN QIAN** (ID No: **12AGB04025**) has completed this final year project entitled VAPOR CHAMBER EMBEDDED WITH HOLLOW CONDENSER TUBES HEAT SINK under the supervision of Prof. Ir. Dr. Ong Kok Seng (Supervisor) from the Department of Industrial Engineering, Faculty of Engineering and Green Technology.

I hereby give permission to the University to upload softcopy of my final year project in pdf format into UTAR Institutional Repository, which may be made accessible to UTAR community and public.

Yours truly,

_____

(GOH WEN QIAN)

Turnitin Originality Report

FYP thesis by Wen Qian Goh

From FYP IE (FYP May 2016 - Jan 2017)

Processed on 08-Apr-2017 22:50 MYT
ID: 768139794
Word Count: 14260

Similarity Index	Similarity by Source	
5%	Internet Sources:	2%
	Publications:	3%
	Student Papers:	1%

sources:

1 < 1% match (publications)
Naphon, Paisarn, and Songkran Wiriyasart. "Study on the vapor chamber with refrigerant R-141b as working fluid for HDD cooling", International Communications in Heat and Mass Transfer, 2012.

2 < 1% match (publications)
Dinçer, . "Heat Pipes", Refrigeration Systems and Applications Dinçer/Refrigeration Systems and Applications, 2010.

3 < 1% match (Internet from 28-Jun-2014)
http://www.thermalfluidscentral.org/e-resources/download.php?id=250

4 < 1% match (publications)
Ong, K.S., Gabriel Goh, K.H. Tshai, and W.M. Chin. "Thermal resistance of a thermosyphon filled with R410A operating at low evaporator temperature", Applied Thermal Engineering, 2016.

5 < 1% match (student papers from 21-Oct-2013)
Submitted to AUT University on 2013-10-21

6 < 1% match (publications)
Wong, S.C.. "A novel vapor chamber and its performance", International Journal of Heat and Mass Transfer, 201005

7 < 1% match (student papers from 03-May-2016)
Submitted to Universiti Tunku Abdul Rahman on 2016-05-03

8 < 1% match (publications)
Michels, Vanessa, Fernando H. Milanez, and Marcia B. H. Mantelli. "Vapor chamber heat sink with hollow fins", Journal of the Brazilian Society of Mechanical Sciences and Engineering, 2012.

9 < 1% match (publications)
De Kerpel, Kathleen, Sven De Schampheleire, Heleen Steuperaert, Peter De Jaeger, and Michel De Paepe. "Experimental study of the effect of felt wick porosity on capillary-driven heat pipes", Applied Thermal Engineering, 2016.

10 < 1% match (Internet from 15-Feb-2017)
http://www.mdpi.com/2076-3417/7/2/62/htm

11 < 1% match (Internet from 10-Mar-2016)
http://cdn.intechopen.com/pdfs-wm/20814.pdf

12 < 1% match (Internet from 04-Dec-2015)
http://engj.org/index.php/ej/article/download/574/371

13 < 1% match (Internet from 19-Aug-2016)
http://www.bu.univ-rennes2.fr/discovery/results?filter%5B0%5D=addfacetfilter%28ContentProvider%3AHyRead+Journal%29&filter%5B%5D=addfacetfilter%28Journal%3A%E6%B5%B7%E6%B4%8B%E5%AD%B8%E5%88%8A%29&lookfor=thermal+conductivity&type=Subject

14 < 1% match (publications)
KOITO, Yasushi, Hideaki IMURA, Masataka MOCHIZUKI, Yuji SAITO, and Shuichi TORII. "Fundamental Experiments and Numerical Analyses on Heat Transfer Characteristics of a Vapor Chamber (Effect of Heat Source Size)", JSME International Journal Series B, 2006.

15 < 1% match (publications)
Hu, X.. "Experimental investigation on flow and thermal characteristics of a micro phase-change cooling system with a microgroove evaporator", International Journal of Thermal Sciences, 200711

16 < 1% match (publications)
Li, Ji, and Lucang Lv. "Experimental studies on a novel thin flat heat pipe heat spreader", Applied Thermal Engineering, 2016.

17 < 1% match (Internet from 04-Oct-2010)
http://www.engr.mun.ca/~yuri/PAPERS/2004/Impingement%20Thermal%20Resistance%20-%202004%20ITHERM%20Conference.pdf

18 < 1% match (Internet from 07-Oct-2016)
https://journalofsolidstatelighting.springeropen.com/articles/10.1186/s40539-014-0012-7

19 < 1% match (publications)
Wang, Jung-Chang. "3-D numerical and experimental models for flat and embedded heat pipes applied in high-end VGA card cooling system", International Communications in Heat and Mass Transfer, 2012.

20 < 1% match (publications)
De Schampheleire, Sven, Kathleen De Kerpel, Thomas Deruyter, Peter De Jaeger, and Michel De Paepe. "Experimental study of small diameter fibres as wick material for capillary-driven heat pipes", Applied Thermal Engineering, 2015.

21 < 1% match (student papers from 08-Sep-2015)
Submitted to Universiti Tunku Abdul Rahman on 2015-09-08

22 < 1% match (Internet from 02-Jan-2017)
http://bombaytechnologist.org/index.php/bt/article/download/6/4

23 < 1% match (publications)
Chingulpitak, Sakkarin, Nares Chimres, Kitti Nilpueng, and Somchai Wongwises. "Experimental and numerical investigations of heat transfer and flow characteristics of cross-cut heat sinks", International Journal of Heat and Mass Transfer, 2016.

24 < 1% match (publications)
Reyes, M.. "Experimental and theoretical study of a vapour chamber based heat spreader for avionics applications", Applied Thermal Engineering, 201205

25 < 1% match (publications)

F. Gerard, "Thermoelectric cooling of high power extremely localized heat sources: system aspects", Eighteenth International Conference on Thermoelectrics Proceedings ICT 99 (Cat No 99TH8407) ICT-99, 1999

26 < 1% match (student papers from 12-Aug-2014)
Submitted to Universiti Tunku Abdul Rahman on 2014-08-12

27 < 1% match (student papers from 07-Jun-2013)
Submitted to Monash University Sunway Campus Malaysia Sdn Bhd on 2013-06-07

28 < 1% match (publications)
Lu, Longsheng, Yingxi Xie, Feixiang Zhang, Huosheng Liao, Xiaokang Liu, and Yong Tang. "Influence of a sintered central column on the thermal hydraulic performance of a vapor chamber: A numerical analysis", Applied Thermal Engineering, 2016.

29 < 1% match (student papers from 23-Apr-2012)
Submitted to The University of Manchester on 2012-04-23

30 < 1% match (Internet from 02-Jul-2014)
http://tijst.net/issues/2013/no3/TIJSAT%202013%20No3%20Full.pdf

31 < 1% match (publications)
Li, H.Y.. "Thermal performance of plate-fin heat sinks under confined impinging jet conditions", International Journal of Heat and Mass Transfer, 200705

32 < 1% match (publications)
Aghel, Babak, Masoud Rahimi, and Saeed Almasi. "Heat-transfer enhancement of two-phase closed thermosyphon using a novel cross-flow condenser", Heat and Mass Transfer, 2016.

33 < 1% match (Internet from 06-May-2014)
http://thermalfluidscentral.com/journals/index.php/Heat_Pipes/article/view/287/311

< 1% match (Internet from 16-Dec-2015)

34 http://eprints.aston.ac.uk/21397/1/Studentthesis-2014.pdf

35 < 1% match (publications)
Li, Yong, Zixi Li, Wenjie Zhou, Zhixin Zeng, Yuying Yan, and Bo Li. "Experimental investigation of vapor chambers with different wick structures at various parameters", Experimental Thermal and Fluid Science, 2016.

36 < 1% match (publications)
Renjith Singh, R., V. Selladurai, P.K. Ponkarthik, and A. Brusly Solomon. "Effect of anodization on the heat transfer performance of flat thermosyphon", Experimental Thermal and Fluid Science, 2015.

37 < 1% match (publications)
Tharayil, Trijo, Lazarus Godson Asirvatham, Vysakh Ravindran, and Somchai Wongwises. "Effect of filling ratio on the performance of a novel miniature loop heat pipe having different diameter transport lines", Applied Thermal Engineering, 2016.

38 < 1% match (publications)
Mohan, P.. "Review heat transfer to Newtonian fluids in mechanically agitated vessels", Experimental Thermal and Fluid Science, 199211

39 < 1% match (Internet from 24-Feb-2017)
http://www.dtic.mil/dtic/tr/fulltext/u2/a271458.pdf

40 < 1% match (Internet from 07-Feb-2014)
http://risk.earthmind.net/files/ERN-AL_2011.pdf

41 < 1% match (Internet from 14-Dec-2014)
http://www.science.gov/topicpages/p/paired+fin+skeletons.html

42 < 1% match (Internet from 24-Apr-2016)
http://media.proquest.com/media/pq/classic/doc/2332119251/fmt/ai/rep/NPDF?_s=is4sF8YNmphsdoxO87YpAOJAnzg%3D

43 < 1% match (publications)
Li, H.Y.. "Thermal performance of plate-fin vapor chamber heat sinks", International Communications in Heat and Mass Transfer, 201008

44 < 1% match (publications)
Jeng, Tzer-Ming. "Combined convection and radiation heat transfer of the radially finned heat sink with a built-in motor fan and multiple vertical passages", International Journal of Heat and Mass Transfer, 2015.

45 < 1% match (publications)
Remsburg, . "Convection Heat Transfer in Electronic Equipment", Electronics Handbook Series, 2000.

46 < 1% match (publications)
Tsai, Meng-Chang, Shung-Wen Kang, and Kleber Vieira de Paiva. "Experimental studies of thermal resistance in a vapor chamber heat spreader", Applied Thermal Engineering, 2013.

47 < 1% match (publications)
Jang, Daeseok, Dong Rip Kim, and Kwan-Soo Lee. "Correlation of cross-cut cylindrical heat sink to improve the orientation effect of LED light bulbs", International Journal of Heat and Mass Transfer, 2015.

48 < 1% match (publications)
Wang, Rong-Tsu, and Jung-Chang Wang. "Optimization of heat flow analysis for exceeding hundred watts in HI-LEDs projectors", International Communications in Heat and Mass Transfer, 2015.

49 < 1% match (publications)
Amatachaya, P.. "Comparative heat transfer characteristics of a flat two-phase closed thermosyphon (FTPCT) and a conventional two-phase closed thermosyphon (CTPCT)", International Communications in Heat and Mass Transfer, 201003

50 < 1% match (publications)
Ersöz, Mustafa Ali, and Abdullah Yıldız. "Thermoeconomic analysis of thermosyphon heat pipes", Renewable and Sustainable Energy Reviews, 2016.

paper text:

CHAPTER 1 INTRODUCTION 1.1 Background of Experimental Study Heat pipes are known as the heat transfer devices for transferring of huge amount of the heat efficiently. They are evacuated vessels with high effective thermal conductivity. The cross section is basically circular in shape, and filled up with small amount of the working fluid. This is due to the pipe which is able to transfer the heat effectively through

long distances and had a minimal temperature variation between both the cold ends and hot ends of pipe, or to the isothermalize surfaces. The common material for making heat pipe is copper with an internal wick structure where the wick structure allows the working fluid to flow from condenser to evaporator through capillaries. The distilled water will be act as the fill liquid in the pipe itself. Basically, a heat pipe is divided into condenser and evaporator section which it demonstrate a closed evaporator-condenser system. The heating part in the system is called evaporator section while the cooling part is called condenser section. They are separated by an adiabatic section in between. Compare to solid conductors like aluminum or copper, heat pipes can transfer heat more even as they have got lower total thermal resistance. This is due to the working fluid filled up in heat pipe is in saturation pressure where water will boil at 100oc if it is at atmospheric pressure. During saturation pressure, the water in the heat pipe can boil at any temperature as long as it is above its freezing point. Heat pipes are mainly used in wide range of transferring heat application. For instance, electronic cooling, heat transfer on space application and others are where heat pipes can perform ideally. As such, they are reliable enough to use in many kind of applications due to no moving parts of the pipes. One of the examples of flat heat pipes is called vapor chamber. A vapor chamber (VC) consists of the bottom (evaporator) and upper (condenser) part. The bottom part will absorb heat while upper part which is the evaporator will dissipates heat to the surrounding which is the ambient. Heat transfer occurs from bottom to upper section where the fluid from bottom and then condense at the upper part. The working fluid is recycling in the system of VC. Apart from that, a conventional fin heat sink (FHS) has fins attached at the top of flat metal where the metal is usually covered by aluminum or copper. A typical of FHS- VC heat sink device where the FHS is placed on top the VC as shown in Figure 1. Figure 1: Cross section of a vapor chamber With the aids of cooling fins, the heat will dissipate out efficiently to the ambient. The fins attached act as the large surface area which helps to have better contact with the surrounding air and transfer effectively. VC can improve the cooling of electronic devices better than the traditional design of heat sink from solid base plate attached with fins. The temperature distribution between the traditional solid base plate heat sink attached with fins and the conventional FHS-VC heat sink

18**as shown in Figure** 2 **and** 3. **Figure 2:** Temperature distribution of **heat**

sink with vapor chamber base Figure 3: Temperature distribution of heat sink with solid metal base Research of both heat sinks show the FHS-VC heat sink has better temperature distribution as they are more uniform than traditional solid base plate heat sink. When temperature distribution is more uniform, the overall thermal resistance will be improved. Thermal resistance exists between the bottom of FHS and VC. It is a heat property that resists the transferring of heat across a medium. For instance, during the process occurs in evaporator and condenser. The overall thermal resistance of VC-FHS includes the contact resistance (CR), spreading resistance, resistance of condenser and internal resistance. Likewise, the total thermal resistance created by the bottom part of VC will be minimized when it operate efficiently under the optimal conditions. The good performance of VC that minimizes the overall thermal resistance is used in the thermal management in electronic packaging nowadays. It helps to cool down the components and enhance the overall performance of the devices. In real life, thermal management is crucial especially in electronic industry as high temperature in the electronic device will shorten the life cycle of the components and eventually causes the device failure and leads to degradation. 1.2 Problem Statement Power transistors or Light Emitting Diodes (LEDs) are high power semiconductor devices. They generate a large amount of heat which means to be dissipated to the ambient surrounding. The major problem encountered in thermal management of electronic device is to remove the heat of high power semiconductor devices more efficiently. Industries are searching for efficient and small heat sinks. Therefore, it is crucial to study and to provide a better solution to improve the heat dissipating rate. Thermal engineers are investigating two-phase cooling solutions with the aid of VCs and HPs. Conventional heat sinks with metal base plates do not have enough capacity to cool down the semiconductors. This is because of the hot spots generated on the base of the heat sink resulting high thermal heat spreading resistance. A VC used in conjunction with a conventional heat sink can achieve a better and more even heat flux distribution. This results in increased heat dissipation rate. Heat sink with fins is introduced with VC to increase

16**in the total** surface area **of the** cooling **system. By** incorporating **the heat**

spreading effectiveness of VC

42**and the heat transfer area of the** fins, **the**

overall thermal contact resistance between VC and FHS can be eliminated.

26**1.3 Aims and Objectives The objective in** this research **is to** study **the** thermal **performance of**

VC with embedded multi hollow fins heat sink. Experiments are carried out under natural and forced convection air cooling.

34**1.4 Outline of Thesis CHAPTER 1:** INTRODUCTION **This chapter**

introduce about the conventional heat sink and vapor chamber fin heat sink and its working principles and applications. We discuss the problem arises in electronic industry and the objective of the study. CHAPTER 2: LITERATURE SURVEY This chapter is doing literature survey

12**on:** ▪ **Thermal performance of Vapor Chamber** Finned **Heat Sink** (VC-FHS). ▪ **Heat transfer**

characteristics on Vapor Chamber. ▪ Experiment Study of Grooved Vapor Chamber ▪ Flat thermosyphon and system they work. CHAPTER 3: THEORETICAL INVESTIGATION This chapter discussed on: ▪ Theoretical model of Vapor Chamber Fin Heat Sink ▪ Theoretical calculations to determine the performance of VC-FHS. CHAPTER 4: EXPERIMENTAL INVESTIGATION This chapter discussed on: ▪ Apparatus used in the experiment. ▪ Experimental Procedure and the preliminary investigation. ▪ Experimental Results. CHAPTER 5: DISCUSSION OF RESULTS This chapter discussed on: ▪ Effect of Fill Ratio ▪ Effect of Natural and Forced convection ▪ Effect of Power ▪ Comparison of Vapor Chamber #1 and #2 ▪ Thermal resistance and coefficient of heat transfer ▪ FHS with VC-FHS CHAPTER 6: SUGGESTION FOR FURTHER STUDIES This chapter discussed on the suggestions that can be done for further improvements in future. CHAPTER 7: CONCLUSION This chapter finalizes the whole project by concluding the results of investigation. CHAPTER 2 LITERATURE REVIEW 2.1

1**Thermal Performance of Vapor Chamber** Finned **Heat Sink** (VC-FHS) (Attia **et al,**

2012) carried out experiment investigation on VC with the variation of working fluids by varies the charge ratio. The experiment is tested out to evaluate thermal performance of 2mm high and 50mm diameter VC with methyl alcohol and water with difference of the charge ratios. Furthermore, Propylene Glycol as well as water with two different concentrations which are 15% and 50% was carry out experiment to examine the effect of surfactant to treat as enhancement agent of working fluid. Total thermal resistances to study in this experiment are divided into three parts. They are junction, internal and condenser resistance in order to indentify which part of thermal resistance will give the better effect on the VC thermal resistance. Based on the experiment study shown, water is better compare to methyl alcohol. This is because the total thermal resistance when water as working fluid is lower. When using propylene glycol as the water surfactant, the VC total thermal resistance reduces to about 50% compare to using only pure water. Besides, the 30% charge ratio shows the most significant for all of the working fluids that used to test. Furthermore, the junction resistance shows the greatest value of total thermal resistance which is around 90%. (Jeng, 2015) proposed a novel fin heat sink designed with motor fan and many vertical passages that

could be applied for heat dissipation of LED lamp. There was a total 6 models of finned heat sink being built with different specifications in order to investigate the effects of motor fan, multiple

44**vertical passages and** separation on **the chamber of** the **heat sink**

on heat transfer rate of fin heat sink. Based on Table 1, it shows different specifications of fin heat sink. Model Motor fan Fan's maximum air flow rate (CFM) Multiple vertical passages Separation A - - - - B - - ? ? -? C1 ?? 3.5 ?? -? C2 ?? 3.5 ?? Complete D ?? 5.3 ?? Complete E ? 17.16 ? Complete Table 1: Specifications of finned heat sinks In this study, the Nusselt number (Nu) was took to analyze overall thermal performance of heat sinks. Different models of heat sinks were compared with the power input of 15.48W. The Nu values obtained for models A, B and C1 are similar and significantly lower than model C2 by 22-29% and 41-50% lower than model D and E. The presence of motor fan illustrates the internally forced convection of transferring of heat for the heat sink. The study showed that forced convection has high impact on overall thermal performance of heat sink with fins. (Li et al., 2010) investigate that

25**with the use of** VC compare to **the** conventional **heat sink,**

25**heat transferred** rate **to the** bases of **heat sink**

for VC is more uniform. They carried out experiment by study the performance of VC with plate fins heat sink with the method of infrared thermography. They use vary number of fin, width and height of the fin as well as Reynolds number to investigate on overall thermal performance of VC heat sink. After the experiment, data was computed and compare with the conventional aluminum heat sink. They found out that it is true that VC as base plate can transferred heat evenly more than the conventional type. Overall thermal resistance also shows a decreasing value. At a fixed Reynolds number, with increased fins height, fins width and number of fins, the VC heat sinks would have larger heat transfer area for convection which

gradually reduces thermal resistance of conduction across it. In brief, lower Reynolds number shows greater results with the various dimensions of fin. (Luo et al., 2010) presented a differently VC with coupled fin heat sink. In their research, this particular type VC is carry out experiment and allows to input to high power of the LED light source (20W)for determining the overall performance of VC coupled fin heat sink on heat dissipation for higher power of the LED device.

39**In order to get a better** significant of **the results,**

they compare the results with another fin heat sink device fabricated. The experiment was carried out with two prototypes and results were computed. 20 thermocouples were put and used do the measurement of temperature of PCB board. Results show that VC coupled fin heat sink can get the better heat dissipation rate and the temperature distribute more evenly. The thermal resistance of VC is only 0.05KW. The overall thermal resistance get is 0.654K/W when surrounding temperature reached 27oc. The solution presented are computed and used to solve the hotspot problems of LED appliances to apply in the LED industry. (Michels, Milanez and Mantelli, 2012) presented a prototype of VC heat sink with hollow fins with thin copper tubes to replace the conventional solid fins in order to maximize the fins efficiency. The hollow fins makes the heat transfer is to be larger and will not easily dry out. The experiment was study with forced convection and different fill ratio was being used. They have found that with higher filling ratios which are 25%, 35% and 60%, the thermal resistance values obtained will be significantly lower with increasing heat source output. The lower filling ratio of 15% and 20%, the overall thermal resistance values is larger. With higher heat source output, the heat transfer coefficient will be higher and the higher vapor of mass flow will results in lower thermal resistance. However, with heat source output above 150W, there is a signature of dry-out occurs where condensation is inefficient enough to transfer the condensate to back to VC. Therefore, overall thermal resistance is high. Result shows that the best filling ratio is 25% with lowest thermal resistance which start from 0.12K/W to 0.20K/W. In brief, the prototype presented showed that the VC heat sink with hollow fins could achieve 20% less overall thermal resistance when we compared with conventional solid fins. (Naphonand Wiriyasart, 2015) carry out experiment to determine the thermal performance and heat transfer characteristics of VC in presence and absence of the micro-channel under fixed of the heat flux. Based on the experiment, the model that they are using for VC is attached a two-phase VC along with wick structure. The method they use to carry out experiment is by finite volume method. They computed the temperature distribution of VC with the effect of micro-channel presence or absence. They compared the results obtained and make a conclusion. The conclusion of the experiment obtained is discussed. They found out that the VC with micro-channel shows a greater result on temperature distribution as well as the thermal performance of VC. With the results, designer could be use to improve the design of VC for cooling systems of electronic devices for a better cooling performance in future. (Shih, 2011) invent a heat sink embedded with VC to see the performance of the heat sink. The equipment includes a VC and heat conduction plate. For the heat conduction plate, it has one side formed of radiation fins while two lateral edges formed in another side. The objective of the invention model is to find out a better heat transfer model to increase the cooling effect. In order to save material, they reduce the weight and in order to pull up rate of heat transfer by fabricates particular model with a smaller thickness. However, result shows that with a smaller thickness, the fastening force apply will cause distortion and deform the whole model and this affects the heat transfer effect. Apart from that, there will be a gap between the plate and VC if deformation occurs. This will also affects the performance of the VC. The drawing of invention was use as reference of the drawing for future. (Shukla et al, 2013) investigate the thermal performance of VC without wick with different working fluids. The working fluids used in this experiment is nano fluids. A VC with 64mm width and 78mm length was used to fabricate on thickness of 5mm then it was used to test with aluminum-water as well as the copper-water nano fluids. 30% of the nano fluids were filled in the VC. It is tested with the power input of 90-150W. The motive on the experiment is to present on thermal resistance of VC with 2 of the working fluids. The results of the experiment showed that nano fluids charge of VC perform a better performance than the de-ionized water charge of VC. Based on results obtained in the experiment, the total thermal resistance was reduced about 5% when there was an increase of weight percentage of nano particles. This investigation proves that the VC- heat sink with the filling of nano fluids can collaborate with the components to carry out the function of heat dissipating and use widely in the application of cooling of electronics. (Wang et al, 2011) tested

18**on thermal performance of** a **vapor chamber** with **the** used **of**

window program VCTM V1.0 and apply

13**findings to a high-performance server. The** experiment used a **method from a novel formula** to investigate **the effective thermal conductivity of a**

VC to determine the thermal performance. Throughout findings in the experiment, it can be summarized that copper and aluminum heat spreader has poorer effective thermal conductivities than VC. 100W/cm2 was the maximum heat flux of VC. The thermal conductivity affected by the power input. There are error for the experiment which is not more than ±3%. For one or two dimensional VC, the thermal conductivity is around 100 W/moc which is less than the single solid phase metals. Besides, the thermal conductivity based on three dimensional VC is about 870W/moc which is many times more than copper base plate.

33**(Wong et al, 2010)** investigate **a novel vapor chamber and**

carried out experiment using the vapor chamber. The conventional wick on top plate was replaced by parallel grooves with inter-grooves openings which place at the plate inner surface. While the layer of porous wick place was placed at bottom part of plate as evaporator. The vapor chamber for this experiment was 10cm x 8.9cm. The heating area used was a 0.021m x 0.021m or a 0.011m x 0.011m. The resistance of VC was measured ranging from 80W- 300W. From the results obtained for the heating area of 0.21m x 0.21m, VC

8thermal resistance ranged from 0. 08 K /W to 0. 04 K /W for the

heating power ranged from 80W to 460W. The resistance decreased while the heat source power increased. For the heating area of 0.011m x 0.011m, the VC performance on an area base is

60.14Kcm2/W and the heat flux is 120W/cm2. Based on the

experiment, evaporator resistance of VC resistance was a dominator. Based on the investigation, the

6heat transfer coefficients associated with the evaporation was a few times larger than that associated with the condensation.

2.2 Heat Transfer Characteristics of VC (Kang et al, 2012) study on the uniformity of temperature and the

3heating rate of heat spreader with multi- well. It is simulate and analyze by CFD software on natural convection. In the

study, they used the

3multi-well heat spreader that made up of copper, aluminium, silver and

VC. The four types of multi-well heat spreader are used to simulate and the results was used to compare. They used dual and six heat sources to apply to the

3heating power of 1200W. For six heat sources which is at heating power of

188W, 300W, 600W and 1200W, the heating rate are used to study. Based on the results of simulation, the lower heating power will greatly effect on the surrounding temperature. Hence, the temperature will rise in curve line. With higher heating power there was little effect on the surrounding temperature. The results also prove that six heating sources are better than dual sources as the temperature uniformity is better. From the study, the results obtained from the simulation are vapor chamber multi-well heat spreader shows the greater uniformity, follow by silver, copper and aluminum. (Reyes, Alonso, Arias and Velazquez, 2012) carried out experiment to study the performance of a vertically placed VC based heat spreader with the dimension of 190mm x 140mm x 15mm. It is used in avionics applications. They also study the effect of natural convection as to act as the

24failure mode of the aircraft supply system to be use in the actual design. In the

experiment, they use various heat spreader geometries, with a metal rectangular shape fins heat sink to be the reference model. The result shows that VC heat spreader has the highest performance which they are efficiently spread the heat even though they have a higher weight. It is better compare to the metallic heat sinks counterparts. The surface temperature found was in the range of 80oc to 100oc, and the suitable power input is ranged from 95W to 145W. Apart from that, they also get a conclusion that natural convection shows good performance with the use of VC heat spreader. The results are computed and use to find out the minimum weight that is most suitable to use in the actual design of heat spreader. (Tan et al, 2010) study about the wick structure on FPHP to investigate the performance of liquid flows inside. They used various sources of heat to carry out study which are line, discrete, strip heaters. The Green' function approach are used to simulate. The results were then used to simulate the different heat source used to carry out experiment on the heat pipe. In the research, the analytical liquid flow model in this study was about to show quantitatively on the pressure and velocity distribution on the model with the various heating conditions. The result on the analytical model is able to use to obtain the optimum position of IC chip on PCB so that designer can provide a better position of the chips. (Tsai, Kang and Vieira de Paiva, 2013) have presented a model of a VC

12heat spreader two-phase heat transfer device. This is because the

increasing heat dissipation in electronic packaging that has to be solved for a better future. They have built a prototype of VC with a dimension of 90mm x 90mm x 3.5mm to study its thermal performance by determining the thermal resistances under five different orientations. By analyzing the results obtained, the inclination did not show a clear impact on the temperature uniformity. However, it was found that the VC had the highest resistance of spread which is 0.718K/Wwhile

19total thermal resistance is 0. 89K /W with the inclination of

90º due to the effect of gravity on the VC mechanism. Research shows that spreading resistance that exists between the

15heater and the bottom surface of the VC was affecting the thermal resistance in

big portion. Besides that, they also varied the power input from 5W to 50W and it was found that with increasing power input, the overall thermal resistance of VC will be reduced. Likewise, result indicates

46that spreading resistance act as a crucial role for the overall thermal resistance

as it will affect the higher or lower value of thermal resistance. (Wang et al, 2011) carried out experiments on FPHP to determine the effect of the length on evaporator and condenser that will affect the performance of their model. Experiments were used a FPHP with a heat transfer length and width of 25.5cm and 2.5cm. The working fluid used is water. The results were used to compare with vapor chamber and the traditional heat pipe. From the results obtained, FPHP could achieve a long distance of heat transfer than vapor chamber. It had a big contact area on heat sources when compare with traditional heat pipe. The length of evaporator is proportionally to the heat transfer limit while inversely proportional to thermal resistance. Besides, FPHP will dry out at low heating power when condenser length increases. The closer to the length of condenser and evaporator, the easier to achieve the thermal performance of FPHP. (Wiriyasart et al, 2013) study on the characteristic of transferring of heat on VC that has no Micro-channel to cool the computer processing unit (CPU). The mathematical model of a VC in the investigation is on two-phase closed chamber of presence on wick column and sheet. In their research, pressure as well as temperature distributions of VC was presented using equation of momentum, energy, and continuity to solve. The CPU

30in the experiment is replaced by two heaters as heat source. The input of

power is 80W for heater. The result was compared with the measured data. It was found that the predicted results and the measured data had a difference in 1.4% which is acceptable. The good agreement obtained from the numerical results can be used in future for designer to design a better thermal performance of a VC while remove the trial and error test in future. (Yang et al, 2015) carried out investigation on a new design of flat polymer heat pipe. The purpose of the investigation was to determine

how much heat can be eliminating based on the heat source with various conditions. The design of the heat pipe is 1mm of thickness for the copper frame which in between the up and down of FR4 polymer for getting a VC. Table 2 showed the five of the flat heap pipes specifications. Case Thermal via Filling ratio (%) Weight (g) A - 36 6.87 B ?? 0 8.37 C ?? 20 8.57 D ?? 28 8.65 E ?? 36 8.73 Table 2: Specifications of flat heat pipes The heat pipe overall thermal resistance was used a TDIM method to measure which known as transient dual interface method. Based on experiment results obtained, the heat pipe containing working fluid will minimize the thermal resistance compared to the heat pipe with the absence of working fluid. With input power of 6-16W, the thermal resistance of filling ratio of 28% is the lowest. Overall using the system to measure the total thermal resistance, a reduction of 57% achieved. (Yu et al, 2012) study the performance of a FPHP heat spreader by using different wick structures. The experiment was conducted with various parameters ranging from 5W to 20W. Eight varieties of wick were used during the experiment to determine the optimum wick. A variety of liquids was used to carry out the experiment as working fluids. For instance, water, acetone, ethanol, TiO2 nanofluids. The results obtained shows that TiO2nanofluids was the best working fluid as it showed the best heat spreading performance of FPHP heat spreader. The best filling ratio was about 50% to 60%. By using the present study of experiment, a simulation was conducted. In brief, simulation results give a strong agreement with present research. 2.3 Experiment Study of Grooved Vapor Chamber (Zhang et al, 2009) study on a new design of grooved VC. VC with grooves structure helps to achieve better radial as well as axial heat transfer. Besides, the study shows that the structure can form capillary loop between the condenser and evaporator surfaces. In the experiment, effect of fill ratio, heat flux as well as the performance of VC was studies. The working fluid used in the experiment was water. The faces for condenser and evaporator have a diameter and thickness of 8.5cm and 0.3cm. The depth and width of the grooves are 0.03cm and 0.02cm. Based on results obtained, VC achieves better performance from fill ratio of working fluid with the weight of 1 to 2g where the optimal amount is 1.43g where the liquid was filled for 40.4%. The heat flux attached with the particular working fluid ratio was 3.05 x 105W/m2. The experimental results were used to compare with numerical simulation results to show reliability. 2.4 Thermal Performance of Flat Thermosyphon (Zhang et al, 2008)

do research to investigate thermal performance of flat thermosyphon. In the study, they used a transparent two phase thermosyphon to study and observe. The area of study in this experiment was characteristics of phase change of heat transfer, performance with various fill ratios and the surface of evaporator to groove. Based on the experiment, it was found that the water shows the best results compare to ethanol. Thermal resistance when using ethanol as working fluid is higher than using of water. Moreover, the thermal resistance will decrease when the heating flux increases. Besides, the presence of grooved surface shows better transferring of heat compare with the absence of grooved. In brief, the two phase thermosyphon gives a good result of leveling the temperature at condenser surface. CHAPTER 3 THEORETICAL INVESTIGATION 3.1 Theoretical Model The model that investigates in this thesis is vapor chamber with multi hollow fins heat sink. VC with multi hollow fins heat sink is a type of 2 dimensional flows VC which the bottom part of the VC acts as the evaporator and the fins act as the condenser. The distilled water that filling up the VC will undergoes evaporation and evaporates through the evaporator to the fins as water vapor. When the water vapor reaches the fins which are the condensers, they will condense back to the evaporator in liquid. This causes the recycling occurs. The power input from the heating element to the base of the VC with an aluminum block place between them. VC will acts as the heat spreader to spread out the heat to the fins when power input. During the heat spreading process, there are thermal resistance exist. The thermal resistances includes are resistance of the fins (Rfin) and resistance of VC (Rvc)

> 17**as shown in Figure** 4. **The** overall **thermal resistance is**

the sum of the two resistances and it has to be reduced or minimize in order to maximize the efficiency of VC so that the heat transfer process happens more effective. (a) Cross-section of VC. (b) Resistance network of VC. Figure 4: Thermal Resistance Network Besides, during the heat spreading process, we also discovered about the convection

> 5**heat transfer coefficient. It is a quantitative characteristic of** convection occurs in **heat transfer between a fluid medium and the** wall **surface flowed over by fluid. It** depends mainly **on the** thermal properties **of**

a medium and the thermal boundary conditions. The SI unit for overall heat transfer coefficient is W/m2K. There are numerous methods and formulas that can be used to calculate ha. In the study of this case, we only used two formulas

> 38**for the calculation of** hfin which are **the heat transfer** coefficient **of the**

fins. The formulas are discussed later on. 3.2 Theoretical Calculations

> 11**Power input to the electric heater,** PEH **is calculated** by **using**

Ohm's Law Formula. PEH = VI (1) Where V is the voltage input, V I is the current input, I The formulas to compute thermal resistance of the VC with multi hollow fins heat sink are as shown: RVC = ThsP−ETHfin (2) Rfin = TfinP−ETHamb (3) Rtotal = RVC + Rfin (4) Where Rvc is the

> 35**resistance of the VC,** K/W Rfin **is the** resistance **of the** multi hollow fins **heat**

sink, K/W Rtotal is the total

> 28**thermal resistance, K/W Ths is the temperature** of evaporator, ℃ Tevap **is the temperature of**

VC heat sink, ℃ Tfin

> 31**is the temperature of the** multi hollow fins **heat sink** (condenser), ℃ Tamb **is the** ambient **temperature, ℃ The**

formulas to compute the heat transfer coefficient of fin, hfin of VC with multi hollow fins heat sink are as shown: Afin = Nfins(πDfinLfin) (5) Abase = πD2 (Nfins) 4 (6) Aplate = 2(1 + √2)α2 (7) ∑A = Aplate − Abase + Afin (8) hfin = Rfin∑A 1 (9) hfin = ∑A(TfPinE−HTamb) (10) Where Nfinsis the number of fin Dfin is the diameter of the fin, m Lfin is the height or the length of the fin, m Afin is the area of the fin, m2 Abase is the base area of the fin, m2 Aplate is the area of the copper plate, m2 ∑Ais the total area of condenser, m2 CHAPTER 4 EXPERIMENTAL INVESTIGATION 4.1 Experimental Set Up The experiment investigation carried out by using two VCFHSs fabricated from 55 mm O/D x 1 mm thick x 35 mm long copper transition sockets capped with 1 mm thick copper plates on top. An array of 1 mm thick x 10 mm OD copper tubes were brazed on the copper plate in a radial symmetrical pattern to act as fins. There are eight tubes each

25 mm long in VC#1 and four tubes each 35 mm long in VC#2. Attachments were provided at the top of the central tube in each of the VC to fit vacuum gauges and to provide connections to a vacuum pump. Figure 5 shows the VC #1 and VC#2 with hollow copper tubes that built to help to determine the result. Figure 5: Vapor chamber with embedded hollow condenser tube heat sink The apparatus set up in the experiment is to determine the influence of different fill ratio of water in the copper ring on natural and forced convection, different power input on the heating element on natural and forced convection. We determine the suitable fill ratio and power input that minimize the overall thermal resistance. The same VC is used when carried out the experiment with different fill ratio of water. The fill ratio that used in this experiment is fill ratio of 1 and 0.5 respectively. The equipments that used to conduct the experimental setup are thermocouples, control valve, pressure gauge, aluminum block, aluminum string, thermal paste, insulation wool, heating element, voltmeter, ammeter, voltage regulator, data logger and cooling fan. The VC with multi hollow fins heat sink attached to the aluminum block and then to heating element with thermal paste applied in between. Thermal paste is a heat conductive paste that able to provide a better surface contact by

minimizing the air trapped in between two

15**surfaces. In order to** minimize the **heat loss to the**

surrounding during the experiment, the VC heat sink is insulated with insulating wool with only the multi-hollow-fins heat sink and the octagonal shape copper plate being exposed. The voltage regulator is connected to the heating element and the power input is determined by measuring the

37**voltage and current** input **using voltmeter and ammeter** respectively according **to the**

formula (P=VI). A pressure gauge

20**is used to measure the** vapor pressure inside **the** VC **heat sink**

and a control valve attached is closed during the experiment to prevent air flow and keep the VC heat sink held in vacuum state. Data logger is used to record the temperature of thermocouples attached on the VC. The VCFHS was heated with a 50 mm diameter electric heating element. A 50 mm diameter x 10 mm thick aluminium block inserted in between the heating element and the VCFHS ensured uniform heating. Power input was measured with ac voltmeter and ammeter. Insulation was provided all around as shown. Figure 6 shows the schematic diagram of the experimental setup. Fan * Hollo w fins Cooling Vapor chamber A Aluminium V + - Heat source Block Insulation ion Figure 6: Schematic Diagram of the Experimental Setup Natural convection of the experiment carries out with normal air flow in the air conditional room. A cooling fan is used for the forced convection experiment with different power input and fill ratio of water.

8**It is to** enhance **the** convective **heat transfer** process throughout **the** VC **heat sink.** When **the**

boiling and evaporating rate of the VC is greater than the condensing, dry out condition will occurs and results in lower composition of distilled water after a long run due to the trapping of water in the hollow copper tubes that unable to flow back to the vapor chamber of the evaporator section. Figure 7 and 8 shows the experimental setup for natural and forced convection. Pressure Gauge Vapor Chamber G-Clamp Insulation Wool Thermocouples Figure 7: Photograph of experimental set up (Natural convection) Cooling Fan Vapor Chamber Pressure G-Clamp Gauge Thermocouples Insulation Wool Figure 8: Photograph of experimental set up (Forced convection) For VC #1, the experiment carried out used a total of 20 thermocouples placed in different position in order to measure the temperature. For VC #2, the experiment carried out using 16 thermocouples. Figure 9 shows the schematic diagram for the locations of the thermocouples for VC#1. Type T (copper-constanten) thermocouples (+ 0.5oC accuracy) were employed to measure temperatures. Four temperature probes were inserted into grooves machined on the aluminum block to measure the heating surface temperatures (Ths). Other thermocouples were mechanically attached with binding wire and thermal paste to measure the surface

4**temperatures. Ambient temperature (Tamb) and insulation surface temperatures**

(Tins) were measured by other thermocouple probes as shown. Ambient

4**temperature was not controlled** and **varied by about + 1.**

0oC. All thermocouple readings were recorded on a Graphtec multi-point millivolt recorder. Figure 9: Schematic diagram showing the locations of thermocouples 4.2 Experimental Procedure Experiments

21**were carried out to determine** the **thermal resistance** across **the**

VC (RVC)

2**and the thermal resistance of the** multi hollow fins **heat sink**

(Rfin) under natural convection with low and high power. The experiments were conducted by using the same VC but with different fill ratio of water, which is fill ratio 1.0 and 0.5. 1. VC was filled with 100% of distilled water using syringe with needle. 2. VC was vacuumed for 1 hour using vacuum pump to ensure it is kept in vacuum condition. 3. VC was left inside the lab for a day to ensure that no leakage occurs. 4. VC is being insulated using insulation

14**wool to minimize** the **heat loss to the** surrounding during **the experiment.**

5. Data logger was switched on to check the initial temperature of all the thermocouples (T1-T20). 6. Voltage regulator was being switched on to provide power input of 10W to the heating element attached to the VC. 7. The voltage input, current input, actual power input and initial pressure were recorded. 8. The apparatus was left under natural convection for 2.5 hours. 9. After 2.5 hour, the thermocouples' temperature shown in the data logger was recorded (T1-T20). 10. The

9**thermal resistance of** VC (RVC) **and the thermal resistance of the** multi hollow fins **heat**

sink (Rfin) were calculated. 11. Steps 6 to 10 were repeated with power input of 20W. 12. Steps 1 to 11 were repeated by using fill ratio of 0.5. 13. Steps 1 to 12 were repeated by using VC #2. Experiments

21**were carried out to determine** the **thermal resistance** across **the**

VC (RVC),

2**and the thermal resistance of the** multi hollow fins **heat sink**

(Rcond) under forced convection with low and high power. The experiments were conducted by using the same VC but with different fill ratio of water, which is fill ratio 1.0 and 0.5. 1. VC was filled with 100% of distilled water using syringe with needle. 2. VC was vacuumed for 1 hour using vacuum pump to ensure it is kept in vacuum condition. 3. VC was left inside the lab for a day to ensure that no leakage occurs. 4. VC is being insulated using insulation

14**wool to minimize** the **heat loss to the** surrounding during **the experiment.**

5. Data logger was switched on to check the initial temperature of all the thermocouples (T1-T20). 6. Voltage regulator was being switched on to provide power input of 10W to the heating element attached to the VC. 7. A fan was positioned with an angle of 10o to the plane to maximize the efficiency of heat transfer process. 8. The voltage input, current input, actual power input and initial pressure were recorded. 9. The apparatus was left under forced convection for 2 hours. 10. After 2 hour, the thermocouples' temperature shown in the data logger was recorded (T1-T20). 11. The

shown in the data logger was recorded (T1-T20). 11. The

> 9**thermal resistance of** VC (RVC) **and the thermal resistance of the** multi hollow fins **heat**

sink (Rfin) were calculated. 12. Steps 6 to 11 were repeated with power input of 20W. 13. Steps 1 to 12 were repeated by using fill ratio of 0.5. 14. Steps 1 to 13 were repeated by using VC #2. 4.3 Experimental Results

> 10**Experiments were** performed **with power inputs** (PEHs) of **10 and 20 W under** both **natural convection (NC) and forced convection (FC) air cooling**

modes. At each power setting, temperatures were recorded until steady state was reached. Experiments were repeated three times to determine repeatability of results. Results were found to be repeatable to be better than + 1.0oC. A summary of the experimental runs conducted and the operating conditions are tabulated in Table 1. Mean average evaporator (Tevap), fin (Tfin) and heating surface (Ths) temperatures are shown in Table 3. Insulation surface temperature (Tins) varied from 20 - 27oC, depending upon cooling modes and power input.The

> 40**summary of the results** is tabulated **in Table 4. The**

graphs were plotted on the temperature and resistance distribution to show the effect of input power, natural and forced convection and fill ratio of water for both VC. Besides, we plotted graphs which compare the thermal performance of both VC to determine which to choose There are a total of 42 graphs for this experimental investigation. Figure 10: Transient Temperature of Tfin for VC#1 under NC and FR=1.0 (Runs#1&2) Figure 11: Transient Temperature of Tevap for VC#1 under NC and FR = 1.0(Runs#1&2) Figure 12: Transient Temperature of Ths for VC#1 under NC and FR = 1.0 (Runs#1&2) Figure 13: Transient Temperature of Tfin for VC#1 under FC and FR = 1.0 (Runs #3 & 4) Figure 14: Transient Temperature of Tevap for VC#1 under FC and FR = 1.0 (Runs#3&4) Figure 15: Transient Temperature of Ths for VC#1under FC and FR = 1.0 (Runs#3&4) Figure 16: Transient Temperature of Tfin for VC#1 under NC and FR = 0.5 (Runs#5&6) Figure 17: Transient Temperature of Tevap for VC#1 under NC and FR = 0.5 (Runs#5&6) Figure 18: Transient Temperature of Ths for VC#1 under NC and FR = 0.5 (Runs#5&6) Figure 19: Transient Temperature of Tfin for VC#1 under FC and FR = 0.5 (Runs#7&8) Figure 20: Transient Temperature of Tevap for VC#1 under FC and FR = 0.5 (Runs#7&8) Figure 21: Transient Temperature of Ths for VC#1under FC and FR = 0.5 (Runs#7&8) Figure 22: Temperature distribution showing effect of Power Input (PEH) and Convection (NC/FC) for FR = 1.0 [VC#1] Figure 23: Temperature distribution showing effect of Power Input (PEH) and Convection (NC/FC) for FR = 0.5 [VC#1] Figure 24: Temperature distribution showing effect of Power Input (PEH) and Fill Ratio (FR) under Natural Convection [VC#1] Figure 25: Temperature distribution showing effect of Power Input (PEH) and Fill Ratio (FR) under Force Convection [VC#1] Figure 26: Effect of Power Input (PEH) and Convection (NC/FC) on Thermal Resistance for FR = 1.0 [VC#1] Figure 27: Effect of Power Input (PEH) and Convection (NC/FC) on Thermal Resistance For FR = 0.5 [VC#1] Figure 28: Effect of Power Input (PEH) and Fill Ratio (FR) on Thermal Resistance on NC [VC#1] Figure 29: Effect of Power Input (PEH) and Fill Ratio (FR) on Thermal Resistance on FC [VC#1] Figure 30: Transient Temperature of Tfin for VC#2 under NC and FR=1.0 (Runs#9&10) Figure 31: Transient Temperature of Tevap for VC#2 under NC and FR=1.0 (Runs#9&10) Figure 32: Transient Temperature of Thsfor VC#2 under NC and FR=1.0 (Runs#9&10) Figure 33: Transient Temperature of Tfin for VC#2 under FC and FR=1.0 (Runs#11&12) Figure 34: Transient Temperature of Tevap for VC#2 under FC and FR=1.0 (Runs#11&12) Figure 35: Transient Temperature of Thsfor VC#2 under FC and FR=1.0 (Runs#11&12) Figure 36: Transient Temperature of Tfin for VC#2 under NC and FR=0.5 (Runs#13&14) Figure 37: Transient Temperature of Tevap for VC#2 under NC and FR=0.5 (Runs#13&14) Figure 38: Transient Temperature of Thsfor VC#2 under NC and FR=0.5 (Runs#13&14) Figure 39: Transient Temperature of Tfin for VC#2 under FC and FR=0.5 (Runs#15&16) Figure 40: Transient Temperature of Tevap for VC#2 under FC and FR=0.5 (Runs#15&16) Figure 41: Transient Temperature of Thsfor VC#2 under FC and FR=0.5 (Runs#15&16) Figure 42: Temperature distribution showing effect of Power Input (PEH) and Convection (NC/FC) for FR = 1.0 [VC#2] Figure 43: Temperature distribution showing effect of Power Input (PEH) and Convection (NC/FC) for FR = 0.5 [VC#2] Figure 44: Temperature distribution showing effect of Power Input (PEH) and Fill Ratio (FR) under Natural Convection [VC#1] Figure 45: Temperature distribution showing effect of Power Input (PEH) and Fill Ratio (FR) under Force Convection [VC#2] Figure 46: Effect of Power Input (PEH) and Convection (NC/FC) on Thermal Resistance for FR = 1.0 [VC#2] Figure 47: Effect of Power Input (PEH) and Convection (NC/FC) on Thermal Resistance for FR = 0.5 [VC#2] Figure 48: Effect of Power Input (PEH) and Fill Ratio (FR) on Thermal Resistance on NC [VC#2] Figure 49: Effect of Power Input (PEH) and Fill Ratio (FR) on Thermal Resistance on FC [VC#2] Figure 50: Total Thermal Resistance showing effect of Fill Ratio for VC1 & VC2 under Natural Convection Figure 51: Total Thermal Resistance showing effect of Fill Ratio for VC1 & VC2 under Force Convection 32 Run # VC FR NC/FC Peh(W) Psat(psi) Tsat(oc) Tamb(oc) Tins1(oc) Tins2(oc) Tevap(oc) Tfin(oc) Ths(oc) Rfin(K/W) Rvc(K/W) ∑R(K/W) hfin 1. a b c Avg 1 1 NC 10 2.5 56.5 22.1 22 21.6 21.9 25.3 24.8 23.2 24.4 26.6 26.2 25.2 26 69.6 68.6 68.2 68.8 61.6 60.5 60.8 61 73.5 72.6 72.5 72.9 4 3.9 3.9 3.9 1.2 1.2 1.2 1.2 5.2 5.1 5.1 5.1 26 2. a b c Avg 20 11 92.1 22.3 22.4 22.2 22.2 26.4 26.3 26 26.2 28 27.5 26.7 27.4 106.2 105.3 105.8 105.8 92.5 92.6 93 92.7 112.8 112 112.5 112.4 3.5 3.5 3.5 3.5 1.0 1.0 1.0 1.0 4.5 4.5 4.5 4.5 29 3. FC 10 0.5 26.4 21.3 21.5 23.4 36.8 29.7 40.6 0.8 1.1 1.9 127 4. 20 1 38.7 21.3 21.9 24.7 49.8 37.8 57.3 0.8 1.0 1.8 127 5. 0.5 NC 10 2 52.2 21.9 24.1 25 65.8 58.4 69.6 3.7 1.1 4.8 27 6. 20 10 89.5 22 25.6 27.7 98.4 85.1 105.5 3.2 1.0 4.3 32 7. FC 10 0.5 26.4 21.4 22.4 24.3 42.9 35.3 46 1.4 1.1 2.5 73 8. 20 1 38.7 21.9 23.4 24.9 62.5 49.9 70.7 1.4 1.0 2.4 73 9. a b c Avg 2 1 NC 10 2.2 54.2 19.5 19.4 21 20 20.7 20.8 22.9 21.5 23.6 23.5 24.4 23.8 65.3 64.2 66.2 65.2 61 60.8 62.6 61.5 69.7 69.6 70.9 70 4.2 4.1 4.2 4.2 0.9 0.9 0.8 0.9 5.1 5 5 5.1 30 10. a b c Avg 20 9.5 88.2 19.6 19.4 21 20 21.7 21.8 22.9 22.1 26.6 26.5 27.4 26.8 108.4 108.1 107.9 108 99.2 98.4 99.2 98.9 114.8 114.7 115.2 114.9 4 3.9 3.9 3.9 0.8 0.8 0.8 0.8 4.8 4.8 4.7 4.7 32 11. FC 10 0.5 26.4 20.2 20 21.7 35.7 30.9 39.7 1.1 0.9 2 114 12. 20 1 38.7 20.8 21.4 22.9 53.9 42 61.1 1.1 0.9 2 114 13. 0.5 NC 10 2 52.2 22.6 23.6 25.2 64.4 61.4 69.4 3.9 0.8 4.7 33 14. 20 9 86.8 22.2 23.2 26.8 104.9 96.1 112.9 3.7 0.8 4.5 34 15. FC 10 0.5 26.4 20.5 20 23.4 36.3 29.9 42 0.9 1.2 2.1 140 16. 20 1 38.7 20.5 20 23.7 53.2 40.7 63.9 1.0 1.1 2.1 126 13(2) NC 10 2 52.2 22.4 23.4 25.1 67.2 61.5/63.4* 71.8 3.9/4.1* 1/0.8* 4.9/4.9* 32/31* 14(2) Run# VC# FR NC/FC PEH(W) Tamb(oc) Tins1(oc) 20 9 86.8 22.5 Tins2(oc) Tfin(oc) Tevap(oc) Ths 23.3 25.9 105.3 96.7/99.8* (oc) Rfin(K/W) RVC(K/W) 113.4 3.7/3.9* 0.8/0.7* 4.5/4.6* 34/32* ∑R(K/W) hfin Table 3: Experimental Results 33 1 1 1 NC 10 21.9 24.4 26 61 68.6 72.9 3.9 1.2 5.1 26 2 20 22.2 26.2 27.4 92.7 105.8 112.4 3.5 1.0 4.5 29 3 FC 10 21.3 21.5 23.4 29.7 36.8 40.6 0.8 1.1 1.9 127 4 20 21.3 21.9 24.7 37.8 49.8 57.3 0.8 1.0 1.8 127 5 0.5 NC 10 21.9 24.1 25 58.4 65.8 69.6 3.7 1.1 4.8 27 6 20 22 25.6 27.7 85.1 98.4 105.5 3.2 1.0 4.3 32 7 FC 10 21.4 22.4 24.3 35.3 42.9 46 1.4 1.1 2.5 73 8 20 21.9 23.4 24.9 49.9 62.5 70.7 1.4 1.0 2.4 73 9 2 1 NC 10 20 21.5 23.8 61.5 65.2 70 4.2 0.9 5.1 30 10 20 20 22.1 26.8 98.9 108 114.9 3.9 0.8 4.7 32 11 FC 10 20.2 20 21.7 30.9 35.7 39.7 1.1 0.9 2 114 12 20 20.8 21.4 22.9 42 53.9 61.1 1.1 0.9 2 114 13 0.5 NC 10 22.6 23.6 25.2 61.4 64.4 69.4 3.9 0.8 4.7 33 14 20 22.2 23.2 26.8 96.1 104.9 112.9 3.7 0.8 4.5 34 15 FC 10 20.5 20 23.4 29.9 36.3 42 0.9 1.2 2.1 140 16 20 20.5 20 23.7 40.7 53.2 63.9 1.0 1.1 2.1 126 Table 4: Summary of the Experimental Results 120 100 T emperature (oc) 80 60 40 20 0 P = 10W P = 20W 0 40 80 120 160 200 240 280 320 360 Time (min) Tfin1 Tfin2 Tfin3 Tfin4 Tfin5 Tfin6 Tfin7 Tfin8 Figure 10: Transient Temperature of Tfin for VC#1 under NC and FR = 1.00 (Runs #1 & 2). 120 T emperature (oc) 100 80 60 40 Tevap1 Tevap2 Tevap3 20 P = 10W P = 20W Tevap4 0 0 40 80 120 160 200 240 280 320 360 Time (min) Figure 11: Transient Temperature of Tevap for VC#1 under NC and FR = 1.00 (Runs #1 & 2). 120 T emperature (oc) 100 80 60 P = 20W Ths1 Ths2 40 P = 10W Ths3 20 Ths4 0 0 40 80 120 160 200 240 280 320 360 Time (min) Figure 12: Transient Temperature of Ths for VC#1 under NC and FR = 1.00 (Runs #1 & 2). 100 T emperature (oc) 80 60 P = 10W P = 20W 40 20 0 0 10 20 30 40 50 60 70 80 90 100 110 120 Time (min) Tfin1 Tfin2 Tfin3 Tfin4 Tfin5 Tfin6 Tfin7 Tfin8 Figure 13: Transient Temperature of Tfin for VC#1 under FC and FR = 1.00 (Runs #3 & 4). 120 100 Temperature (oc) 80 60 P = 10W P = 20W Tevap1 40 20 0 Tevap2 Tevap3 Tevap4 0 10 20 30 40 50 60 70 80 90 100 110 120 Time (min) Figure 14: Transient Temperature of Tevap for VC#1 under FC and FR = 1.00 (Runs #3 & 4). 120 100 Temperature (oc) 80 P = 10W P = 20W Ths1 60 40 20 0 Ths2 Ths3 Ths4 0 10 20 30 40 50 60 70 80 90 100 110 120 Time (min) Figure 15: Transient Temperature of Ths for VC#1 under FC and FR = 1.00 (Runs #3 & 4) 100 Temperature (oc) 80 60 40 20 0 P = 10W P = 20W 0 20 40 60 80 100 120 140 160 180 200 220 240 Time (min) Tfin1 Tfin2 Tfin3 Tfin4 Tfin5 Tfin6 Tfin7 Tfin8 Figure 16: Transient Temperature of Tfin for VC#1 under NC and FR = 0.5 (Runs #5 & 6). 120 100 Temperature (oc) 40 80 60 Tevap1 Tevap2 Tevap3 20 0 P = 10W P = 20W Tevap4 0 20 40 60 80 100 120 140 160 180 200 220 240

Time (min) Figure 17: Transient Temperature of Tevap for VC#1 under NC and FR = 0.5 (Runs #5 & 6). 120 100 Temperature (oc) 80 60 Ths1 Ths2 40 20 0 P = 10W P = 20W Ths3 Ths4 0 20 40 60 80 100 120 140 160 180 200 220 240 Time (min) Figure 18: Transient Temperature of Ths for VC#1 under NC and FR = 0.5 (Runs #5 & 6) 100 Temperature (oc) 60 80 P = 20W 40 20

220 P = 10W 0 10 20 30 40 50 60 70 80 90 100 110 120 Time (min)

Tfin1 Tfin2 Tfin3 Tfin4 Tfin5 Tfin6 Tfin7 Tfin8 Figure 19: Transient Temperature of Tfin for VC#1 under FC and FR = 0.5 (Runs #7 & 8). 120 100 Temperature (oc) 80 P = 20W 60 P = 10W 40 20 0 0 10 20 30 40 50 60 70 80 90 100 110 120 Time (min) Tevap1 Tevap2 Tevap3 Tevap4 Figure 20: Transient Temperature of Tevap for VC#1 under FC and FR = 0.5 (Runs #7 & 8). 120 100 P = 20W Temperature (oc) 80 60 40 20 0 P = 10W Ths1 Ths2 Ths3 Ths4 0 10 20 30 40 50 60 70 80 90 100 110 120 Time (min) Figure 21: Transient Temperature of Ths for VC#1 under FC and FR = 0.5 (Runs #7 & 8). FR=1.0 T emperature (oc) 100 P = 20W 80 } NC 60 P = 10W 40 P = 20W } FC 20 P = 10W 0 Tamb Tins1 Tins2 Tfin Tevap Ths Figure 22: Temperature distribution showing effect of Power Input (PEH) and Convection (NC/FC) for FR = 1.0 120 FR = 0.5 T emperature (oc) P = 20W 80 } NC 100 60 P = 10W } P = 20W FC 40 P = 10W 20 0 Tamb Tins1 Tins2 Tfin Tevap Ths Figure 23: Temperature distribution showing effect of Power Input (PEH) and Convection (NC/FC) for FR = 0.5 100 Natural Convection FR=1.0 } 20W T emperature (oc) 80 FR=0.5 60 FR=1.0 } 10W 40 FR=0.5 20 0 Tamb Tins1 Tins2 Tfin Tevap Ths Figure 24: Temperature distribution showing effect of Power Input (PEH) and Fill Ratio (FR) for Natural Convection 120 Force Convection 100 T emperature (oc) 80 60

7FR=0.5 } 20W 40 FR=1.0 FR=0.5 } 10W FR=1.0

20 0 Tamb Tins1 Tins2 Tfin Tevap Ths Figure 25: Temperature distribution showing effect of Power Input (PEH) and Fill Ratio (FR) under Force Convection FR = 1.0 Thermal Resistance (K/W) 5 4 P = 10W } NC P = 20W 3 P = 10W } FC 2 P = 20W 1 0 Rvc Rfin ∑R Figure 26: Effect of Power Input (PEH) and Convection (NC/FC) on Thermal Resistance for FR = 1.0 6 FR = 0.5 Thermal Resistance (K/W) 5 P = 10W } NC 4 P = 20W 3 } FC 2 P = 10W P = 20W 1 0 Rvc Rfin ∑R Figure 27: Effect of Power Input (PEH) and Convection (NC/FC) on Thermal Resistance for FR = 0.5 Natural Convection Thermal Resistance (K/W) 5 } 10W FR=1

7.0 FR=0.5 4 } 20W FR=1.0 FR=0.5

3 2 1 0 Rvc Rfin ∑R Figure 28: Effect of Power Input (PEH) and Fill Ratio (FR) on Thermal Resistance on NC 6 Force Convection Thermal Resistance (K/W) 5 4 3 P=10W } FR=0.5 2 P=20W P=10W } FR=1.0 1 P=20W 0 Rvc Rfin ∑R Figure 29: Effect of Power Input (PEH) and Fill Ratio (FR) on Thermal Resistance on FC 120 100 T emperature (oc) 80 60 Tfin1 Tfin2 40 Tfin3 P= 10W P= 20W Tfin4 20 0 0 20 40 60 80 100 120 140 160 180 200 220 240 Time (min) Figure 30: Transient Temperature of Tfin for VC#2 under NC and FR = 1.00 (Runs #9 & 10). 120 T emperature (oc) 100 80 60 40 20 Tevap1 Tevap2 Tevap3 Tevap4 0 P= 10W P= 20W 0 20 40 60 80 100 120 140 160 180 200 220 240 Time (min) Figure 31: Transient Temperature of Tevap for VC#2 under NC and FR = 1.00 (Runs #9 & 10). 120 100 T emperature (oc) 80 60 40 Ths1 Ths2 Ths3 Ths4 20 P= 10W P= 20W 0 0 20 40 60 80 100 120 140 160 180 200 220 240 Time (min) Figure 32: Transient Temperature of Ths for VC#2 under NC and FR = 1.00 (Runs #9 & 10). 100 T emperature (oc) 80 60 Tfin1 P= 10W P= 20W Tfin2 40 Tfin3 Tfin4 20 0 0 10 20 30 40 50 60 70 80 90 100 110 120 Time (min) Figure 33: Transient Temperature of Tfin for VC#2 under FC and FR = 1.00 (Runs #11 & 12). 120 100 T emperature (oc) 80 60 P= 10W Tevap1 Tevap2 40 20 0 P= 20W Tevap3 Tevap4 0 10 20 30 40 50 60 70 80 90 100 110 120 Time (min) Figure 34: Transient Temperature of Tevapfor VC#2 under FC and FR = 1.00 (Runs #11 & 12). 120 100 Temperature (oc) 80 60 40 Ths1 Ths2 Ths3 Ths4 20 P= 10W P= 20W 0 0 10 20 30 40 50 60 70 80 90 100 110 120 Time (min) Figure 35: Transient Temperature of Ths for VC#2 under FC and FR = 1.00 (Runs #11 & 12). 100 T emperature (oc) 80 60 40 Tfin1 Tfin2 Tfin3 20 0 P= 10W P= 20W Tfin4 0 20 40 60 80 100 120 140 160 180 200 220 240 Time (min) Figure 36: Transient Temperature of Tfin for VC#2 under NC and FR = 0.5 (Runs #13 & 14). 120 100 Temperature (oc) 80 60 Tevap1 Tevap2 P= 10W P= 20W 40 Tevap3 Tevap4 20 0 0 20 40 60 80 100 120 140 160 180 200 220 240 Time (min) Figure 37: Transient Temperature of Tevap for VC#2 under NC and FR = 0.5 (Runs #13 & 14). 120 100 Temperature (oc) 80 60 Ths1 P= 10W P= 20W Ths2 40 Ths3 Ths4 20 0 0 20 40 60 80 100 120 140 160 180 200 220 240 Time (min) Figure 38: Transient Temperature of Ths for VC#2 under NC and FR = 0.5 (Runs #13 & 14). 100 T emperature (oc) 80 60 P= 10W P= 20W Tfin1 Tfin2 40 20 0 Tfin3 Tfin4 0 10 20 30 40 50 60 70 80 90 100 110 120 Time (min) Figure 39: Transient Temperature of Tfin for VC#2 under FC and FR = 0.5 (Runs #15 & 16). 120 100 T emperature (oc) 80 P= 10W P= 20W Tevap1 60 40 20 0 Tevap2 Tevap3 Tevap4 0 10 20 30 40 50 60 70 80 90 100 110 120 Time (min) Figure 40: Transient Temperature of Tevapfor VC#2 under FC and FR = 0.5 (Runs #15 & 16). 120 100 Temperature (oc) 80 60 40 Ths1 Ths2 Ths3 Ths4 P= 10W P= 20W 20 0 0 10 20 30 40 50 60 70 80 90 100 110 120 Time (min) Figure 41: Transient Temperature of Ths for VC#2 under FC and FR = 0.5 (Runs #15 & 16). FR=1.0 T emperature (oc) 100 80 P = 20W, NC P = 10W, NC 60 40 P = 20W, FC 20 P = 10W, FC 0 Tamb Tins2 Tfin Tevap Ths Figure 42: Temperature distribution showing effect of Power Input (PEH) and Convection (NC/FC) for FR = 1.0 120 100 FR=0.5 T emperature (oc) 80 P = 20W, NC 60 P = 10W, NC 40 P = 10W, FC 20 P = 20W, FC 0 Tamb Tins2 Tfin Tevap Ths Figure 43: Temperature distribution showing effect of Power Input (PEH) and Convection (NC/FC) for FR = 0.5 100 Natural Convection P = 20W, FR=1.0 T emperature (oc) 80 P = 20W, FR=0.5 60 40 P = 10W, FR=1.0 P = 10W, FR=0.5 20 0 Tamb Tins1 Tins2 Tfin Tevap Ths Figure 44: Temperature distribution showing effect of Power Input (PEH) and Fill Ratio for Natural Convection 120 T emperature (oc) 100 80 Force Convection 60 P = 20W, FR=0.5 P = 20W, FR=1.0 40 P = 10W, FR=0.5 P = 10W, FR=1.0 20 0 Tamb Tins1 Tins2 Tfin Tevap Ths Figure 45: Temperature distribution showing effect of Power Input (PEH) and Fill Ratio for Force Convection FR=1.0 Thermal Resistance (K/W) P = 10W, NC 4 P = 20W, NC 3 5 2 P = 10W, FC P = 20W, FC 1 0 Rvc Rfin ∑R Figure 46: Effect of Power Input (PEH) and Convection (NC/FC) on Thermal Resistance for FR = 1.0 6 FR=0.5 Thermal Resistance (K/W) P = 10W, NC 4 5 P = 20W, NC 3 2 P = 10W, FC P = 20W, FC 1 0 Rvc Rfin ∑R Figure 47: Effect of Power Input (PEH) and Convection (NC/FC) on Thermal Resistance for FR = 0.5 Natural Convection Thermal Resistance (K/W) 4 P = 10W, FR=0.5 5 P = 10W, FR=1.0 P = 20W, FR=1.0 3 P = 20W, FR=0.5 2 1 0 Rvc Rfin ∑R Figure 48: Effect of Power Input (PEH) and Fill Ratio on Thermal Resistance for Natural Convection 5 Force Convection Thermal Resistance (K/W) 4 3 2 P = 20W, FR=0.5 1 P = 20W, FR=1.0 P = 10W, FR=0.5 P = 10W, FR=1.0 0 Rvc Rfin ∑R Figure 49: Effect of Power Input (PEH) and Fill Ratio on Thermal Resistance for Force Convection T otal Thermal Resistance (K/W) Natural Convection 5 4 FR = 1, VC2 3 FR = 1, VC1 FR = 0.5, VC1 2 FR = 0.5, VC2 1 10 20 Power Input of Electric Heater, PEH (W) Figure 50: Total Thermal Resistance showing effect of Fill Ratio for VC1 & VC2 under Natural Convection 6 Total Thermal Resistance (K/W) Force Convection 5 4 FR = 0.5, VC2 FR = 0.5, VC1 3 2 1 FR = 1, VC1 FR = 1, VC2 0 10 20 Power Input of Electric Heater, PEH (W) Figure 51: Total Thermal Resistance showing effect of Fill Ratio for VC1 & VC2 under Force Convection CHAPTER 5 DISCUSSION OF RESULTS 5.1 Repeatability test of the results (Runs #1, 2, 9, 10) Based on the experiment of study, same test were run repeatedly with the same working fluid and fill ratio. For run #1 and 2 which are using the VC #1,same test were repeated for three times on the four runs under natural convection with fill ratio of 1.0 for water. From the results obtained for run #1 which the power input was 10W, the temperatures for the run were found to be repeatable within ±1.0oC in 120 minutes or7200 seconds. For run #2 which the power input for 20W, the temperatures for the run were found to be repeatable within ±0.5oC in 280 minutes or 16800 seconds. For run #9 and 10 which are using the VC #2, same test were repeated for three times on the four runs under natural convection with the fill ratio of 1.0 for water. Based on the results obtained for run #9, the power input of 10W has the repeatability of temperature within ±1.0oC in 120 minutes. For run #10 which the power input for 20W, the temperatures for the run were found to be repeatable within ±0.5oC in 120 minutes. In order to calculate the average transient temperature of the repeated experiment for computing the total thermal resistance and heat transfer coefficient, we take the average of the value for the three repeated results. Figure 10 to 12 present on the transient temperature for run #1 and 2 where Figure 30 to 32 present on the transient temperature for run #9 and 10. 5.2Transient Temperature Results (Runs #1 to 16) The transient temperature results were plotted in Figure 10 to 21 and Figure 30 to 41. In the Figures, the results of temperatures along the fins and evaporator were also plotted. From the Figures, the temperature of the VC was increasing from the room temperature due to the heat transfer from the power input to the VC. The power input used for the study was 10W and 20W where each power input of the experiment will heat up the VC until it achieved steady state. Under natural convection for power input of 10W on VC #1 and 2, it was noticed that all the temperature achieved its steady state around 120 minutes of heat up. For power input of 20W on VC #1 and 2, the temperature achieved its steady state at around 120 to 150 minutes. Under force convection for power input of 10W on VC #1 and 2, it was noticed that the temperature achieved its steady state at around 60 minutes. For power input of 20W on VC #1 and 2, the

temperature achieved its steady state at around 50-60 minutes. At higher power input, the temperature of the VC will be higher. This is because when the power input is higher, more heat will transfer to the device. Under natural convection, the highest temperature was up to 114.9oC which was on run #10 VC #2. Under force convection, the highest temperature was up to 70.7oC which was on run #10 VC #1. By comparison of the natural convection and force convection, the surface temperature of VC on natural convection is higher. This is because the condensing rate is expected to be slower under NC as it is using the natural air flow speed. This would result in less condensate return to the evaporator section of the VC. Hence the larger pool of un-evaporated liquid in the evaporator section would result in poorer performance of the NC. 5.3Effect of Fill Ratio on Vapor Chamber 5.3.1 Effect of Fill Ratio on VC #1 In order to compare the effect of fill ratio and power input under natural and force convection, the temperature distribution of the VC #1 were plotted in Figure 24 and 25. In Figure 24, result showed that the fill ratio of 0.5 performed better than the fill ratio of 1.0 under natural convection. On power input of 20W, the surface temperature of aluminum block reached about 112oC in FR of 1.0, where in FR of 0.5 the temperature reached about 106oC. On power input of 10W, the surface temperature of aluminum block reached about 73oC in FR of 1.0, where in FR of 0.5 the temperature is slightly lower which is about 70oC. The reason of the poorer performance of the high fill ratio in natural convection might be due to the higher rate of evaporation than the rate of condensation. With high fill ratio, the working fluid was “stuck” at the fins causes the rate of condensation

return to be lesser. Hence, the evaporator was to be “starved”. On the other hand, Figure 25 showed that the fill ratio of 1.0 performed better than the fill ratio of 0.5 under force convection. On the power input of 10W, the surface temperature of aluminum block reached about 41oC in high fill ratio, where in low fill ratio the temperature reached about 46oC. On power input of 20W, the surface temperature of aluminum block was about 57oC in high fill ratio where the temperature increase to about 71oC in low fill ratio. The fin temperature for high fill ratio is around 38oC where the low fill ratio is about 50oC. This showed that there are better cooling effect on high fill ratio. The reason for the better performance of high fill ratio in force convection might be due to the rate of condensation of working fluid return to the evaporator section is high enough. Therefore, the high fill ratio of working fluid will be better to transfer the heat with higher rate to the condenser section. 5.3.2 Effect of Fill Ratio on VC #2 In order to compare the effect of fill ratio and power input under natural and force convection, the temperature distribution of the VC #2 were plotted in Figure 44 and 45. In Figure 44, result showed that the fill ratio of 0.5 performed better than the fill ratio of 1.0 under natural convection. On power input of 10W, the surface temperature of aluminum block reached about 70oC in FR of 1.0, where in FR of 0.5 the temperature is slightly lower which is about 69oC. The decrease in temperature is not significant on both of the fill ratio. On power input of 20W, the surface temperature of aluminum block reached about 115oC in FR of 1.0, where in FR of 0.5 the temperature reached about 113oC. Again, the temperature difference was not much. But as overall, the performance of low fill ratio performed better in natural convection because it has a lower temperature at the heat source. The lower temperature obtained was

> 20**due to the** higher **heat transfer rate** in **the** VC. **The**

possible reason behind had been explained earlier in part 6.3.1 which isthe higher rate of evaporation than the rate of condensation that causes “stuck up” at the condenser section. Meanwhile for the force convection on Figure 45, the result showed that the fill ratio of 1.0 performed better than the fill ratio of 0.5 as the temperature distribution of high fill ratio is lower. On the power input of 10W, the surface temperature of aluminum block reached about 40oC in high fill ratio, where in low fill ratio the temperature reached about 42oC, with a 2oC of difference. On power input of 20W, the surface temperature of aluminum block was about 61oC in high fill ratio where the temperature increase to about 64oC in low fill ratio. The result showed that better cooling effect on high fill ratio. The heat transfer occurs faster in liquid than in solid state. Therefore, when the fill ratio is higher and the rate of condensation return to the evaporator is high enough, more working fluid filled in the VC will transfer the heat faster, hence results in better cooling and higher heat transfer coefficient. 5.4Effect of Convection on Vapor Chamber 5.4.1 Effect of convection on VC #1 In order to compare the effect of convection and power input respective with the fill ratio of VC #1, Figure 22 and 23 were plotted for the temperature distribution. Convection is the flow of heat or heat transfer from a hot to cold region. Based on Figure 22, the temperature distribution of natural convection shows a higher temperature than the force convection for high fill ratio. The surface temperature of aluminum block for natural convection for power input of 10W to 20W ranged from 73oC to 112oC. On the other side, the surface temperature of aluminum block for force convection ranged from 41oC to 57oC. In higher power for both natural and force convection results in higher temperature. The temperature distribution for natural convection on high fill ratio with low power input is from 61oC to 73oC. For high power input the temperature distribution is from 93oC to 112oC. Meanwhile, the temperature distribution for force convection on high fill ratio with low power input is from 30oC to 41oC. For high power input the temperature distribution is from 38oC to 57oC. The probable reason for such results might be there is external agent involved on the fluid motion in force convection. In natural convection, the fluid motion is natural. Therefore, the heat transfer rate in lower which results in higher temperature and poorer cooling effect. Moreover, in Figure 23 shows the temperature distribution on convection with high and low input power in low fill ratio. The result obtained was similar to the concept of the temperature distribution in high fill ratio. Natural convection results in higher temperature compare to force convection. The temperature distribution for natural convection on low fill ratio with low power input is from 58oC to 70oC. For high power input the temperature distribution is from 85oC to 106oC. Meanwhile, the temperature distribution for force convection on low fill ratio with low power input is from 35oC to 46oC. For high power input the temperature distribution is from 50oC to 71oC. 5.4.2 Effect of convection on VC #2 In order to compare the effect of convection and power input respective with the fill ratio of VC #2, Figure 42 and 43 were plotted for the temperature distribution. Natural convection occurs on the flow of fluid motion with buoyancy effect while force convection occurs with the flow of fluid motion with external device input on it. For instance, cooling fan. No difference with the VC #1, the temperature distribution of natural convection shows a higher temperature than the force convection. In higher power for both natural and force convection results in higher temperature. The temperature distribution for natural convection on high fill ratio with low power input is from 62oC to 70oC. For high power input the temperature distribution is from 99oC to 115oC. Meanwhile, the temperature distribution for force convection on high fill ratio with low power input is from 31oC to 40oC. For high power input the temperature distribution is from 42oC to 61oC. The heat transfer process occurs in force convection is faster. The faster the

> 17**heat transfer** process, **the** higher **heat transfer coefficient will be**

acquired. In forced convection, the process was accelerated by a fan. Hence the increase in temperature of the working fluid occurs faster in the VC and higher heat transfer coefficient. Figure 43 shows the temperature distribution on convection with high and low input power in low fill ratio. Based on the result obtained, the higher power of natural and force convection have a higher temperature. This is because higher energy produced in every second to the device when the power increases. Besides, natural convection results in higher temperature compare to force convection. The temperature distribution for

natural convection on low fill ratio with low power input is from 61oC to 69oC. For high power input the temperature distribution is from 96oC to 113oC. Meanwhile, the temperature distribution for force convection on low fill ratio with low power input is from 30oC to 42oC. For high power input the temperature distribution is from 41oC to 64oC. 5.5Effect of Fill Ratio on Total Thermal Resistance 5.5.1 Total Thermal Resistance on VC #1 In order to compare the

> 4**effect of fill ratio and power** input **on**

total thermal resistance for convection on VC #1, Figure 28 and 29 were plotted to investigate. Thermal resistance is defined as the resistance of a system or medium to the heat flow through the boundaries and dependent upon the thermal properties of the system. For instance, this is thermal conductivity of the material. Under natural convection, Figure 28 shows the total

> 1**thermal resistance for** low power **is higher than the** high power. **The**

resistance that included in the study is resistance of fin which is the condenser and the resistance of VC.

> 1**The total thermal resistance is** calculated using **the summation of the** Rfin and

RVC. **The** total thermal **resistance**

for high fill ratio under natural convection ranged from 4.5K/W to 5.1K/W where for low fill ratio it ranged from 4.3K/W to 4.8K/W.

23**Based on the results, the** total **thermal resistance**

of high fill ratio is higher than low fill ratio. This is because the heat transfer rate in natural convection is slower. Therefore with the high fill ratio, the possibility that the working fluid to “stuck up” at the fin is higher. When there is less condensate return

2**to the evaporator** section, **the heat transfer coefficient**

will be smaller results in higher total thermal resistance. Under force convection, Figure 29 shows the total

1**thermal resistance for** low power **is higher than the** high power. **The**

total thermal resistance for high fill ratio under force convection ranged from 1.8K/W to 1.9K/W where for low fill ratio it ranged from 2.4K/W to 2.5K/W. The variation of total thermal resistance on both fill ratios is small. Based on the results obtained, the total thermal resistance for high fill ratio is lower than low fill ratio which is opposed to the natural convection experiment. In force convection, the rate of condensate to return to the evaporator is high due to the external force apply at the condenser part. Therefore, high filled working fluid will helps to transfer the heat faster from the heat source. Hence, result in the lower thermal resistance. 5.5.2 Total Thermal Resistance on VC #2 In order to compare the

4**effect of fill ratio and power** input **on**

total thermal resistance for convection on VC #2, Figure 48 and 49 were plotted to investigate. The

2**evaporator and condenser resistances are** calculated **based on the outer surface area of the**

wall. Under natural convection, Figure 48 shows the total

1**thermal resistance for** low power **is higher than the** high power. **The**

mainpurpose of the study

29**is to reduce the overall thermal resistance by increasing the** rate of **heat transfer**

to get a better cooling device for electronic industry. The total thermal resistance for high fill ratio under natural convection ranged from 4.7K/W to 5.1K/W where for low fill ratio it ranged from 4.5K/W to 4.7K/W.

23**Based on the results, the** total **thermal resistance**

of high fill ratio is higher than low fill ratio. The heat transfer of working fluid that pass through the wick structure of the wall of VC from condenser to evaporator is slower under natural convection as been described earlier in part 6.3.1. Under force convection, Figure 49 shows the total thermal resistance is same for both high and low powers. The total thermal resistance for high fill ratio under force convection is 2K/W where for low fill ratio it is 2.1K/W. The total thermal resistance on both fill ratios is the same. Based on the results obtained, the total thermal resistance for high fill ratio is slightly lower than low fill ratio which is opposed to the natural convection experiment. The variation of overall thermal resistance is only 0.1K/W. In force convection, the rate of condensate to return to the evaporator is high due to the external force apply at the condenser part. Therefore, working fluid of fill ratio of 0.5 to 1.0 can give a good performance which helps to transfer the heat faster from the heat source. However, the results obtained showed that the optimum fill ratio is 1.0. 5.6Effect of Convection on Total Thermal Resistance 5.6.1 Total Thermal Resistance on VC #1 In order to compare the effect of convection and power input respective with the fill ratio for VC #1, Figure 26 and 27 were plotted for the overall thermal resistance. Convection is the flow of heat or heat transfer of a medium from a hot to cold region. Based on Figure 26, the power input of natural convection shows a higher thermal resistance than the force convection for high fill ratio. The overall thermal resistance for natural convection for power input of 10W to 20W ranged from 4.5K/W to 5.1K/W. On the other side, the total thermal resistance for force convection ranged from 1.8K/W to 1.9K/W which is only 0.1K/W of variation. In higher power for both natural and force convection results in lower thermal resistance. This is because during high power, the energy pass through per second was higher to overcome the resistance to become smaller. When the power increases, there is more heat transfer through the device resulting in higher heat transfer coefficient. As for force convection on high fill ratio, the overall thermal resistance is not much variation due to the external sources forcing on the condenser part resulting in better cooling effect. Based on Figure 27, the

1**thermal resistance for** natural convection **is higher than for** force convection. When **the** power increase, **the**

thermal resistance is reduce. The overall thermal resistance for natural convection for power input of 10W to 20W ranged from 4.3K/W to 4.8K/W. Besides, the total thermal resistance for force convection ranged from 2.4K/W to 2.5K/W which is also with 0.1K/W of variation. As for natural and force convection for low fill ratio, the resistance of fin is higher than the resistance of VC. As for force convection, the variation of thermal resistance is small indicating the rate of heat transfer for high and low power is almost equal. 5.6.2 Total Thermal Resistance on VC #2 In order to compare the effect of convection and power input respective with the fill ratio for VC #2, Figure 46 and 47 were plotted for the overall thermal resistance. Based on Figure 46, the power input of natural convection shows a higher thermal resistance than the force convection for high fill ratio. This is because the air flow for natural convection is slower compare to force convection with external force on the air flow. The cooling effect is poorer results in rate of heat transfer is slower. The overall thermal resistance for natural convection for power input of 10W to 20W ranged from 4.7K/W to 5.1K/W. On the other side, the total thermal resistance for force convection for high and low power is the same which is 2K/W. In higher power for natural convection tends to result in lower thermal resistance. This is because during high power, the energy pass through per second was higher to overcome the resistance to become smaller. While on the other hand for force convection, the total thermal resistance did not change shows that 10 and 20W of power did not affect much for the thermal resistance due to the external air used to cool down the VC. Based on Figure 47, the same theory get in previous part where the

1**thermal resistance for** natural convection **is higher than for** force convection. When **the** power increase, **the**

thermal resistance is reduce. The overall thermal resistance for natural convection for power input of 10W to 20W ranged from 4.5K/W to 4.7K/W. Besides, the total thermal resistance for force convection is the same which is 2.1K/W. As for natural for low fill ratio, the resistance of fin is higher than the resistance of VC. As for force convection, the resistance of VC is higher than the resistance of fin. This can be mean by the

36**heat transfer** rate **at the condenser is** lower **than the evaporator**

part for natural convection. While for force convection, the fin has lower thermal resistance indicates the heat transfer rate is higher than the evaporator part. 5.7Thermal Performance of VC #1 and VC #2

41**In order to** compare **the thermal performance of the**

two VC, Figure 50 and 51 were plotted on the thermal resistance to show the effect of fill ratio and input power under natural and force convection. The variation of both VC is the number of fins where VC #1 has eight fins meanwhile VC #2 has four fins. 5.7.1 Natural Convection Based on Figure 50, the total thermal

resistance for VC #1 and VC #2 with the fill ratio of 1.0 at power of 10W is the highest which is 5.1K/W under natural convection. During the power of 10W, the VC #2 of fill ratio of 0.5 has the lowest thermal resistance which is 4.7K/W. This concludes that under natural convection, the fill ratio of 0.5 performed better than the fill ratio of 1.0 with the power of 10W. Compared with the fill ratio of 0.5 for VC #1 and VC #2 with power of 10W, VC #2 performs better than VC #1. This may be due to less condensate return

50**to the evaporator section** and more “stuck” **of working fluid** at **the**

condenser for VC #1, therefore with the increase in the number of fins, the condensate that “stuck” at the fins will be greater. Hence the un-evaporated liquid from the evaporator session will lower down the heat transfer rate from the condenser to evaporator. Meanwhile, when we see for the power input of 20W, the highest total thermal resistance is on the VC #2 with fill ratio of 1.0 which is 4.7K/W. Besides, the thermal resistance for VC #1 with fill ratio of 1.0 and VC #2 with fill ratio of 0.5 are the same which is 4.5KW. The lowest total thermal resistance is VC #1 with the fill ratio of 0.5 which is 4.3K/W. The total thermal resistance for VC #1 and VC #2 with fill ratio of 0.5 has a variation of only 0.2K/W which is not significant enough to make any conclusion. The probable reason for such results might be due to the power for 20W is strong enough to perform better

32**to transfer** the **heat from the evaporator to the condenser.** Hence, with **the**

increase of surface area by

43**increasing the number of fins, the heat transfer**

rate is higher for VC #1 with fill ratio of 0.5. 5.7.2 Force Convection Based on Figure 51,the total thermal resistance for VC #1 with the fill ratio of 0.5 at power of 10W is the highest which is 2.5K/W under force convection. During the power of 10W, the VC #1 of fill ratio of 1.0 has the lowest thermal resistance which is 1.9K/W. Besides, the second highest total thermal resistance is VC #2 with the fill ratio of 0.5 which is 2.1K/W. This concludes that under force convection, the fill ratio of 1.0 performed better than the fill ratio of 0.5 with the power of 10W. Compared with the fill ratio of 1.0 for VC #1 and VC #2 with power of 10W, VC #1 performs better than VC #2. This is because during force convection experiment carried out with the cooling fan, the surface of the fin will have a better cooling effect, the condensate return to the evaporator section with me more. The number of fins increase will results in the increasing of total surface area of condenser. The larger the total surface area, the more surface it exposed to the air to cool down the evaporated liquid in the fin heat sink. In brief, the heat transfer coefficient of the force convection will be larger than in the natural convection. If we look into the power of 20W, the ranking of the highest and lowest thermal resistance is the same with the ranking of power 10W. The total thermal resistance for force convection on power 10W and 20W has not much variation. The highest thermal resistance for power 20W is 2.4K/W where the

19**lowest total thermal resistance is** 1.8K **/W.** Whereas **for the**

VC #2 with the

27**fill ratio of 0.5, the total thermal resistance** remains the same **with the** power **of** 10W **and**

20W. Therefore, if we were to use force convection on the cooling of electronic device, the fill ratio is the better choice compare to the half fill ratio. In brief, if we compare the Figure 50 and 51, the overall thermal resistance for natural convection is higher than force convection. The concept that shows the results obtained has been explain earlier. Based on the experiment study, there is heat loss to the surrounding by convection and radiation. In order to investigate the error form with the heat loss, another experiment of run #13(2) and #14(2) were repeated with the same power and fill ratio on VC #2. In the experiment, insulation was added on the thermocouples head on the fins in order to investigate the temperature difference with and without the insulation. Results were tabulated in Table 3. 5.8Heat transfer Coefficient of VC Heat transfer is the process of exchanging of the thermal energy between the systems. Heat can be travel through three ways which are conduction, convection as well as radiation. When the heat is transfer between a surface wall and a working fluid at a variation of temperature is known as convective heat transfer. Based on the study of VC- FHS, the working fluid of water is transferring heat by convection

16**to the surface** wall **of the flat** plate **heat pipe**

with capillary tube. Heat is transfer from the high temperature end to the low temperature end. Heat loss to the surrounding from the VC-FHS to the surrounding air is by conduction and radiation. The convective heat transfer coefficient is based on the working fluid properties such as velocity, viscosity and temperature. The heat transfer coefficient that can be measured in this study is the convective heat transfer coefficient. In this study, heat transfer coefficient of the fin, hfin had been calculated to investigate the performance of both VC to determine the optimum fins to use on VC-FHS system. Based on the results that had been calculated, the

45**heat transfer coefficient** of force **convection is** higher **than in** natural **convection.**

This applied to both of the VC. The reason is because natural convection is solely caused by the buoyancy force due to the variation of density with different temperatures in the working fluid. Natural convection is never induced by external force which applies free convection for the transferring of heat through the system. The highest heat transfer coefficient is 140W/m2K which is force convection on VC #2 with the fill ratio of 0.5. The higher the heat transfer coefficient, the higher the rate of heat transfers through the system. The lowest heat transfer coefficient is 26W/m2K on natural convection on VC #1 with the fill ratio of 1.0. The range of heat transfer coefficient for natural convection is from 26W/m2K to 34W/m2K. Meanwhile, the range of heat transfer coefficient for force convection is from 73W/m2K to 140W/m2K. This shows that the thermal resistance will be lower for force convection process as the heat transfer rate is higher through the working fluid. The study of experiment has been neglect the issue of heat loss to surrounding by convection and radiation.

48**In order to** determine **the accuracy of the results,**

another experiment of run #13(2) and #14(2) were tested by apply insulation to the fin. Based on the results, the fin temperature increase about 3% for both the power inputs. The resistance of fin is believed to be increased by around 5%. This is because when insulation applies to the fin, heat loss to the

surrounding will be limited and hence the heat was trapped inside the fins that increase the temperature of fin. With this result, the reduction of the resistance of VC is about 12.5% to 20%. When

47 **the thermal resistance of the fin** is **increased, the**

heat transfer coefficient will be smaller. The higher the thermal resistance, thus the smaller the

49 **heat transfer coefficient. The heat transfer coefficient is**

about to reduce from 3% to 6%. The results obtained for this experiment can be assume to use in other runs of experiment in earlier stage with the correction of error. 5.9 Comparison of VC-FHS with FHS Based on the research study, simulation was

11 **carried out in order to** compare **the thermal performance of**

VC-FHS and FHS. The simulation was done with the MATHCAD program. Different model of VC-FHS and FHS with different dimension were used to compare. Based on the simulation results of FHS, the RF1D obtained for natural convection is around 11-12K/W. From the results obtained in my research, the total thermal resistance is around 4-5K/W. This proved that with the VC embedded in the FHS, the overall performance will be improved. This is because VC is the flat heat pipe provide wick structure which will distribute the temperature of the working fluid in the pipe evenly through capillary, thus the rate of condensation and evaporation will be higher in order to results in better cooling. When the temperature is lower, the cooling effect is better. Thus, lower thermal resistance we get. CHAPTER 6 SUGGESTIONS FOR FUTURE STUDIES • Carry out experiment study on FR of 0.25 or 0.75. • Change the working fluid with another liquid like acetone. • Varied the fins height and width. • Varied the size of the VC heat sink. • Used a better insulator in order to prevent the likelihood of heat loss to the surroundings. CHAPTER 7 CONCLUSIONS The conclusions of the study are as shown: ? FC performs better with lower thermal resistance compared to NC. ? Under NC, lower FR (FR=0.5) performs better. ? Under FC, higher FR (FR=1.0) performs better. ? Under NC, lower FR does not affect the performance of VC1&VC2. ? Under FC and at low FR, VC2 performs better than VC1. REFERENCES ? Attia, A. A., & El-Assal, B. T. (2012). Experimental investigation of vapor chamber with different working fluids at different charge ratios. Ain Shams Engineering Journal, 3(3), 289-297. ? Jeng, T. (2015). Combined convection and radiation heat transfer of the radially finned heat sink with a built-in motor fan and multiple vertical passages. International Journal of Heat and Mass Transfer, 80, pp.411-423. ? Kang, S. W., Chen, Y. T., Hsu, C. H., & Lin, J. Y. (2012). Temperature Uniformity Analysis of a Multi-well Vapor Chamber Heat Spreader. Frontiers in Heat Pipes (FHP), 3(1). ? Li, H., Chiang, M., Lee, C. and Yang, W. (2010). Thermal performance of plate-fin vapor chamber heat sinks. International Communications in Heat and Mass Transfer, 37(7), pp.731-738. ? Luo, X., Hu, R., Guo, T., Zhu, X., Chen, W., Mao, Z. and Liu, S., (2010), June. Low thermal resistance LED light source with vapor chamber coupled fin heat sink. In 2010 Proceedings 60th Electronic Components and Technology Conference (ECTC) (pp. 1347-1352). IEEE. ? Michels, V., Milanez, F. and Mantelli, M. (2012). Vapor chamber heat sink with hollow fins. J. Braz. Soc. Mech. Sci. & Eng., 34(3), pp.233-237. ? Ming, Z., Zhongliang, L., &Guoyuan, M. (2009). The experimental and numerical investigation of a grooved vapor chamber. Applied Thermal Engineering, 29(2), 422- 430. ? Naphon, P. and Wiriyasart, S., (2015). On the Thermal Performance of the Vapor Chamber with Micro-channel for Unmixed Air Flow Cooling. Engineering Journal, 19(1), pp.125-137. ? Reyes, M., Alonso, D., Arias, J.R. and Velazquez, A., (2012).

Experimental and theoretical study of a vapour chamber based heat spreader for avionics applications. Applied Thermal Engineering, 37, pp.51-59. ? Shih, D., (2011). Heat sink equipped with a vapor chamber. U.S. Patent Application 13/029,878. ? Shukla, K., Solomon, A., & Pillai, B. (2013). Thermal Performance of Vapor Chamber with Nanofluids. Frontiers in Heat Pipes (FHP), 3(3). ? Tan, B. K., Wong, T. N., &Ooi, K. T. (2010). A study of liquid flow in a flat plate heat pipe under localized heating. International Journal of Thermal Sciences, 49(1), 99-108. ? Tsai, M.C., Kang, S.W. and de Paiva, K.V., (2013). Experimental studies of thermal resistance in a vapor chamber heat spreader. Applied Thermal Engineering, 56(1), pp.38-44. ? Wang, R. T., Wang, J. C., & Chang, T. L. (2011). Experimental analysis for thermal performance of a vapor chamber applied to high-performance servers. Journal of Marine Science and Technology, 19(4), 353-360. ? Wang, S., Chen, J., Hu, Y., & Zhang, W. (2011). Effect of evaporation section and condensation section length on thermal performance of flat plate heat pipe. Applied Thermal Engineering, 31(14), 2367-2373. ? Wiriyasart, S., &Naphon, P. (2013). Study on the Heat Transfer Characteristics of a Vapor Chamber without Micro-channel for Cooling an Electronic Component. Thammasat International Journal of Science and Technology, 18(3), 16- 22. ? Wong, S. C., Hsieh, K. C., Wu, J. D., & Han, W. L. (2010). A novel vapor chamber and its performance. International Journal of Heat and Mass Transfer, 53(11), 2377- 2384. ? Yang, K. S., Yang, T. Y., Tu, C. W., Yeh, C. T., & Lee, M. T. (2015). A novel flat polymer heat pipe with thermal via for cooling electronic devices. Energy Conversion and Management, 100, 37-44. ? Yu, I. S., Rhi, S. H., & Cha, K. I. (2012). Micro and nano thermal flow characteristics of a flat plate heat pipe heat spreader. International Journal of Physical Sciences, 7(11), 1762-1772. ? Zhang, M., Liu, Z., & Ma, G. (2008). The experimental investigation on thermal performance of a flat two-phase thermosyphon. International Journal of Thermal Sciences, 47(9),1195-1203. APPENDICES Thermal conductivity aluminium (W/mK): kfin ?? 200 Fin dimensions (m): Hfin ?? 0.03 Sfin ?? 0.01 tfin ?? 0.0035 ?x base ?? 0.005 Wfin ?? 0.049 Assume: Natural convection coefficient (W/m2K): ha ?? 5 Wfin Nfin ?? ? 4.9 Sfin Afin ?? ? 2.Hfin ? tfin? Wfin?5 ? 0.016 x ?? ?? Wfin?? ? tfin ? 6.3 ? 10? 3 At ?? Afin ? 0.0024 ? 0.018 ?5? Fin efficiency: 0.5 mfin ?? ? ha ?? 2Wfin ? 2 ?tfin? ? ? kfin?Wfin?tfin ? ? 3.912 ? ? Hfinc ?? Hfin ? tfin 2 ? 0.032 ? fin ?? tanh? mfin?Hfinc? mfin?Hfinc ? 0.995 ?o ?? 1 ? Nfin?Afin?? 1 ? ?fin? ? 0.978 A t Fin resistance (K/W): Rfin?? 1 ha?At??o ? 11.384 Rbase ?? kfin?Wfin?Sfin?Nfin ?x base ? 0.01 Rf1D?? Rfin? Rbase ? 11.395 Thermal conductivity aluminium (W/mK): kfin ?? 200 Fin dimensions (m): Hfin ?? 0.03 Sfin ?? 0.01 tfin ?? 0.0035 ?x base ?? 0.005 Wfin ?? 0.049 Assume: Force convection coefficient (W/m2K): ha ?? 40 Wfin Nfin ?? ? 4.9 Sfin Afin ?? ? 2.Hfin ? tfin? Wfin?5 ? 0.016 x ?? ? ? Wfin? ? ? tfin ? 6.3 ? 10 ?3 At ?? Afin ? 0.0024 ? 0.018 ? 5 ? Fin efficiency: 0.5 mfin ?? ? ha ?? 2Wfin ? 2?tfin? ? ? kfin?Wfin?tfin ? ? 11.066 ? ? Hfinc ?? Hfin ? tfin 2 ? 0.032 ?fin ?? tanh? mfin?Hfinc? mfin?Hfinc ? 0.961 ?o ?? 1 ? Nfin?Afin??1 ? ?fin? ? 0.834 A t Fin resistance (K/W): Rfin?? ha?At??o 1 ? 1.67 Rbase ?? kfin?Wfin?Sfin?Nfin ?x base ? 0.01 Rf1D?? Rfin? Rbase ? 1.681 1 2 3 4 5 6 7 8 9 10 11 12 13 14 15 16 17 18 19 20 21 22 23 24 25 26 27 28 29 30 31 34 35 120 36 37 120 38 39 120 40 41 120 42 120 43 6 44 6 45 46 47 120 48 49 120 50 51 120 52 53 120 54 120 55 6 56 6 57 6 58 59 60 61 62 63 64 65 66 67 68 69 70 71 72 73 74 75 76 77 78 79 80 81